# Elemental Analysis of Aqueous Process Samples with Wavelength Dispersive X-ray Fluorescence Spectrometry

Master's Thesis

University of Jyväskylä

Department of Chemistry

6th May, 2022

Jenni Heikkilä

## Abstract

In the literature review of this Master's thesis work, topics related to quantitative analysis of aqueous samples with x-ray fluorescence (XRF) techniques were covered. XRF techniques are fast, highly stable and accurate methods for analysing several elements in wide concentration ranges. The techniques have a variety of applications in industry and research.

According to the literature, XRF techniques are less typically used for measuring aqueous samples, and many researchers have used preconcentration techniques to obtain sufficient detection limits. In XRF, the analyte signal is strongly affected by the physical and chemical properties of the sample matrix, and several matrix correction procedures have been developed. Strong background scattering is typical for aqueous matrices.

In the experimental part of the work, a method for measuring aqueous process samples with wavelength dispersive XRF instrumentation (WDXRF) was developed. The method was calibrated with aqueous standard solutions, and it included 10 elements (Na, Mg, Si, P, S, Cl, K, Ca, Mn, Fe). The samples were measured directly as liquids using liquid sample cups. Calibrations were linear, and the limits of quantitation were between 3.4 – 24.6 ppm depending on the analyte.

Method performance was tested with standard solutions and spiked samples, and the results were compared to the results from reference methods. Recoveries for sodium were 70 – 90% whereas for other elements the recoveries were 100 – 120%. Except for sodium, the results from XRF were generally higher than the results from reference methods. Relative standard deviation of results was 2 – 16%. Variance was greater for Na and Cl than for other elements.

Sample pretreatment tests were performed for two typical sample types, one being an organic-in-water emulsion and the other having a clear aqueous phase. Sample pretreatment by funnel separation, filtration and centrifugation was tested. For both sample types, the XRF results were close to the results from reference methods. The measured analyte concentrations were similar after each pretreatment procedure, and the results were not affected by the changes in the sample temperature.

# Tiivistelmä

Tämän pro gradu -työn kirjallisessa osassa perehdyttiin vesinäytteiden kvantitatiiviseen röntgenfluoresenssianalytiikkaan (XRF) liittyviin teemoihin. XRF on nopea, stabiili ja tarkka analyysimenetelmä, joka soveltuu useiden alkuaineiden mittaamiseen laajalla pitoisuusalueella. XRF-tekniikoilla on useita sovelluskohteita tutkimuksessa ja teollisuudessa.

Kirjallisuuskatsauksen perusteella XRF-tekniikkaa ei yleisesti sovelleta vesinäytteiden mittaamiseen, ja useat tutkijat ovat hyödyntäneet näytteiden konsentrointia suoran nestefaasimittauksen sijaan. XRF-analytiikassa näytematriisin kemialliset ja fysikaaliset ominaisuudet vaikuttavat voimakkaasti mitattavaan signaaliin, ja matriisivaikutusten korjaamiseen on kehitetty lukuisia menetelmiä. Taustasäteilyn voimakas sironta on tyypillistä vesipohjaisilla näytteillä.

Työn kokeellisessa osassa kehitettiin mittausmenetelmä vesipohjaisten prosessinäytteiden ja jätevesien mittaamiseen aallonpituus-dispersiivisellä XRF-tekniikalla (WDXRF). Kalibrointi tehtiin vesipohjaisilla standardiliuoksilla kymmenelle alkuaineelle (Na, Mg, Si, P, S, Cl, K, Ca, Mn, Fe). Näytteet mitattiin nestefaasissa käyttäen nestenäytteille tarkoitettuja näytekuppeja. Kalibroinnit olivat lineaarisia, ja määritysrajat asettuivat alkuaineesta riippuen 3,4–24,6 ppm tasolle.

Menetelmän toimivuutta testattiin mittaamalla standardiliuoksia sekä näytteitä, joissa alkuaineiden pitoisuuksia oli kasvatettu lisäämällä standardiliuosta näytteeseen. XRF-menetelmän tuloksia verrattiin referenssimenetelmien tuloksiin. Saantoprosentit olivat natriumille 70–90 %, ja muille alkuaineille yleisesti 100–120 %. XRF-menetelmän tulokset olivat yleisesti suurempia kuin referenssimenetelmien tulokset, lukuun ottamatta natriumia. Tulosten suhteellinen hajonta XRF-menetelmällä oli 2–16 %. Hajonta oli suurempaa natriumilla ja kloorilla kuin muilla alkuaineilla.

Esikäsittelytesteihin valittiin kaksi erilaista näytetyyppiä, joista toinen oli öljy vedessä -emulsio ja toisessa oli kirkas vesifaasi. Esikäsittelyinä testattiin erotusta erotussuppilossa, suodatusta ja sentrifugointia. XRF-menetelmällä mitatut tulokset olivat lähellä referenssimenetelmien tuloksia molemmilla näytetyypeillä. Esikäsittelyillä ei ollut vaikutusta näytteistä mitattuihin alkuainepitoisuuksiin, eikä näytteen lämpötila vaikuttanut mittaukseen.

# Foreword

This master thesis project was done between November 2021 and April 2022 at the UPM-Kymmene Oyj North European Research Center in Lappeenranta, and the topic for the experimental part was provided by the UPM Biofuels Growth Program. The supervisors of the work were Senior Researcher Satu Tikkakoski from UPM and University Lecturer Jarmo Louhelainen from University of Jyväskylä. Senior Researcher Andrea Gutierrez represented the customer Biofuels Growth Program and was also supervising the experimental project.

The literature review was limited to cover the topics that were relevant for the experimental project. The experimental part was planned to answer the most crucial research questions, and other possible sample types or further applications were excluded.

Books and articles related to instrumental analysis techniques and x-ray fluorescence theory and applications were used as information sources. The introductory publications and operation manuals by instrument manufacturers were also used. The scientific publications were searched mostly through Elsevier's ScienceDirect tool, and generic internet search was also applied.

I wish to thank UPM-Kymmene Oyj for providing me with such an interesting thesis project and all the resources for working with it. Special thanks to my supervisor Satu, who has been supporting me and giving advice on a weekly basis through the whole project. I also want to thank Jarmo for supervision and comments, and my Team Manager Tuomas Mäkinen at UPM for all the support.

Thank you, Andrea, for coming up with the project idea and all the advice through the project. I also want to thank Senior Researcher Jaana Käkölä and Manager Kati Vilonen for all the advice and conversations, and the Research Center laboratories for running the reference measurement and answering all my questions. Special thanks to the people at Biorefinery Development Center laboratory – for sampling, help with measurements, advice and discussions.

Finally, thank you to my family and friends for all the support.

In Lappeenranta, 30th March 2022

Jenni Heikkilä

# Contents

# Abbreviations

| | |
|---|---|
| CNT | Carbon nanotube |
| CSE | Counting statistical error |
| EDXRF | Energy dispersive x-ray fluorescence spectrometry |
| FAAS | Flame atomic absorption spectrometry |
| FC | Flow proportional counter |
| FP | Fundamental parameters |
| GFAAS | Graphite furnace atomic absorption spectrometry |
| IC | Ion chromatography |
| ICP-MS | Inductively coupled plasma mass spectrometry |
| ICP-OES | Inductively coupled plasma optical emission spectrometry |
| LLD | Lowest limit of detection |
| LOD | Limit of detection |
| LOQ | Limit of quantitation |
| ppm | parts per million, in experimental part used as equal to mg $L^{-1}$ |
| SC | Scintillation counter |
| SPE | Solid phase extraction |
| TOC | Total organic carbon |
| TXRF | Total reflection x-ray fluorescence spectrometry |
| UP water | Ultrapure water |

LITERATURE REVIEW

# 1 Introduction

In x-ray fluorescence spectrometry (XRF), x-rays are used to excite the analyte atoms. Characteristic fluorescent radiation from inner shell electron transitions is measured to both identify and quantify analytes. X-ray fluorescence spectrometry is a widely used multi-elemental analysis technique to determine trace, minor and major elements in various sample types and application.[1e)] Typical applications include the routine analysis of geological samples, steels and alloys, archaeological samples, cement and other construction materials and different kind of forensics and environmental samples.[2] Different instrument configurations from high power floor-standing models to table-top laboratory instruments and field portable hand-held units are available.[1a)]

Whereas many elemental analysis techniques are developed for liquid sample analysis, XRF techniques are well suitable for analysing solid specimens and bulk powder, which makes them a good choice in many industrial quality control tasks. Wavelength dispersive instruments (WDXRF) are suitable for fast and accurate routine analysis of specific elements, whereas energy dispersive systems (EDXRF) give the overview of all elements in the sample simultaneously, but lack the resolution compared to WDXRF.[1e)] In theory, the analysis of all elements from beryllium to uranium is possible with the XRF techniques, including non-metallic elements.[2]

XRF techniques are suitable for both qualitative and quantitative analysis since the intensity of the fluorescent radiation is generally proportional to the analyte concentration. Quantitative analysis requires the consideration of strong matrix effects that are characteristic for the technique. The matrix effects originate from chemical effects (absorption and enhancement of the signal) as well as physical properties (particle size and sample surface homogeneity).[1b)] In general, XRF technique is considered fast and accurate, and concentrations from ppb level to 100% can be measured.[3]

Analysis of a wide range of aqueous samples is crucial in the modern society. These samples include purified waters, natural waters and environmental samples as well as sewage waters and different kinds of industrial waters.[4] Industrial effluents are eventually discharged to natural waters, so their composition needs to be known in order to evaluate the effect on the receiving water system. The emission of pollutants is regulated by the authorities, which makes it necessary for the company to monitor several constituents in the disposed waters.[5]

In addition to monitoring the effluents, the analysis of different aqueous process stream samples can also give information to the process control. The results can be used to evaluate process efficiency, or they can indicate upcoming process problems, e.g., corrosion of steel parts. Since the sample matrix is typically complex, the standard analytical methods may need to be modified in order to meet requirements for both speed and accuracy.[5] In elemental analysis of aqueous samples, inductively coupled plasma optical emission spectrometry (ICP-OES) is one of the most commonly used analytical techniques.

The experimental part of this thesis work was done at the UPM Research Center in Lappeenranta. The aim of the work was to develop a method for measuring aqueous process samples with a WDXRF instrument. As the method was designed for process monitoring and control, it was expected to be fast and easy to operate and have sufficient accuracy for the intended use. Method development also included the testing of suitable and required sample pretreatment.

The first chapter in this thesis paper covers the general practices in water analysis and shortly introduces the more commonly used analytical techniques for elemental analysis. Next, the theoretical background and instrumentation of XRF techniques are presented. Aspects of quantitative analysis, liquid sample analysis and aqueous sample pretreatment are covered in the following chapters. At last, validation and quality control of analytical measurement methods are shortly described. The experimental part describes the method development and testing and represents the key findings. Finally, the thesis project is summarised together with final conclusions and suggestions for further work.

# 2 Analysis of aqueous samples

## 2.1 General practices

The analysis of aqueous samples starts with representative sample, that is collected and handled without contamination or loss of the analytes. The samples are suggested to be analysed as soon as possible.[4] Standard method series ISO EN 5667 states the guidance for sampling and sample handling of water samples, and the third part focuses on preservation and handling of the samples.[6] According to the standard, water samples should be stored in low temperatures, inside inert containers, minimising the exposure to light and air. The standard also states the preferred pH, storage time and possible additives considering the intended analysis. The separation of suspended solids by filtration with 0.45 µm filter is suggested to be done to all samples before storing.[4,6]

Depending on the sample, many types of determinations are commonly done. The colour, taste and smell of the sample can be evaluated by physical senses. Typical analysis also includes the determination of temperature, conductivity, redox potential and pH, as well as a variety of organic and inorganic constituents.[4] For industrial effluents, common organic and inorganic analysis include the determination of oil or grease content, total organic carbon, chemical and biological oxygen demand, ammonia and nitrogen content, and various anions and metallic ions.[5]

A variety of standard methods considering water samples have been published, some focusing on specific analyte and some on specific analysis method. The publication “Standard Methods for the Examination of Water and Wastewater” by American Public Health Association[7] collects a wide range of standard methods for many types of water samples. The methods are categorised by constituents, but the book also introduces the widely used analytical techniques. Attention is paid to quality assurance and high-quality laboratory work.

For the determination of some single inorganic constituents (e.g., silicates and phosphates), titrations, spectrophotometric analysis or other specific methods are suggested as standard methods. Ion chromatography is commonly used for determining anions, whereas atomic absorption and emission spectrometry are the widely used instrumental techniques for determining metallic ions. Also, different kind of sensors and test chips can be applied for fast monitoring of waters.[4]

## 2.2 Common instrumental methods for elemental analysis

### 2.2.1 Atomic absorption techniques

Atomic absorption methods are widely used for determining single dissolved metallic analytes. The techniques are based on atomising the analytes and detecting the absorption of electromagnetic radiation, as the atoms are excited to a higher energy level.[8,9b)] Flame atomic absorption spectrometry (FAAS) uses flame to evaporate the solvent and atomise the sample that is sprayed into the flame as aerosol. Graphite furnace atomization (GFAAS) uses rapidly heating graphite furnace to atomise a small volume of sample introduced in the furnace tube.[9b)]

Qualitative analysis is performed by measuring known solution and plotting the detected intensity against concentration. The absorption intensity is linearly proportional to analyte concentration only on a restricted concentration range.[8] Atomic absorption techniques have a great disadvantage of being able to measure only one element at the time. On the other hand, FAAS instrumentation is relatively simple and inexpensive and GFAAS has moderate sensitivity for many applications.[2]

Chemical interferences are common in atomic absorption spectrometry if compounds with low volatility are formed during atomization. Ionization and other chemical reactions may reduce the amount of free gaseous atoms. Also, matrix effects may be present and affect the aerosol formation or atomization. Overlapping of the spectral lines is not that common, since the analytes are excited with their characteristic excitation wavelengths.[9b)]

### 2.2.2 Optical emission and mass spectrometry techniques

Optical emission spectrometry (OES) is one of the most widely used techniques for multi-elemental analysis of a wide range of samples, inductively coupled plasma (ICP) being the most used atomization source.[9c)] The plasma is generated by ionising argon gas in an oscillating radio frequency magnetic field. Typical plasma powers of 0.5 – 2.5 kW result in high temperature plasma at around 7000 – 8000 K.[10] Liquid sample is introduced to the plasma as fine aerosol, where the solvent is evaporated (flushing with nitrogen or argon gas helps to remove water) and the compounds are dissociated to free gaseous atoms or ions. Plasma energy excites the elements, and the characteristic emission formed during the following relaxation is detected as the analytical signal, intensity of the signal being proportional to the analyte concentration.[10]

With ICP-OES, all the analytes can be detected simultaneously, and non-metals can also be measured. High temperatures in plasma result in more complete atomization, and therefore there are less interferences from ionization reactions.[9c)] The method is relatively stable and sensitive, but compromises in operation conditions may be needed if different kind of elements are determined. Many elements have several emission lines to choose from if spectral interferences occur with some, but on the other hand, resolving the emission spectra requires more complex optical system compared to atomic absorption spectra.[9c)]

Atomization by inductively coupled plasma can also be combined to a detection system based on mass spectrometry (ICP-MS). After atomization, the elements are ionised, and the ions are separated by their mass-to-charge ratio. ICP-MS has lower detection limits than ICP-OES, and the spectra is simpler. ICP-MS has typically been more expensive to acquire, and it may have some special and complex interferences and matrix effects.[9d)] Nevertheless, ICP-MS has been growing its popularity in many applications recently.

### 2.2.3 Challenges in atomic absorption and emission techniques

Reproducible and representative sample introduction is one of the main challenges with atomic absorption and emission techniques. Only a small portion of sample enters the atomization source as fine aerosol carried by a gas flow.[9a)] Separation of the sample during aerosol formation or memory effects due to insufficient flushing of the sample introduction system may lead to errors. Also, the atomization needs to be reproducible, and the temperature fluctuations can have severe effects on the excitation of the atoms. Emission spectrometry is especially sensitive for plasma temperature fluctuations.[9a)]

As the spectral interferences in ICP-OES analysis are typically well known, non-spectral interferences may occur when samples with complex matrices are measured (e.g., industrial effluents or wastewaters). Matrix-based interferences may occur if the sample properties affecting sample transport and nebulization, e.g., viscosity and surface tension, are changed. Also, changes in plasma excitation properties, including plasma temperature and the number of electrons in plasma, can result in interferences.[11] The interferences can be reduced by matrix-matching (diluting the sample, matching the acid background and possibly adding major matrix components to calibration standards), using internal standard correction or calibrating the method by analyte addition procedure. Carbon from organic compounds may give rise to emission background and consume the plasma energy. Also, burning carbon in plasma may form carbon deposits in the torch parts or injector tube.[11]

# 3 X-ray fluorescence spectrometry: theory and instrumentation

X-ray fluorescence spectrometry is based on exciting the sample's atoms with x-rays and measuring the radiation generated in the resulting electron transfers. X-rays interact with the matter in multiple ways, and in addition to fluorescence, scattering of primary photons and the emission of photoelectrons are relevant processes in XRF measurements. XRF spectrometers consist typically of radiation source, sample chamber and the spectrometer system for detection of the fluorescent radiation. XRF spectrometry has advantages in many types of applications, as long as x-ray safety is considered.[1a)d)]

## 3.1 Theoretical background

### 3.1.1 X-rays

In x-ray fluorescence spectrometry the sample is excited with x-rays. X-rays are electromagnetic radiation with the wavelength in the range from 0.01 to 10 nm. X-rays can also be illustrated as photons having the energies in the range from 0.125 to 125 keV.[3] The most common source of x-rays is an x-ray tube, but also radioactive material or a synchrotron can be used to generate the radiation.[1a),3] X-ray tube generates radiation with a continuous band of energies called Bremsstrahlung as well as the peaks of characteristic radiation of the tube material (see Figure 1).[1a)]

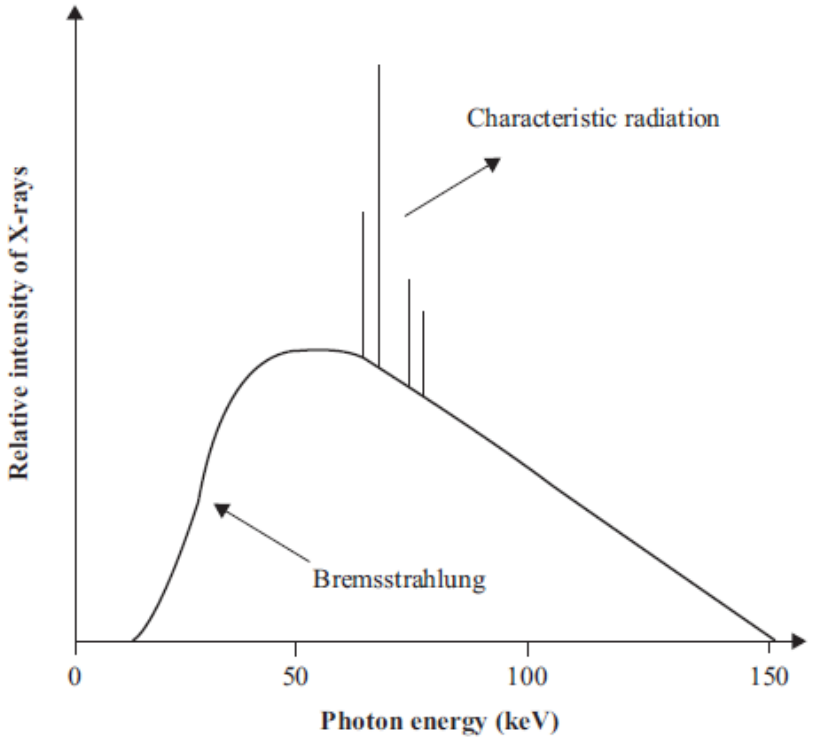


Figure 1 X-ray tube spectrum.[1a)]



### 3.1.2 X-ray interactions with the matter

The x-rays interact with the electrons of the atoms in the target matter. When a beam of x-ray photons is in contact with the matter, a fraction of the radiation will pass through, a fraction is absorbed in the material and a part of the photons scatter back.[3] If the photons collide with tightly bound electrons, they cause the electron to oscillate and emit radiation that have the same energy as the primary beam. This phenomenon is called Rayleigh scattering or elastic scattering. The photon may also loose a part of its energy due to a collision with a more loosely bound electron and as a result, the scattering radiation has lower energy as the primary beam. This phenomenon is called Compton scattering, or inelastic scattering.[3,12] Lighter elements (low atomic number Z) in the sample give rise to scattering, and for heavier elements the scattered fraction is relatively low. [12]

The fraction of primary beam that is absorbed in the material can produce the fluorescent radiation that is detected as an analytical signal in x-ray fluorescence spectrometry. If the energy of the primary x-ray photon is greater than the binding energy of an electron, the x-ray photon can expel an electron from the atom. The energies of the primary x-ray photons are in the same range with the binding energies of the electrons in the inner shells of the electron configuration, called K- and L-shells in the Bohr's atomic model (see Figure 2).[3] The energy transfer from primary photon to the inner shell electron is greatest when the energy of the primary photon is just above the binding energy of the electron (also, called the absorption edge).[12]

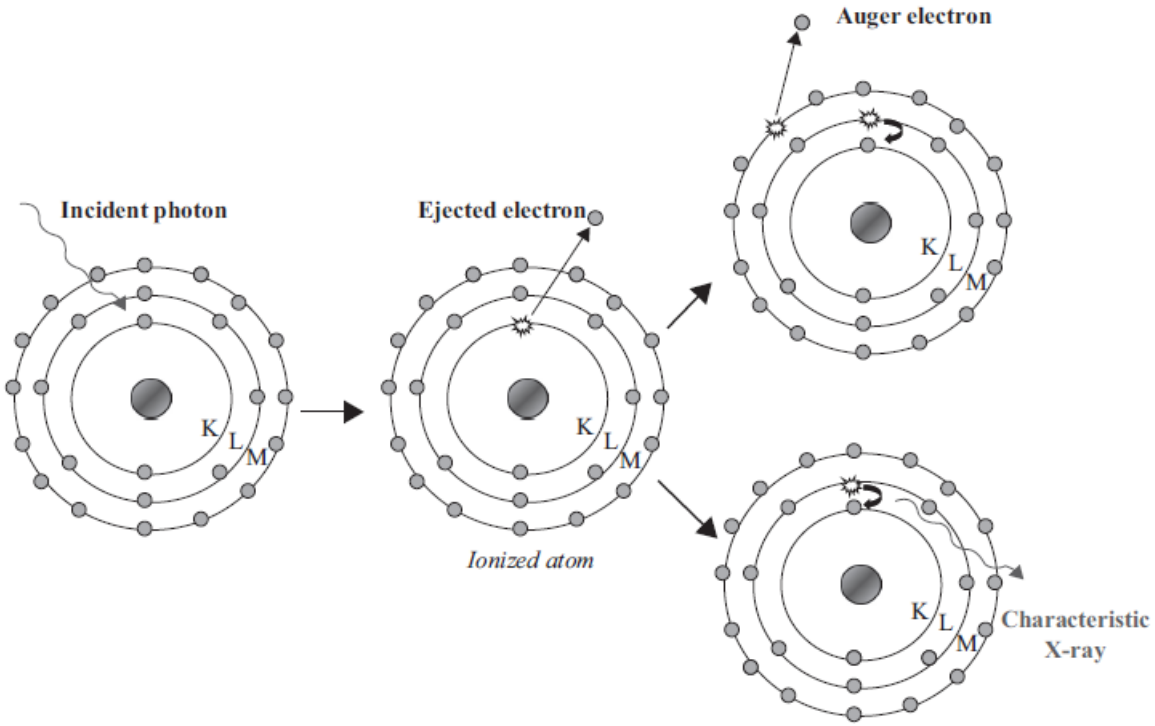


Figure 2 Generation of fluorescent radiation and Auger-electrons.[1a)]



Expelling an electron from the K- or L-shell of the atom leads into unstable excited state that has higher energy as the original state. The original electron configuration is restored when an electron from outer shell is transferred to the inner shell. The excess of the energy is emitted as an x-ray photon that can be detected as fluorescent radiation, as illustrated in Figure 2. Since all elements have their specific energy levels, the resulting radiation is characteristic for the elements.[3]

Another way of reaching the original state after an electron has been expelled is the Auger effect, meaning the rearrangement of electrons resulting in emitting a photoelectron (see Figure 2).[1a),12] Therefore, the intensity of emitted characteristic fluorescence is dependent of the effectiveness of Auger effect compared to the effectiveness of fluorescence. This relation is called the fluorescence yield, and it's value is great for heavier elements but low for light elements.[1a)] All interactions are illustrated in Figure 3.

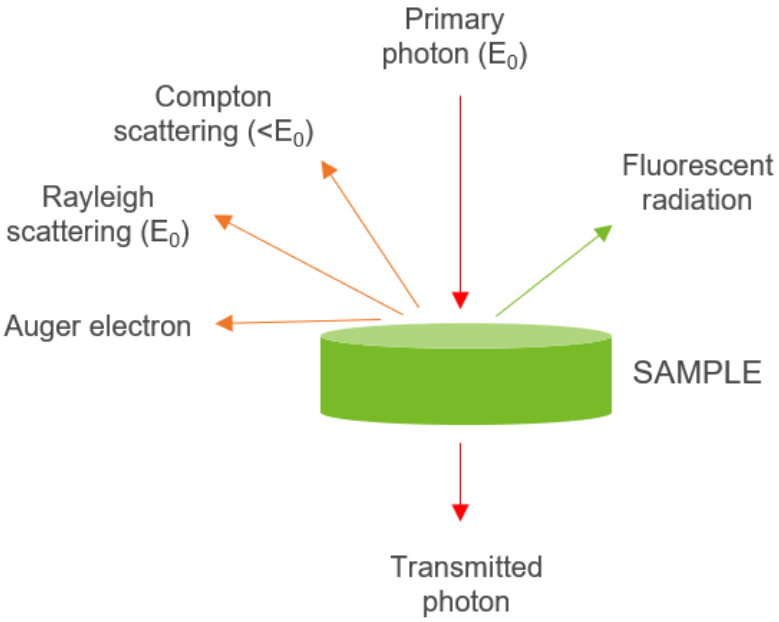


Figure 3 X-ray photon interactions with sample material.

### 3.1.3 Fluorescent lines

The energy of the characteristic radiation depends on where the electron was expelled and from where the replacing electron was transferred, meaning the energy difference between the corresponding electron states. Therefore, one element emits characteristic radiation with a few different energies, also called the "lines" for that element. A commonly used notation to name the transitions is the Siegbahn notation. The Siegbahn notation includes the symbol of the element, the name of the shell from which the electron was expelled, a Greek letter indicating the relative intensity of the line (α being the most intense line), and a number indicating electron subshells (e.g., Na Kα1).[1a)] The strongest lines are the K-lines, followed by the L-lines, M-lines and so on.[3] Atomic transitions for commonly measured fluorescent lines are represented in Figure 4.

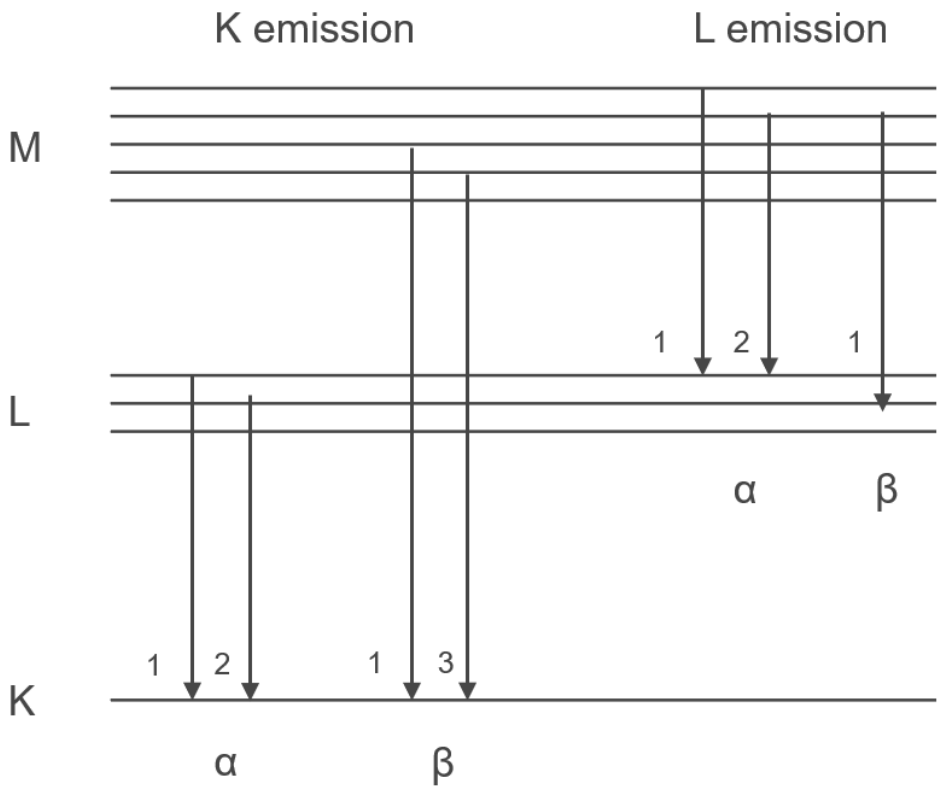


Figure 4 A few common atomic transitions in x-ray spectrometry.[1a),3,12]

3.2 WDXRF instrumentation

Wavelength-dispersive x-ray fluorescence (WDXRF) instrumentation generally consists of radiation source, sample holder, focusing optics and detection system. Table-top and floor-standing models are available, and the power varies between about 50 – 4000 watts. Figure *5* visualises the main components and the beam path in a WDXRF spectrometer.

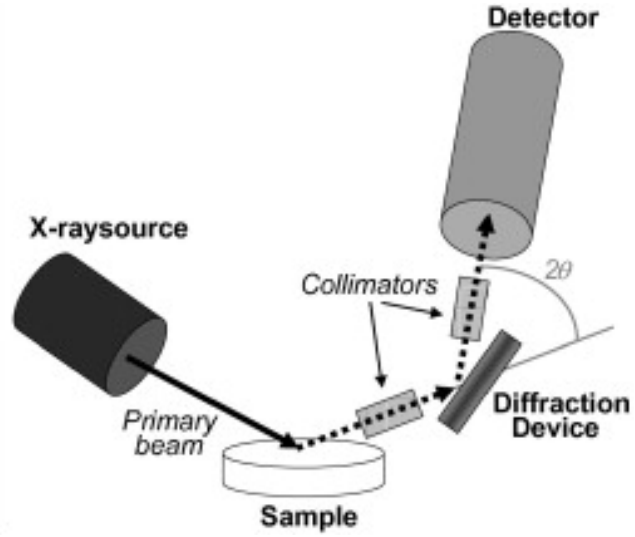


Figure 5 Instrument configuration of WDXRF spectrometer.[13]



In the x-ray tube the electrons from the cathode filament are accelerated towards the anode by high voltage between the cathode and the anode. The electrons hit the anode and cause the emission of x-ray photons.[1a)] The photons leave the tube through a thin (typically 75 μm[12]) beryllium window. The anode material and the used current and voltage determine the elements that can be excited, and the power of the tube is closely related to instrument sensitivity.[1a)]

Samples are introduced into a sample chamber. Because the molecules of air absorb x-ray radiation, solid samples are commonly measured under vacuum. For volatile samples (liquid or gas) the sample chamber is filled with helium which doesn't absorb the radiation of the analytes.[3] Some XRF instruments use sample spinner to reduce the effect of sample non-homogeneity.[1a)]

Filters between x-ray source and sample can be used to reduce interfering radiation and improve signal-to-noise ratio. Focusing optics, such as lenses and masks are used to focus the primary x-ray beam toward the specimen or the radiation coming from the sample chamber toward detection system, so that only the radiation from the sample reaches the detector. Collimators are used to convert the x-ray beam from the sample to a parallel beam that meets the diffraction crystal or the detector in the required angle.[1a),3]

The crystals placed between sample and detectors are used to separate and diffract the wavelengths of the fluorescent beam from the sample in different directions. The planes in the crystal diffract the incoming wavelengths in a way that only specific wavelengths have constructing interference, and the others will cancel out for the same angle. Diffraction is based on Bragg's reflection law represented in Equation (1) as

$$n\lambda = 2d \sin\theta \tag{1}$$

where $\lambda$ is the wavelength of the radiation, $d$ is the distance between lattice planes and $\theta$ is the angle of the incident beam. The lattice plane distance $d$ and the angle $\theta$ determine which wavelengths $\lambda$ and their integers $n\lambda$ will have the constructive interference (see Figure 6). Different wavelengths can be measured by placing the detector according to the diffraction angle $\theta$.[3] To measure wide range of elements (multiple different wavelengths), the instruments typically have a few different crystals with different lattice plain distances.[12]

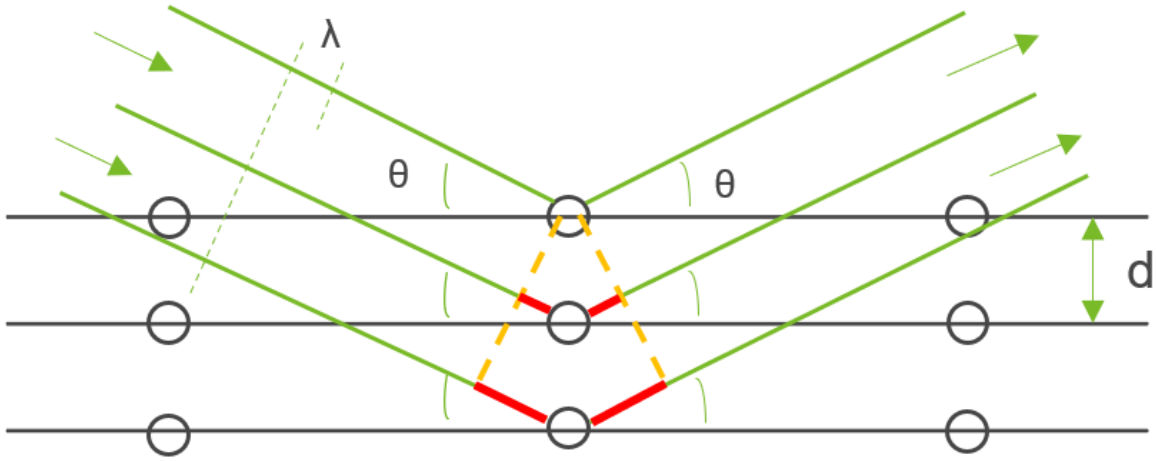


Figure 6 Bragg's diffraction law.

Detectors are needed to convert the beam of x-ray photons into electric pulses, that can be counted and further converted into an analytical signal. The energy (or wavelength) of the photon determines the height of the pulse, and the intensity comes from the number of pulses of a certain height.[1a)] WDXRF instruments commonly use gas-filled detectors and scintillation detectors, of which gas-filled detectors are best suited for detecting lower energies and scintillation detectors for high energies.[3]

Gas-filled detector is a metallic tube filled with inert counting gas and it has a thin tungsten wire with high voltage (see Figure 7). X-ray photons entering the detector generate a cloud of electrons that travel to the anode wire and cause a drop in wire voltage that is detected as the electric pulse. The number of electrons generated, and thus the height of the pulse, is proportional to the energy of the radiation.[1a)]

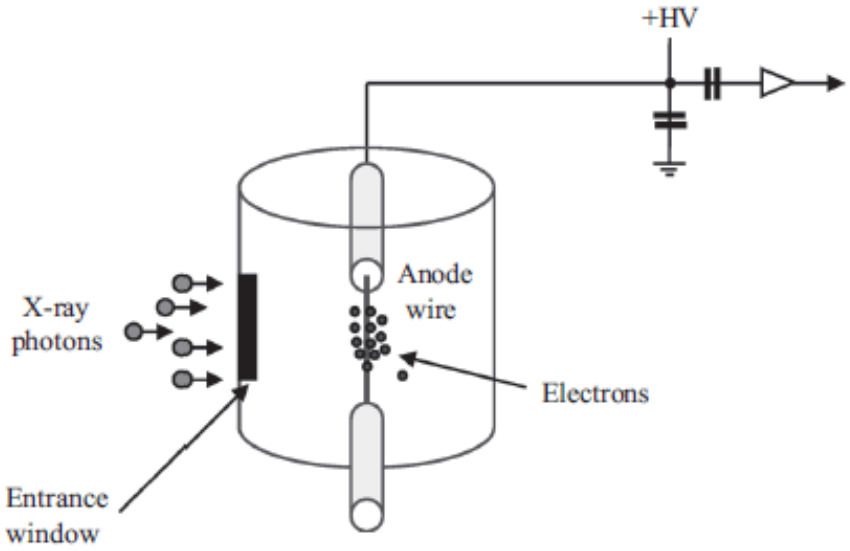


Figure 7 Schematic figure of gas proportional counter. HV = high voltage.[1a)]



The scintillation counter consists of the scintillation crystal and the photomultiplier (see Figure 8). X-rays produce a flash of blue-light electrons in the scintillation crystal, and the number of electrons is proportional to the wavelength of the x-ray photons. The signal is multiplied in the photomultiplier tube, and the electrons cause a drop in the voltage when reaching the anode.[1a)]

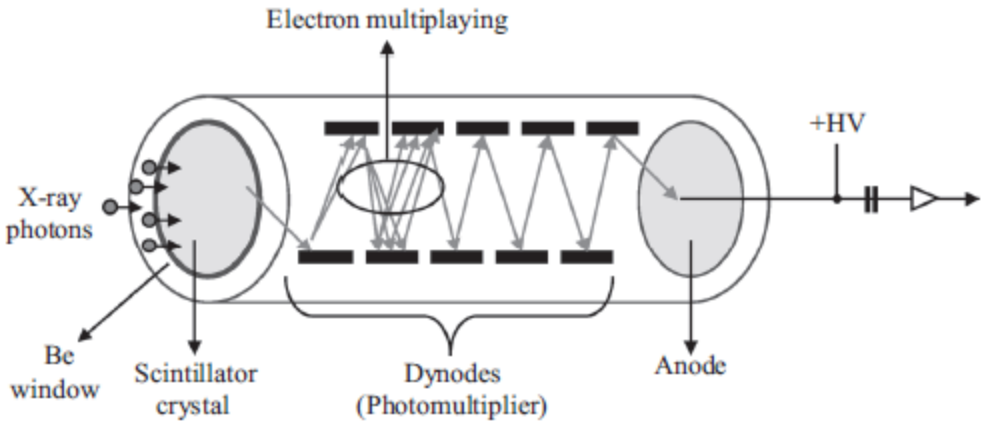


Figure 8 Schematic figure of scintillation counter. HV = high voltage.[1a)]



In sequential WDXRF spectrometer, the detectors move to certain angles to collect the x-rays that are diffracted to that direction from the crystal. The spectral lines of the elements are detected in specific detector positions, or the detector can move through an angular range and detect a range of wavelengths. Simultaneous instruments have fixed crystal-detector angles that detect specific wavelengths.[3]

## 3.3 Other XRF instrumentations

Another common XRF instrumentation setup is the energy dispersive spectrometer (EDXRF). The excitation process in very similar to WDXRF, but EDXRF uses energy dispersive detection system instead of crystal-detector combination to separate signals from different elements. Therefore, EDXRF records a spectrum of energies (or in other words, wavelengths) simultaneously. These detectors commonly have lower sensitivity for low energy lines but good sensitivity and resolution for heavier elements.[3] In simple 2D-optics for EDXRF (see Figure 9), also the scattered radiation reach the detector giving high background and noise. This can be reduced by using 3D-optics, where the x-ray tube irradiates a secondary target and the sample is excited by the fluorescent radiation of the secondary target.[3]

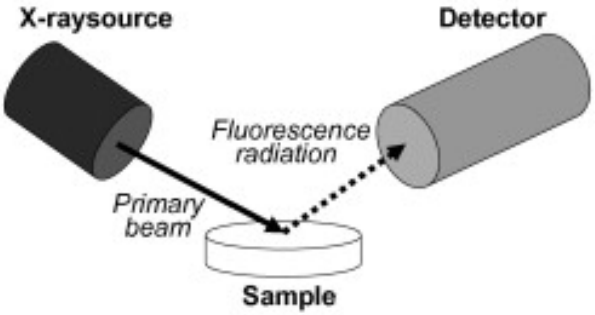


Figure 9 Instrument configuration of 2D EDXRF spectrometer.[13]



Total reflection XRF (TXRF) is a modified technique of EDXRF, where the primary beam is directed to the specimen at a small angle ($\leq 0.1°$), as illustrated in Figure 10. This configuration significantly reduces the background radiation coming to the detector, and the detector can be positioned close to the sample. TXRF has low penetration depth, and the samples are typically introduced as thin films.[1a),18]

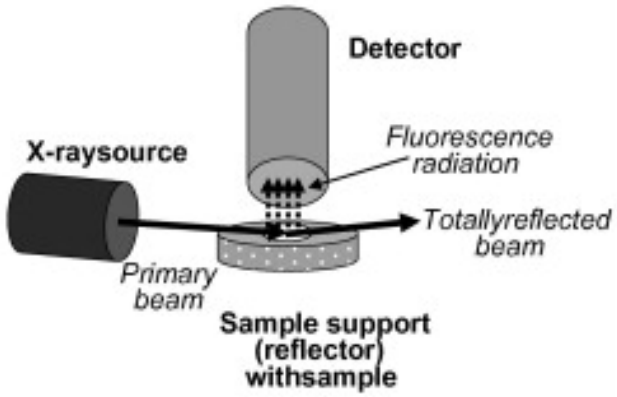


Figure 10 Instrument configuration of TXRF spectrometer.[13]

### 3.4 General advantages and disadvantages of XRF techniques

X-ray fluorescence technique has several advantages in element analysis compared to traditional atomic absorption or emission techniques. Many types of solid and liquid samples can be measured with little or no sample preparation, and there is no need to dilute or digest solid samples. The method is also non-destructive for the sample and doesn't produce liquid waste like AAS or ICP-OES techniques. Multielement analysis of wide range of elements is relatively fast, simple, and inexpensive to operate. X-ray fluorescence also offers high dynamic range from ppm level to almost 100% and good short and long term stability, so that the calibrations are valid for a long time without need for recalibration.[14]

Greatest disadvantages deal with low sensitivity for light elements, and the detection limits for XRF analysis may not always be sufficient for trace element analysis. On the other hand, dilution of high concentration samples is not usually needed.[14] Despite low operational costs, high-power x-ray spectrometers can be relative expensive to acquire. The sequential measurement of WDXRF technique increases analysis time, which might lead to changes in the sample during measurement. Matrix effects and interferences may be challenging to correct. Also, certified reference materials corresponding to sample matrix may be difficult to find, leading to challenges with method calibration. Especially in liquid sample analysis, the spillage of sample inside the spectrometer may lead to severe damage.[14]

The x-ray tube is a source of ionising radiation, and radiation safety needs to be considered when operating with XRF instruments. X-rays ionise matter, and exposure to radiation injures tissues in living organisms. Radiation damages DNA in cells, which may lead to local cell damage and increases the risk of cancer. Radiation dose describes the amount of radiation that a person has been exposed to and the health hazards related to it. The unit of dose is Sievert (Sv), and dose rate is measured as Sieverts per hour (Sv/h). Humans expose to natural radiation from the environment and working with radiation sources may increase the radiation dose.[15]

In Finland, the use of radiation is highly restricted and regulated. Finnish legislation for radiation[16] aims to minimise the health and environment hazards from the use of radiation. The use of radiation requires a licence, and the Finnish Radiation and Nuclear Safety Authority (STUK) guides and controls all activities related to radiation. The licence holder is responsible for radiation safety, and all persons using radiation must be regularly trained. XRF instruments are well protected with radiation shields and have several safety features that prevent misuse and shut down the system if any safety monitoring check is failed.

# 4 Quantitative XRF analysis

In XRF the intensity of fluorescent radiation is measured for specific wavelengths or wavelength ranges. Energy dispersive spectrometers measure a spectrum, and commonly the peak area is used as the measure of peak intensity. For wavelength dispersive XRF-analysis, the peak and background positions are known and set beforehand, and only the intensities in these positions are typically recorded.[3] High intensity, low background and minimum interferences are the main characters of good measurement conditions. The tube voltage is adjusted to obtain primary radiation of optimal energy for each measured element. In WDXRF, the crystals and collimators are responsible for sufficient resolution.[3]

As for many other instrumental analysis techniques, the relationship between measured intensities and analyte concentrations is typically determined by a calibration curve. A series of standard samples is measured with the XRF instrument, and the regression analysis and line fitting are done for the data. In general, the relationship between concentration $C$ and intensity is simply linear, but with XRF, the relation is extended to a form in Equation (2) as

$$C = K \times I \times M \times S \tag{2}$$

where $K$ is a factor related to the instrument and the current analytical method and is commonly defined as the slope of the calibration curve, and $I$ refers to the measured intensity.[17a)] Factor $M$ represents the inter-elemental effects related to XRF analysis. Factor $S$ considers the sample heterogeneity, and its influence can be reduced by sufficient and repeatable sample preparation, which is especially crucial with solid specimens (which may have variations in particle size and porosity, or uneven surfaces). If the samples are considered as homogeneous (e.g., homogenous solutions) and the factor $S$ can be neglected, the biggest interest is in dealing with factor $M$ for inter-elemental or matrix effects.[17a)]

Elements are first identified from the spectrum if the measurement is performed with EDXRF or the scan mode of WDXRF instrument. After the measurement, XRF software can make some corrections automatically to the spectrum.[1b)] Library information based on pure substances is often offered by the instrument manufacturer, and semi-quantitative analysis is possible without matrix specific calibration.[3] As a single XRF calibration is valid for years, the manufacturers offer a range of ready-made application setups (e.g., Geo-Quant and Petro-Quant by Bruker AXS GmbH), or the calibration can be done by the end-user.

For quantitative XRF analysis, the counting time for fluorescent photons, for both the analytical line and possible background correction points, needs to be sufficient so that the counting error is not limiting the analytical performance. The background in the XRF spectrum may be complex, and the peak to background ratios can be relatively low especially for light elements. The counting loss due to detector deadtime becomes important with high intensities.[17a)]

## 4.1 Absorption and enhancement effects

As the x-ray beam passes through matter (e.g., the sample matrix), the intensity of the x-rays decreases because the material absorbs a part of the radiation. Heavier elements absorb radiation better than lighter elements, and low-energy photons are absorbed more easily than high-energy photons. Increase in the density of the matter and in the length of the path that the photons travel in the matter also increases absorption.[12] Absorption effects weaken both the primary x-ray beam entering the sample, as well as the characteristic fluorescence coming out from the sample (see Figure 11).

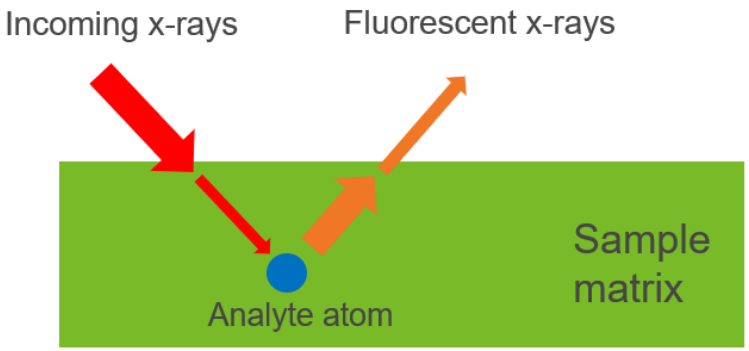


Figure 11 Absorption of x-rays in sample matrix.

The absorption probability of the characteristic fluorescence determines the analysis depth, which means the layer of sample from where the fluorescent x-rays can escape the sample without being absorbed into the sample matrix. Samples, that are thicker than the analysis depth of the analyte, are considered as infinitely thick. For intermediately thick samples the measured intensities depend on the thickness of the sample and therefore identical sample quantities must be used.[3,12]

In addition to absorption effects, the characteristic radiation of the elements can excite other elements in the sample similarly as the primary x-ray radiation (see Figure 12). This phenomena is called secondary enhancement, and the resulting radiation is called secondary fluorescence.[3,12] In addition to fluorescent photons, also the scattered primary photons can further excite other atoms. As the direct excitation is relatively inefficient for light elements, the excitation and enhancement effects may become important.[18]

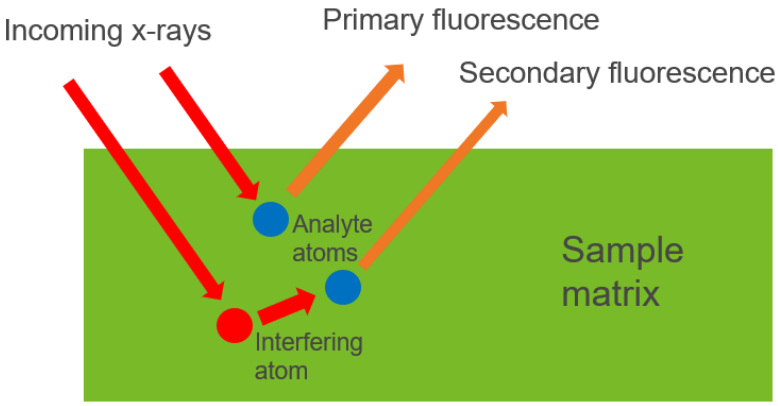


Figure 12 Secondary enhancement in XRF specimen.

4.2 Dealing with matrix effects

Due to the presence of absorption and enhancement effects, the measured analytical signal is highly dependent on the sample matrix around the analyte. In addition to the weight fraction or concentration of the analyte, the detected photon rate depends also on the other elements present in the specimen, the specimen type, preparation, size, and thickness as well as the geometrical setup of the instrument. Therefore, the intensity of the analytical line is not ideally directly proportional to analyte concentrations, and the influence of physical and chemical matrix effects need to be considered in order to obtain reliable results.[1b),18] Jenkins *et al.*[17b)] have listed four different strategies to deal with matrix effects in quantitative XRF analysis: ignoring, minimising, compensating and correcting.

Matrix effects can usually be ignored when the matrix in the standard materials and unknowns is similar. This is called in-type analysis or matrix-matching. Using this strategy only allows measurements in narrow concentration ranges, and suitable standard materials may be difficult to find. Also, matrix effects become negligible when very thin specimens are used, because for thin samples, the absorption and enhancement effects are reduced.[1b),17b)] Dilution can be used

to reduce the effect of interfering elements and minimise the variation in matrix. Simultaneously, the intensity of the analyte is reduced which creates sensitivity problems in trace analysis.[1b)]

Compensation strategies include the use of internal standard, standard addition and the utilization of the information from scattered radiation.[17b)] The internal standard procedure involves adding a fixed amount of analyte that is not present in the samples to all standards and unknowns. The internal standard is expected to be affected similarly as the analyte, which means that in multi-elemental analysis multiple internal standards may need to be used. The use of internal standard also makes the sample preparation more complex.[1b)] In standard addition method, differing known amounts of analyte are added to the unknowns, and the resulting difference in intensities is used to calculate the analyte concentration in the unknown. The information of scattered tube radiation can also be used to compensate for matrix effects, because the type and degree of scattering is dependent of the average atomic number of the sample matrix. However, this method only corrects for absorption effects and it's most suitable for light matrices, since the scattering is increased with decreasing atomic numbers. [1b),17b)]

## 4.3 Mathematical matrix correction models

Matrix correction models based on mathematical equations have been developed for quantitative XRF-analysis. The mathematical corrections became widely used only after the development of sufficient computers that were able to run the calculations.[17b)] The mathematical correction methods rely on fundamental physical parameters or empirical data.

### 4.3.1 Fundamental parameters method

Fundamental parameters (FPs) describe the basic interactions between photons and atoms as mathematical models. This theoretical method involves fundamental physical parameters like wavelengths of lines and absorption edges, attenuation and absorption coefficients, probabilities and ratios for different transitions and theoretical fluorescent yields.[1b),18] Instrumental parameters, like tube current and voltage, filters, distances and angles are also considered.[1b)] Simple models for single-element systems are then extended to more realistic systems having multiple layers of different elements.

The FP equations describe the attenuation coefficients for a sample of defined composition and physical size, and the photo-absorption coefficients for absorption in specific atom shells or subshells. The fundamental parameters also define the equations for excitation and relaxation phenomena based on quantum-mechanical rules as well as Auger-effect and transitions by emitted electrons. The probabilities of different phenomena are included in the model.[18]

### 4.3.2 Influence coefficients method

The starting point for influence coefficient method is the linear relationship between element concentration and the observed photon count rate. Due to the matrix effects, the correlation is not ideally linear for a set of data-points. The method assigns the elements of the matrix with a certain coefficient describing the element's effect to the measured count rate of the analyte.[18] In addition to the characteristics of analyte and matrix elements, the influence coefficients also depend on the wavelength distribution of the primary x-ray radiation and the incidence and emerge angles related to the system.[18]

The influence coefficients can be determined either theoretically or empirically. Theoretically determined coefficients are based on the fundamental parameters equations whereas empirical coefficients are calculated based on experimental data. Some expressions of theoretical coefficients rely on a set of approximations, whereas the fundamental algorithm introduced by Rousseau[19] is algebraically derived from the fundamental parameter equations and corrects for all matrix effects.[19] Theoretical approach uses only a few reference samples to calculate the coefficients, which can then be applied for wide concentration ranges. The use of empirical coefficients requires greater number of reference specimens, and the calculated coefficients can only be used for unknowns of similar concentration. The empirical approach can also be affected by empirical error.[19]

The coefficients can also be categorised according to the incident radiation (mono- or polychromatic), the analytical context (binary or multielement), or the effect of correction (absorption, enhancement or unspecified).[18] The resulting coefficients can be either constant or varying by the concentrations of one or multiple specimen components. Constant coefficients are suitable when enhancement effects are small or the concentration range is limited, whereas variable constants allow the measurement of greater concentration ranges.[1b)]

The algorithms for using the calculated coefficients can be based on either intensities or concentrations, most of them applying a general expression of Equation (3) as

$$W_i = K_i I_i \left( 1 + \sum_j \alpha_{ij} W_j \right) + B_i \qquad (3)$$

where $W_i$ is the analyte concentration, $K_i$ is the sensitivity (or the slope of the calibration curve), $I_i$ is the analyte intensity, $\alpha_{ij}$ is the influence coefficient related to matrix component $j$, $W_j$ is the concentration of the matrix component and $B_i$ is the analyte background.[1b)] The correction term is a sum over all matrix elements.

## 4.4 Measurement background

The background in XRF measurements consists of several phenomena. X-ray tube continuum spectrum and the characteristic anode material lines scatter from the specimen and give rise to the background level. If x-rays interact with the materials in specimen chamber, spectrometer chamber or other instrument parts, characteristic lines from these materials can interfere the measurement. In addition to characteristic fluorescence, x-rays can diffract from highly crystalline specimens resulting in interfering signals. High order diffraction or fluorescence in crystals can also be a source for background.[17c)]

As well as the analytical signals, also the background is matrix dependent. Therefore, the intensity for a blank sample with zero analyte concentrations is usually not the optimal estimation of overall background. A common practice with WDXRF is to measure the background separately for each analyte line, on a suitable position next to the analyte peak.[17c)] Also multiple background measurement points can be used, and the suitable position for background correction might also be matrix-dependent. The net intensity for the analyte peak is calculated by subtracting the background intensity from the gross peak intensity.[17c)]

### 4.5 Trace analysis

Typical features for trace analysis with x-ray spectrometry are low photon counting rates and poor peak-to-background ratios, which lead to severe loss of precision at low concentrations. Counting statistics play an important role when the measured concentrations are close to lowest limit of detection, and the increase in measurement time helps to reduce variance. With long counting times, drift in intensity levels may become notable when using sequential instruments that measure peak and background positions one after another.[17c)] Also, practical aspects like daily sample throughput or foil duration under x-ray radiation limit the measurement time. Defining the lowest limits of detectable and analysable concentrations is crucial for successful analysis.

If the matrix remains constant for all specimens and all analytes are at trace concentrations, inter-elemental effects become negligible and can be ignored. In this case, the absorption by matrix stays constant and enhancement effects are neglected, and a simple linear calibration can be used.[17c)] Elements in major concentrations may interfere the analysis of trace elements through absorption, overlapping peaks or rise in the background.

## 5 Analysis of liquid samples with XRF

X-ray spectrometry has a variety of applications for different sample types. Solid specimens like rock or metal samples can be measured directly. Powdered specimens can be measured as loose powders or after pelletising. Solid specimens can also be converted into glass-like beads by flux fusion in high temperatures.[1c)] XRF instruments can also be applied for liquid sample analysis. Liquids are measured in special sample cups that have a thin foil bottom. Whereas solid specimens are typically measured under vacuum to minimise the absorption of primary and fluorescent radiation, vacuum conditions can’t be used for liquids due to evaporation.[1c),3] Helium gas is typically used as sample chamber gas instead of air because it does not significantly absorb x-rays.[3]

## 5.1 Sample support foils

Liquid samples are introduced into XRF-instruments in liquid cups, that are prepared from plastic rings and a piece of thin sample support foil (see Figure 13). The x-ray spectrum is measured from the bottom of the sample cup through the foil material. The foils need to have sufficient mechanical strength and chemical resistance, durability against x-ray radiation and heat and be free from contamination. Simultaneously, the foil should have low x-ray absorption, because both the primary beam and the fluorescent radiation need to pass through supporting foil.[20,21]

Figure 13 Liquid sample cup accessories (right) and one prepared cup (left).

Generally, good mechanical strength means low transmission of long wavelength x-rays and limits the possibility to analyse light elements. Stretching of the foil change the distances between excitation source, sample plane and detection system as well as the foil thickness, which can result in counting errors and influence the accuracy of the analysis.[20,22] Foil duration also limits the possible analysis time for liquid samples. Preliminary tests for foil duration should be done by placing the actual sample in the sample cup and let the cup stay for example a few hours.[21]

Transmittance of x-rays is related to foil material and thickness as well as the wavelength of the radiation. High-energy radiation penetrate the foil material with minimal absorption, but for longer wavelengths of light element's lines the transmittance can be relatively poor.[20] Commonly used foil materials are polyethylene terephthalate (Mylar®, Du Pont, USA), polypropylene (Prolene®, Chemplex, USA) and polyimide (Kapton®, Du Pont, USA). Polypropylene is especially suitable for acids and alkalis, whereas Mylar and Kapton have good resistance for hydrocarbons.[20,21]

Increasing foil thickness results in better mechanical strength but lowers the transmittance of fluorescent radiation. Foils of nitrogen or oxygen containing material also absorb more than pure hydrocarbons, due to higher average molar mass of the material. The transmittance rate of different analytical lines compared to different foil materials is presented in Figure 14. For example, for Na Kα line the transmittance is only around 40% with 4 µm Prolene foil and practically zero with thick Mylar and Kapton foils. On the other hand, Cu Kα line passes through all foil materials with high transmittance rate.

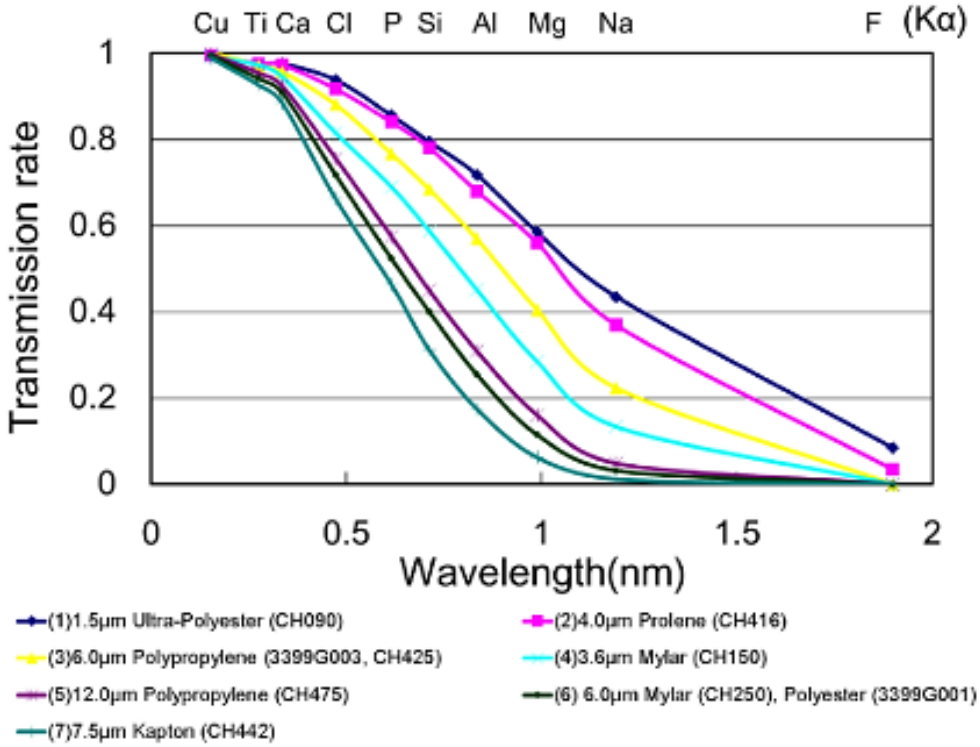


Figure 14 Transmission rate of fluorescent lines through different foil materials.[21]

## 5.2 Advantages and challenges of XRF in liquid sample analysis

Compared to other instrumental elemental analysis methods, XRF has several advantages but also remarkable challenges. XRF analysis is relatively fast due to long-term stability of the calibration and often requires minimal sample preparation. The method is non-destructive, and even though a relatively large amount of sample is needed, it is preserved, and no liquid waste is generated. A wide range of elements from B or Na to U can be determined, including sulphur and halogens, with long dynamic ranges from ppb (heavier elements) or ppm (lighter elements) level up to 100%.[3,14] WDXRF instruments have high resolution and spectral interferences are rare, which makes the analysis highly specific. [13,14]

Liquid matrix (e.g., water, oil, organic solvents) that is generally composed of light elements has low absorption effects. On the other hand, high background from scattered tube radiation result in poor peak to background ratio.[13,22] As the analyte concentrations are typically low (ppm to low percentage range), inter-elemental matrix effects are minor. Liquid samples are of intermediate thickness (not thin or infinitely thick), and this needs to be considered in quantitative analysis.

The sensitivity of the measurement might be insufficient for some applications, since the limits of detections are typically at mg $L^{-1}$ level for direct liquid analysis.[1c),13] The possible generation of bubbles in liquid samples lead to incomplete filling of the sample cup bottom and affect the reproducibility of the measurement.[13,22] Also, finding suitable liquid phase reference samples, especially for higher concentrations, may be difficult.

One of the biggest concerns regarding liquid sample analysis with XRF are leakage and scattering of the sample inside the instrument due to foil breakage. Sample material can cause severe damage to the system, and the replacement of the x-ray tube cause significant costs.[14,21] The risk of spillage can be reduced by limiting the measurement time and having an automatic sample ejection to prevent overexposure. Some instruments also have an automatic recognition of liquid sample cups, which automatically prevents the use of vacuum conditions. X-ray tube can be protected with a shield or hood and the vacuum seal between sample and spectrometer chambers protect the detection systems.[14]

## 5.3 XRF applications for aqueous sample analysis

X-ray fluorescence spectrometry is not a standardised method for analysing aqueous samples, and usually atomic absorption and emission techniques are preferred over XRF. With EDXRF and WDXRF configurations, the preconcentration of the sample is typically suggested to obtain sufficient sensitivity and reproducibility (see also Chapter 6).[13] Considering XRF systems, TXRF configuration measuring small amount of dried sample in minor angles gives the lowest background radiation and best sensitivity. When aqueous samples are measured directly with EDXRF or WDXRF configurations, the limits of detection (LOD) may not be satisfactory for certain environmental or industrial applications.[13]

Instrument manufacturers offer XRF applications mainly for the measurement of solid samples. Also, applications for measuring petrochemistry products are widely available, and standard methods have been published for the XRF analysis of oil and fuel samples. Considering aqueous sample analysis, Rigaku Corporation suggests the use of special sample carrier disks or utilization of the TXRF technique.[23] Bruker offers TXRF system[24] for the analysis of heavy metals and pollutants in aqueous samples, whereas EDXRF and WDXRF instruments are suggested for other analytical applications.

Thermo Fisher Scientific has published an application note for direct measurement of aqueous acid solution samples with the ARL OPTIM'X WDXRF instrument.[25] Na, $SO_4$ and Fe were determined from the samples that were measured with 3.7 µm polypropylene foil, and the results were compared to ICP-OES results. Linear calibration curves were obtained for Fe and $SO_4$, whereas Na measurement had more challenges. XRF and ICP-OES results were close to each other, when Fe was measured at < 10ppm range, Na at 50-360 ppm range, and $SO_4$ at 80-420 ppm range. Two XRF replicates had higher standard deviation for Na and low deviation for Fe.

In scientific literature, papers describing the direct analysis of aqueous samples were challenging to find, as many authors have utilised different preconcentration procedures. On the other hand, industrial applications in single quality assurance labs are rarely published in scientific literature if the methods are developed for in-house use.

However, Lerner *et al*.[26] had developed an EDXRF method for determining tin in beverages by direct liquid measurement. The authors were looking for a fast and simple method without the microwave digestion step required for ICP-OES. Aqueous standard solutions were used for calibration, as the calculated absorption coefficients were close to each other between standards and beverage samples. Limit of determination was 4 mg $L^{-1}$ and limit of quantitation 15 mg $L^{-1}$ The results for spiked samples were close to the results from ICP-OES at approximately 50 and 100 mg $L^{-1}$ level.

XRF techniques have also been used for measuring milk and dairy products, which would need decomposing for AAS and ICP-OES methods. Commonly used sample preparation technique is freeze-drying and pressing pellets, and the direct measurement as liquid is less popular.[27] Rinaldoni *et al*.[28] used direct WDXRF measurement for ultra-filtrated milk and yoghurt. The samples were diluted with water, and Ca, K, Fe and Zn were measured with scan mode. The results were compared to ICP-OES and flame emission spectrometry, which required the decomposition step. According to the authors, XRF proved to be fast and accurate method for the direct determination of dairy samples.

## 6 Sample preparation techniques for aqueous samples

Basic principles of good sample preparation also apply to XRF analysis. The sample must be homogenous, representative of the original material and free of contamination. Sample preparation should be related to intended analysis type (qualitative or quantitative analysis) and kept as simple as possible. As the analysis typically concerns dissolved analytes, traditional separation techniques like filtration and centrifugation can be used to remove possible other matter from samples. In XRF analysis the thickness of the sample is a crucial parameter, and accurate results are obtained with constant sample amount and appropriate correction methods.[1c),14]

X-ray spectrometry has many advantages in multi-element analysis of water, but the main drawbacks are insufficient sensitivity and detection limits for many applications. Therefore, preconcentration methods are widely used in combination with the XRF systems to extend the application range.[29] According to IUPAC definitions,[30] preconcentration is defined as a process to increase the concentration ratio or the amount of mixture components. Preconcentration

simultaneously improves the sensitivity for the analyte and reduces the matrix effects thus improving accuracy. Disadvantages linked to preconcentration procedures are possible loss of analytes and risk of contamination, in addition to making the analysis more complex and time-consuming.[29,31]

Solid specimens for XRF allow the use of vacuum, and XRF operates best on thin solid samples. Also, sensitivity and accuracy are increased for thin and homogenous specimens. Therefore, preconcentration procedures that result in thin, solid and homogeneous specimens are the most favourable ones for XRF analysis.[29,31] Van Grieken[29] reviewed over 170 articles on preconcentration methods already in 1982 and described several procedures used for aqueous samples. The researcher emphasises that the method must be selected according to sample type, number and concentration range of the desired elements, and the need for speed and cost of the analysis, and there is not one universal method that meets all the requirements. Marguí *et al*.[31] reviewed the topic again in 2010, giving an overview on new variations of the traditional methods.

### 6.1 Converting liquid into solid

As mentioned earlier, solid specimens are generally more suitable for XRF analysis than liquids. There are pretreatment strategies that are not preconcentrating the sample but aim to converting liquid into solid-type texture using additives. The resulting specimens can be e.g., jelly-like quasi-solids or glassy polymer specimens.[22]

Eksperiandova *et al.*[32] used ground gelatine and agar to obtain quasi-solid specimens to determine analytes from wastewater. The authors also combined extractive enrichment to producing gel-like specimens, organogels and polymer films. Also, preconcentration by crystallization was used resulting in glassy saccharose-based specimens. Pretreatment by adding gel-forming substances was found to be applicable for wastewater analysis, but the crystallization with saccharose was partial and resulted in poor recoveries.

Zhang *et al*.[33] mixed agaron gel with mineral samples that had been decomposed with aqua regia. After heating to boiling, the mixture formed a quasi-solid gel when cooling to normal temperature. The specimens were measured with WDXRF, and good correlation to certified values was obtained. Detection limits for Pb, Zn and Fe were at 0.1% range.

## 6.2 Preconcentration techniques

### 6.2.1 Physical preconcentration via drying

Physical preconcentration methods of liquid samples involve drying the sample, in other words, evaporating the solvent. Removing the solvent reduces liquid matrix effects and concentrates the analytes, and therefore improves sensitivity and detection limits. In many cases, the dried specimen can be handled as "thin layer" samples, and there is no need for correction of absorption and enhancement effects. Drying as preconcentration is unsuitable for samples that form crystals during drying, and evaporating the solvent might be time consuming. [22,31]

The liquid sample can be pipetted and dried directly on the liquid cup foil, as was done by Gonzalez-Fernandez *et al*.[34]. Infrared lamp was used to dry a 1-6 mL aqueous mining sample on the Prolene x-ray foil that was analysed with WDXRF instrument. The authors used integrated peak area to calculate the result, instead of the commonly used net peak intensity, to improve the limits of detection. Total of 29 elements from Na to Bi were analysed with LODs at mg $L^{-1}$ level, but for lighter elements the results were not correlating to ICP-OES results that well.

Special filter papers are also available for the XRF analysis of water with drying preconcentration. The use of Rigaku's UltraCarry droplet filter paper (see Figure 15) was introduced by Uemura and Moriyama[35]. The MicroCarry and UltraCarry filter papers can hold a bigger amount of liquid sample introduced in the sample area, which improves the limits of detection compared to similar applications. Background scattering and matrix effects are also reduced because the analytes are detected from a thin layer. Thirteen elements from Na to Sr were determined in mineral waters with a WDXRF instrument, with LODs on tens of ppb level and calibration curves showing good correlations.

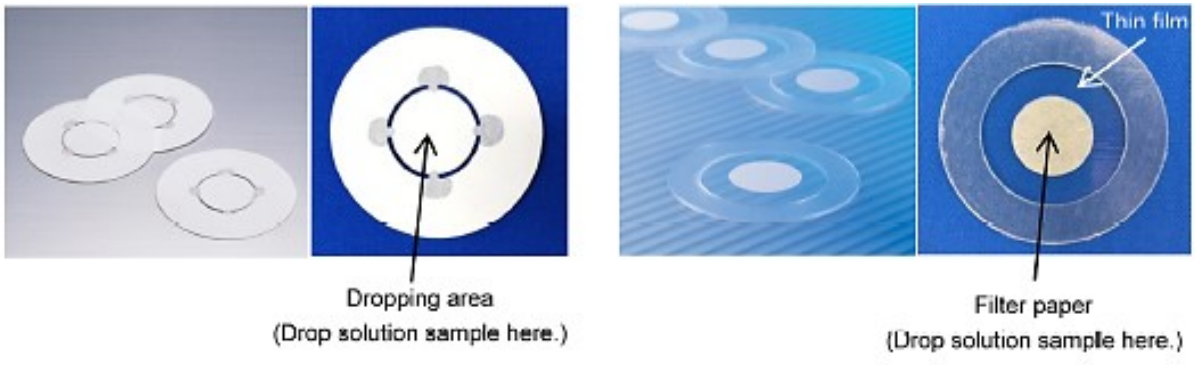


Figure 15 Rigaku's MicroCarry (left) and UltraCarry (right) filter papers.[21]



### 6.2.2 Precipitation and coprecipitation

Metals of interest can be separated from the surrounding aqueous matrix by adding a precipitating agent and collecting the resulting precipitates for XRF analysis. The precipitates can be collected by a filtration procedure, or by liquid-liquid extraction, which can both result in a thin solid sample well suitable for XRF analysis.[31] Although precipitation is widely used and suitable for many different materials, it requires a lot of work and includes a risk of loss of analytes.[22,31] Precipitation agents can be selective towards specific elements, which leads to selective preconcentration of those elements.

Rathod *et al*.[36] used ammonium pyrrolidinedithiocarbamate as a chelating agent for several analytes in sea water and methyl isobutyl ketone to extract the chelates from aqueous solution. The dried samples were measured with EDXRF instrumentation with ppb level LODs and good comparability to ICP-OES results.

### 6.2.3 Extraction procedures

Whereas liquid-liquid extraction is not commonly used in XRF spectrometry, liquid-solid extraction or solid phase extraction (SPE) has many advances as a preconcentration for XRF.[31] In SPE the analytes are transferred from liquid phase to the solid phase. Since the solid phase can be directly measured with XRF, there is no need for elution step after the extraction. SPE preconcentration resulting in a thin-layered sample also reduces the background and matrix effects.[22,31] Solid phase extraction can be performed as a simple filtration procedure when using ion-collecting filters or other functionalised membranes or disks. The possibility to use large

sample volumes results in large preconcentration factors.[31] Highly selective separation or preconcentration is possible with this preconcentration strategy.

Inui *et al.*[37] used ion-exchange resin disks to separate and measure Cr(III) and Cr(IV) in water. The authors examined multiple parameters of the procedure, including the effect of resin disk thickness, pH, and matrix effects. Calibration with good linearity and sub-ppb level LODs were obtained for 1 L water sample, also no severe matrix effects from freshwater major ions were detected.

Preconcentration of Cu, Ni, Zn, Pb and Cd with a commercial SPE-disk functionalised with iminodiacetate groups was examined by Marguí *et al*.[38] The authors used vacuum filter assembly to extract 1 L of aqueous sample and found out that the metals were homogenously loaded on one side of the disk. The capabilities of three different EDXRF systems were compared, and for all metals, there was a linear correlation between initial concentration and loading of the disk. LODs at μg $L^{-1}$ level were obtained and the method was successfully tested with different environmental aqueous samples.

Carbon nanotubes (CNT) have also been used as solid phase extraction material. Zawisza *et al.*[39] reported the use and optimising of the extraction process whereas Marguí *et al.*[40] compared different XRF systems for measuring the resulting samples. CNTs have large surface area, which results in high loading capacity of metals. The authors mixed CNTs with aqueous solution of 10 analytes and collected the loaded CNTs by filtration. The filters loaded with CNTs were dried and analysed with WDXRF spectrometer. The results showed good recoveries for spiked samples as well as detection limits at ng $mL^{-1}$ level for Cr, Mn, Fe, Co, Ni, Cu, Zn and Pb.[39] Marguí *et al.* used the same preparation procedure and found out that elements are loaded homogeneously on the filter paper. Low detection limits were achieved with EDXRF, WDXRF and polarised-EDXRF instruments, and the preconcentration of the analytes was quantitative also from solutions containing high concentrations of alkali metals.[40]

# 7 Validation and quality assurance of an analytical measurement method

The results of chemical measurement methods are often used as a basis for decision making, and therefore, the results need to be reliable and comparable. Reliable results can be obtained, when the methods are suitable for the analysis and the uncertainty of the method is known.[41] The comparability of analytical results is built from proficiency, traceability, accuracy and known uncertainty. Method validation, laboratory quality control, use of certified reference materials and participation in proficiency tests are the crucial tools for assessing the quality and comparability of the results. [42]

## 7.1 Method validation

Validation is a crucial part of the development of a new analytical measurement method. Validation is a process of testing method suitability and performance towards the defined analytical requirements.[41] Validation typically includes the evaluation of selectivity, sensitivity, limits of determination and quantitation, linear range, trueness, precision, ruggedness and uncertainty, but also other parameter can be included in the process.[41,43]

If the method is planned to be published, interlaboratory comparisons are suggested to be included in validation. Methods that are developed or modified for the laboratory's own use can be validated without comparison to other laboratories. Analytical requirements define the parameters that need to be tested, and careful planning allows to save time and costs, which may together with technical possibilities limit the extent of validation. Validation process is carefully documented and reported.[41]

Selectivity describes the ability of the method to determine the analyte from other components that may give interference to the measurement. Interference can increase or decrease the analyte intensity, and the effect may be concentration dependent or fixed. Interference can be tested by measuring reference materials and samples with suspected interference constituents and by comparing results to another method.[41] Sensitivity describes how much the measured signal changes by a change in analyte concentration. Sensitivity is therefore the gradient of the calibration curve.[41]

Limits of determination (LOD) and quantitation (LOQ) need to be defined if low concentrations are measured. Definitions and equations for setting the limits are not well-established, but the aim is to define concentrations that are distinguished from the background variation (LOD) or measured quantitatively (LOQ) with sufficient statistical confidence.[41,44b)]

Typically, LOD is defined by considering three times the standard deviation of the background signal, and LOQ by ten times the variation. The background variation is determined typically by measuring 10 replicates of blank sample. Use of reagent blank gives the instrument related LOD, whereas measuring blank sample that goes through the whole method procedure gives the LOD describing the whole method. Possible sample dilution factor is considered when calculating the final limit values.[41]

Working range is the concentration interval that can be measured with acceptable uncertainty. Inside linear range, the analyte concentration and measured signal are linearly dependent. Optimal working range is usually from the limit of quantitation to the upper end of linear range.[41]

The determination of bias (systematic difference between detected and expected values) gives the trueness of the analytical results and is also the measure of systematic error. Trueness can be evaluated by measuring certified reference materials, comparing the results to another method or instrument and by determining the recovery of spiked samples. Statistical significance tests are a useful tool for comparing the results.[41]

Precision describes the random error of the measurement, and it is commonly expressed as standard deviation or relative standard deviation. Precision is evaluated by measuring replicates of the same sample under constant and specified conditions. Precision is usually concentration dependent, and the tests should be carried out across the working range. Measurements by the same analyst with same instrument give repeatability, but the tests can also be expanded to within-laboratory and inter-laboratory reproducibility.[41]

Ruggedness, or also called robustness, describes the stability and performance of the method under small changes in the method parameters. Ruggedness tests give the information of how much changes the method tolerates and which parameters should be controlled carefully.[41]

### 7.1.1 Method uncertainty

Uncertainty gives an estimation of the error related to the method. Overall error consists of systematic and random error. Systematic error can arise from the measurement method itself (method bias) or from other laboratory procedures related to the method (laboratory bias). Random error includes day-to-day variation in one lab and repeatability between different laboratories.[45] Figure 16 illustrates the formation of overall uncertainty.

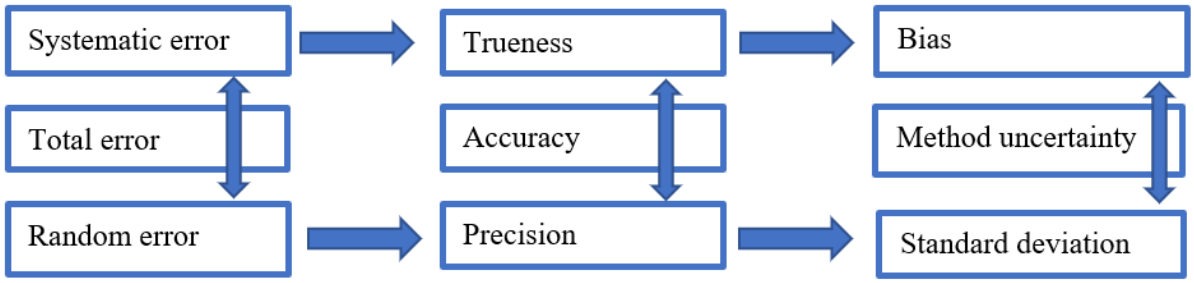


Figure 16 Formation of method uncertainty (according to Hägg[43]).

The process of uncertainty estimation starts with specifying the material and analyte that are analysed. Possible sample pretreatment procedures need to be named, and the decision of including or excluding sampling in the estimation is done beforehand. After setting the scope of the estimation, relevant uncertainty sources are identified. These can include for example sampling and sample storage, reagent purity, instrumental effects and measurement conditions, computational effects and operator errors.[46]

Uncertainty sources are quantified and expressed as standard deviation. Measurement data from validation process, quality control measurements and proficiency testing can usually be utilised, and in addition, specific tests, supplier information and analyst judgement can be used. The aim is to estimate the overall bias and precision related to the method.[45,46] Combined uncertainty is calculated by Equation (4) as

$$u_c = \sqrt{u(R_w)^2 + \left(u(bias)\right)^2} \quad (4)$$

where $u(R_w)$ represents the laboratory reproducibility and $u(bias)$ the method and laboratory bias.[45] Expanded uncertainty is obtained by multiplying $u_c$ with a coefficient representing the confidence level, usually 2 for approximately 95% confidence level. Special software packages,

like MUkit software by Finnish Environment institute SYKE are available for uncertainty calculations.[45]

Method uncertainty can be expressed as relative or absolute value. Typically, some parts of the overall error are proportional to analyte concentration, and others have a fixed effect. In some cases, it is useful to express uncertainty as absolute value for low concentration range, where absolute uncertainty is constant, and as relative value for higher concentration range, where relative uncertainty becomes constant.[45]

## 7.2 Quality control

With quality control, the laboratory makes critical assessment of the methods and laboratory routines to prove and maintain the reliability of the results. Measurement of quality control samples and utilising quality control charts are the main tools for checking that the method is under control. Quality control sample can be a certified reference material, internal standard sample or a stable and well-known routine sample.[47]

X-chart is the simplest quality control chart, which follows the variation of the results for the quality control sample. The chart includes a horizontal middle line that represents the right or expected value of the analyte, and warning and action limits, that are typically set to ±2*s* and ±3*s*, respectively, *s* being the standard deviation (see Figure *17*). If the results are normally distributed, statistically over 95% of the results should fall inside warning limits and over 99% inside action limits.[47] Actions are needed, if single points fall outside action limits, or trends occur.

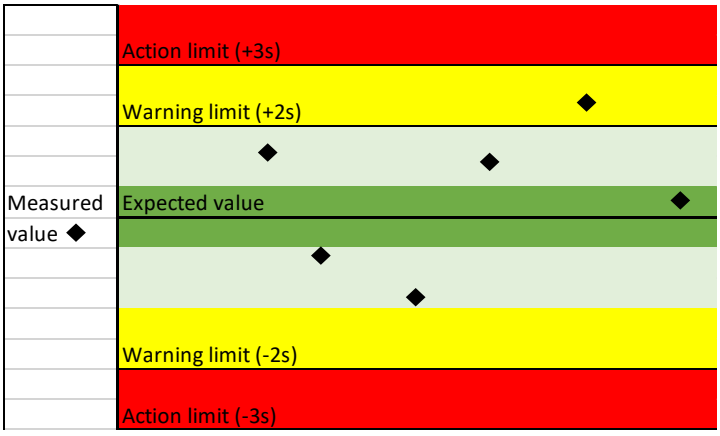


Figure 17 Illustration of X-chart.

Another common quality control chart is the Shewhart chart, which follows the process average of quality control sample results. Middle line is set to the target value $\mu_0$ and warning and action limits to $\mu_0 \pm 2\sigma/\sqrt{n}$ and $\mu_0 \pm 3\sigma/\sqrt{n}$, respectively, $\sigma$ being standard deviation and $n$ the number of results. The criteria for suspecting the method is out of control are: one point outside action limits, two successive points outside warning limits, or eight successive points on the same side of target value.[44a)]

CUSUM chart follows the cumulative sum of the difference between process average and target value. CUSUM chart is interpreted with a v-mask, and if the points fall inside the mask, the method is under control. The advantage of CUSUM chart is that it shows increasing or decreasing trends in results faster that Shewhart chart.[44a)]

EXPERIMENTAL PART

# 8 Background and aim of the work

The aim of the experimental part of this Thesis project was to develop a method for measuring aqueous samples from biorefining processes with WDXRF instrument. The method would be used for internal monitoring of different aqueous process samples from biofuel production, and the main feature of this method was to detect changes in the process, so that the operators can use the information to make required changes to operating parameters. The XRF instrument was already used to measure the oil phase samples from the processes on-site, but the aqueous samples were currently sent to another laboratory for ICP-OES analysis. XRF was expected to provide a fast and easy-to-use measurement method to screen the process in-time, whereas ICP-OES results were available only days after sampling.

First, a modified version of the preinstalled Petro-Quant application was tested for comparison. An empirical XRF method was then developed based on $H_2O$ matrix calibration for Na, Mg, Si, P, S, Cl, K, Ca, Mn and Fe. The development and evaluation of the method continued with the testing of method performance and fitness for purpose. Parameters included in method validation were planned to be tested, although complete validation procedure was not in the scope of this work. The tests covered the measurements for method accuracy, precision, and ruggedness, as well as tests for defining the linear range and limits of determination and quantitation. The results from XRF measurements were compared to ICP-OES results.

At last, the experimental part of this work covered the testing for sample pretreatment procedures. As the method was expected to be fast and simple, the tests focused on optimising the liquid phase analysis of the samples without preconcentration procedures, unlike suggested in the literature. The requirements for sensitivity, limits of determination and accuracy at low concentrations (ppm level) were less crucial features. The sample pretreatment tests covered separations by settling, centrifugation and filtration, and focus was set to dissolved analytes. Two typical sample types were tested, but the same method will be later extended to other sample types making the range for this method significantly wider.

Liquid phase measurements of aqueous samples were expected to have several challenges, as was described in the literature part of this work. The measured elements were relatively light (from Na to Fe), which lead to low fluorescence intensities. Also, the expected concentrations were at trace level (<1000 ppm, or typically even <100 ppm), although higher limits of

quantitation compared to ICP-OES were considered acceptable. The aqueous matrix was known to give high scattering background, and both the matrix and the sample support foil were absorbing the fluorescent radiation. On the other hand, low analyte concentrations were not expected to have complex inter-elemental interferences. Previous tests with the instrument had shown that despite the low intensities of analytical peaks, the instrument was able to determine analyte concentrations at surprisingly low concentrations.

# 9 Instrumentation, reagents and samples

## 9.1 Instrumentation

All XRF measurements were performed with an S8 Tiger 1 kW WDXRF instrument by Bruker AXS GmbH, located in the UPM North European Research Centre. The instrument had an application package called Petro-Quant installed by Bruker, and the empirical method was built up with the SPECTRAplus software's Application Setup tool. Measurement parameters related to the used measurement methods are described in the following chapters.

ICP-OES measurements were performed with iCAP7600 Duo instrument from Thermo Fisher Scientific Inc. The measurements had the following parameters: plasma power 1150 W, nebuliser gas flow 0.6 L $min^{-1}$, cooling gas flow 12 L $min^{-1}$ and auxiliary gas flow 0.5 L $min^{-1}$. The used analytical lines and their instrumental quantitation limits are shown in Table 1. The quantitation limit was defined as 10 times the standard deviation of blank samples. For ICP-OES, calibration was performed separately for each run.

Table 1. Analytical line parameters for the ICP-OES measurements

| Line (nm) | Plasma orientation | Limit of quantitation (ppm) |
|---|---|---|
| Mn 257.610 | Axial | 0.001 |
| Ca 315.887 | Axial | 0.07 |
| Fe 259.940 | Axial | 0.02 |
| K 766.490 | Radial | 0.09 |
| Mg 285.213 | Axial | 0.01 |
| Na 589.592 | Radial | 0.1 |
| P 213.618 | Axial | 0.02 |
| S 180.731 | Axial | 0.02 |
| Si 251.611 | Axial | 0.02 |

Ion chromatography (IC) measurements for chloride were performed with DIONEX ICS-2100 RFIC instrument by Thermo Fisher Scientific Inc. Samples were filtrated through IonPack NG1 guard column to remove organic matter. The instrument used IonPack AG11-HC guard column and IonPack AS11-HC 4 x 250 mm separating column. The flow rate of KOH eluent was 1.00 mL per minute, and the run used concentration gradient from 1 mM to 60 mM. Limit of quantitation was typically 0.3 ppm, and the samples were diluted if interferences were present.

The pH values of the samples were measured with regular pH meters (several instruments) that are calibrated regularly and checked daily. Total organic carbon (TOC) was determined with TOC-$L_{CSH}$ instrument by Shimadzu Corporation. TOC was determined by indirect method, where total carbon and inorganic carbon were first determined, and organic carbon was calculated by subtracting inorganic carbon from total carbon. Suspended solids were determined gravimetrically by filtrating the sample on a Whatman GF/A 1.6 µm glass fibre filter.

9.2 Materials and reagents

Standard solution for Na, Mg, K and Cl was made from analysis grade purity NaCl, $Mg(NO_3)_2$ and $KNO_3$ salts by weighing exact amounts of salts to a volumetric flask and filling to mark with ultrapure (UP) water. For other elements, aqueous standard solutions designed for ICP-OES were used (Merck TraceCERT and VWR, acid matrix of 1-3% $HNO_3$). All used ultrapure

water was from ELGA Purelab Prima instruments and had the resistivity of 18.2 MΩ. The list of used reagents is presented in Table 2.

Table 2. Reagents used in the experimental work

| Reagent | Manufacturer | Concentration |
|---|---|---|
| Supelco EMSURE NaCl | Merck | ≥ 99.5% |
| Supelco EMSURE $Mg(NO_3)_2$ | Merck | ≥ 99% |
| Supelco EMSURE $KNO_3$ | Merck | ≥ 99% |
| Na standard for ICP | VWR | 1000 mg $L^{-1}$ |
| TraceCERT Mg standard for ICP | Sigma Aldrich | 1000 mg $L^{-1}$ |
| TraceCERT Si standard for ICP | Sigma Aldrich | 1000 mg $L^{-1}$ |
| TraceCERT P standard for ICP | Sigma Aldrich | 1000 mg $L^{-1}$ |
| TraceCERT P standard for ICP | Sigma Aldrich | 10,000 mg $L^{-1}$ |
| S standard for ICP | VWR | 1000 mg $L^{-1}$ |
| TraceCERT S standard for ICP | Sigma Aldrich | 10,000 mg $L^{-1}$ |
| Ca standard for ICP | VWR | 1000 mg $L^{-1}$ |
| TraceCERT Mn standard for ICP | Sigma Aldrich | 1000 mg $L^{-1}$ |
| TraceCERT Fe standard for ICP | Sigma Aldrich | 1000 mg $L^{-1}$ |
| Nitric acid | Merck | concentrated (65%) |
| Triton X-100 | Alfa Aesar | - |

## 9.3 Samples and sample handling

First test samples for this work were collected from the oil pretreatment process during November and December 2021. Samples were stored in cold right after sampling. The chemical composition of the samples was expected to remain unchanged, but there were some changes in the physical properties (layering or separation of the phases). More samples were collected from the same process during February and March 2022, when samples were handled right after collection, and different pretreatment procedures were tested.

Samples could be categorised in two groups based on the sample texture: thick, brown emulsions or samples with clear aqueous phase (see Figure 18). This difference in the sample types was a result of different operation conditions in the process. In general, the samples might

also have some solids and, in some cases, an organic phase that separates during storage. Before starting the test measurements with the stored samples, the aqueous phase was separated from the original samples by decanting or in a separating funnel and then filtered with coarse black ribbon filter paper (Grade 589/1, 12-25 µm). Sample handling of the fresh samples is described in chapter 14.

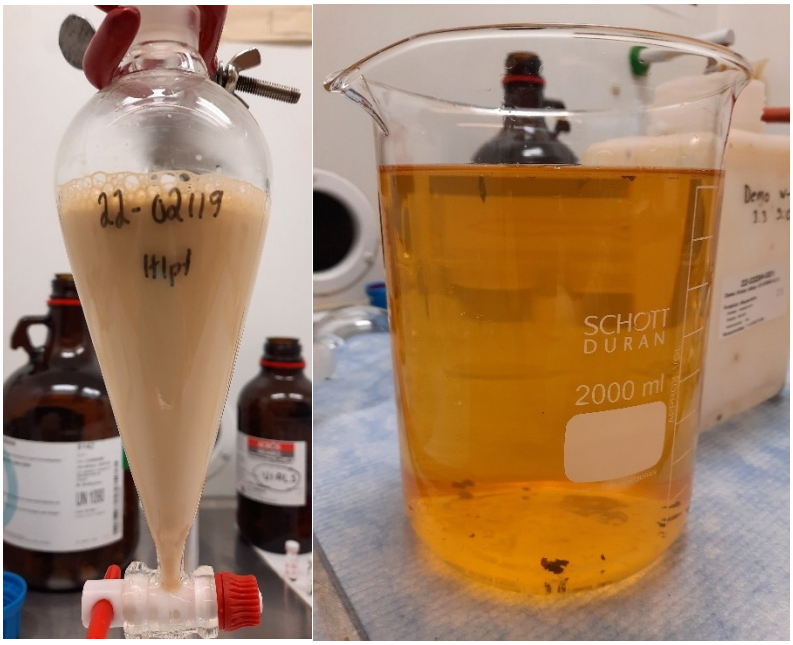


Figure 18 Emulsion-type (left) and clear-type (right) wastewater samples.

The original samples had also been analysed at the Research Center laboratory and therefore, some results describing the sample properties were readily available. The samples were typically acidic, and pH varied between 1.2-2.5. Oil content was estimated by weighing the separated phases, and it varied between samples. In addition, suspended solids, total nitrogen, chemical oxygen demand and total organic carbon (TOC) were determined.

The ICP-OES results were used as background information for planning the calibration ranges for the experimental XRF method. For ICP-OES measurements, the aqueous process samples were routinely pretreated as follows: if the sample clearly had an oil phase, this phase was separated in a separating funnel. The samples were filtrated with coarse black ribbon paper (Macherey-Nagel MN 640 w, 8-10 µm) before the ICP analysis, and again with 0.45 µm polyethylene terephthalate (PET) syringe filter if there were solid particles. All ICP measurements were performed in 5% $HNO_3$ matrix.

The samples were registered in a laboratory information management system (LIMS), where sample information and results were managed. The number codes used for sample identification originate from this system.

# 10 Preliminary preparations

## 10.1 Foil tests

The sample cup foils need to be tested for every new sample type to check the foil compatibility. If the foil would break during the measurement, spillage of sample could make severe damage to the x-ray tube. The prepared cup foils shouldn't have any wrinkles when they are taken into use. Foil tests were performed by adding tested solution to a prepared sample cup, which was then placed on paper that would show possible leakage for a few hours.

Prolene 4 µm foils were tested for three different specimens: 10% v/v nitric acid in water, sample 22-00430 and sample 22-00434. Two replicate tests were performed for each specimen. Approximately 7 g of sample was transferred to cups with a Pasteur pipette and the lid was closed. Samples were checked for immediate leakage or spillage and left to stay on fume hood table. The cups were checked after one, two and three hours, and no wrinkles, sagging or leakage was observed (see Figure 19).

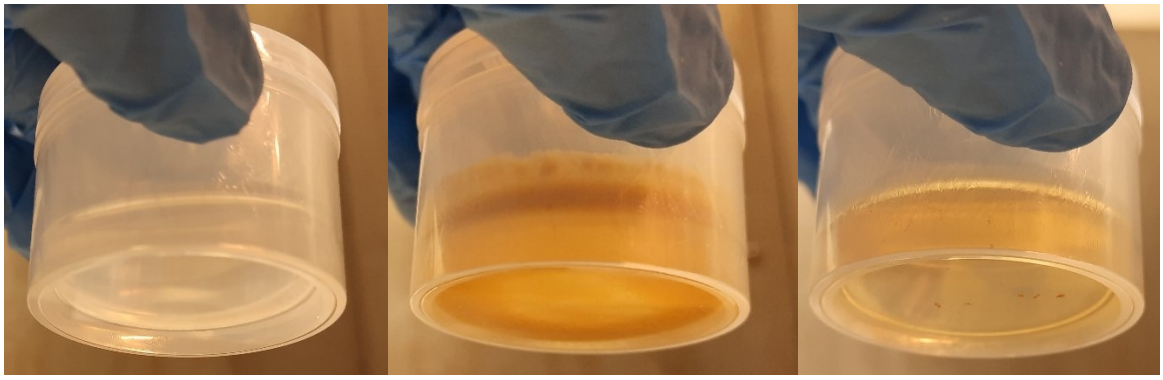

Figure 19. Samples after three hours foil tests. Left: 10 v-% $HNO_3$, middle: 22-00430, right: 22-00434.

## 10.2 Scan measurements

With the Bruker's SPECTRAplus software, it is possible to manually scan the analytical lines defined in the measurement method. A 2θ angle range near the analytical line is measured in the scan mode, and the resulting spectra is displayed as kilo-counts per second vs. 2θ angle. This function can be used to examine peak positions and possible interferences at background correction points. The spectrum also visualises the peak shape and height as well as the noise in the background.

Analytical line scans were done for aqueous standard mixtures to predict what level of intensities different concentrations would give for a few analytical lines. Solutions for Na, Ca, Si and Fe were prepared at concentration range 1000 – 10 ppm. For sodium, the signal for 100 ppm solution was barely visible from the background and the peak for 250 ppm was small (see Figure 20), whereas 10 ppm still gave a clear peak for iron (see Figure 21). For silicon and calcium, 50 ppm signal could somehow be distinguished from the background. The background level was relatively high for some lines, and the signal was noisy. The results from the scans indicated that measuring low concentrations (less than 100 ppm) of light elements in aqueous matrix will, as expected, be challenging due to low peak intensity, and longer reading times may need to be used to overcome noise.

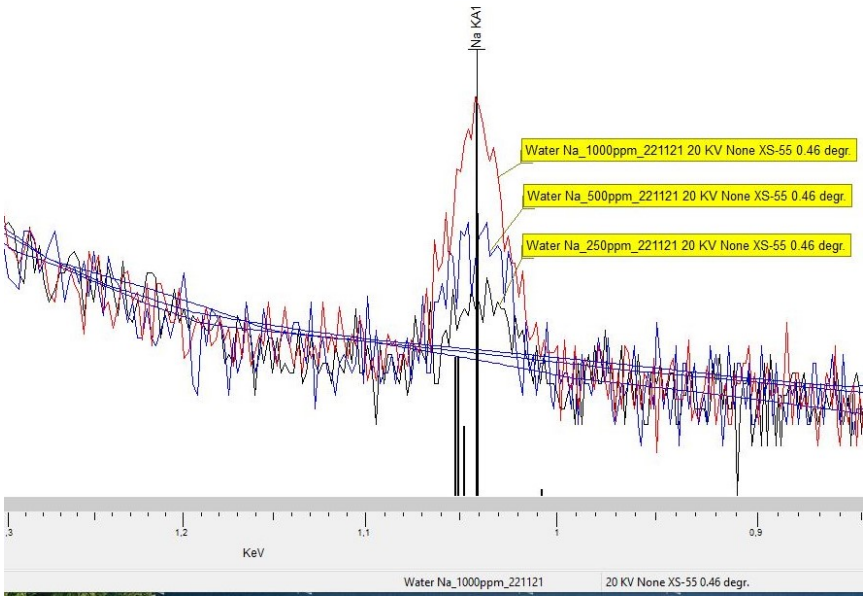


Figure 20 Scan spectrum for Na Kα1 line: 1000 ppm (red), 500 ppm (blue) and 250 ppm (black).

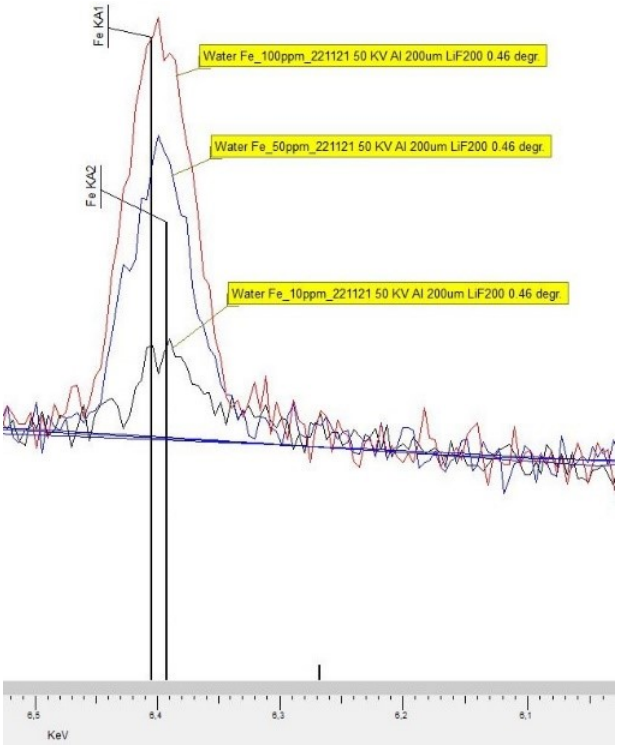


Figure 21 Scan spectrum for Fe Kα1 line: 100 ppm (red), 50 ppm (blue), 10 ppm (black).

During the scan measurements it was also noticed that some bubbles are formed at the bottom of the measurement cup (see Figure 22). The room temperature sample heated up during the measurement, which reduced the amount of gas being dissolved in water and caused the formation of bubbles. Due to strong surface tension, the bubbles did not escape from the bottom of the cup. Heating the sample to 40 °C prior the measurement did not significantly affect the bubble formation. The effect of bubbles in the actual measurement as well as possible ways to prevent bubble formation were to be further studied.

Figure 22 Bubbles at the bottom of the measurement cup.

Pure water was also scanned for possible contaminations. Ultrapure water from one water machine was found to show signal for Si and therefore water for preparing standards was taken from the other machine that gave no visible signal for Si. Also, a small signal for Fe could be seen in all measurements. Prolene foils have some typical trace impurities (Ca, P, Sb, Fe, Zn, Cu, Zr, Ti, Al at ppm level), and the signal for Fe was most probably resulting from foil contaminant. For other elements, no clear peaks were detected.

### 10.3 Determination of chlorine in aqueous samples

Before the start of this project, a method for determining chlorine in aqueous samples had been developed for the XRF instrument. The development work of the method was still ongoing, but some experiences from the previous work gave ideas and guidance to plan this project. The chlorine method was calibrated for 0-200 ppm range with UP-water based standards, and it was routinely used to determine overall chlorine in some aqueous process samples in addition to chloride determination with IC. The lowest limit of detection (LLD) calculated by the software was 4 ppm, and the quantitation limit was thought to be around 10-20 ppm. During this work and for comparison, some samples were also measured with the existing chlorine method.

## 11 Method based on Petro-Quant application

The instrument manufacturer, Bruker, offers an application called Petro-Quant for measuring petrochemistry samples. The method uses library calibration and is optimised for petrochemical measurement of the samples. The Petro-Quant Oil method was routinely used for measuring oil phase samples at the UPM Research Center. In this work, the Petro-Quant based method was modified for aqueous samples and could be used for comparison to the empirical method.

## 11.1 Changes to method and application parameters

A few important changes were made to the Petro-Quant application to create the method "PETRO-QUANT2 Oil-short_aqueous" for measuring aqueous samples. Compared to the original Petro-Quant application, the number of measured elements was reduced to ten (Na, Mg, Si, P, S, Cl, K, Ca, Mn, Fe) and the measurement order was changed from customised order to measuring from the lightest elements to the heaviest. Also, the sample matrix chemical composition was changed from hydrocarbons ($CH_2$) to $H_2O$. Sample cup material was 4 µm Prolene foil and the sample size was maintained the same as for the original method (7 g). The measurement time for Na and Mg was increased to 100s and the preferred LLD limit to 10 ppm. The total measurement time for this new method was approximately 10 minutes. The line parameters are listed in Appendix 1. Calibration information of the method was not available for end-users.

## 11.2 Test measurements with standard solutions

The method was tested with a few different standard test solutions that were prepared from ICP-OES standards and with salt solutions prepared for this purpose. Each solution was measured three times, and the average $\bar{x}$ and standard deviation $s$ of these measurements were calculated in Excel, in addition to the recovery percentage compared to the expected concentration, which was calculated by Equation (5) as

$$\text{Recovery\%} = \frac{\bar{x}}{\mu} * 100\% \quad (5)$$

where $\bar{x}$ is the measured average concentration and $\mu$ is the expected concentration. The results for test solutions 2 and 4 are shown in Table 3 and measurement data is collected in Appendix 2.

Table 3 Results of the tests measurements with Petro-Quant based method

| | Test solution 2 | | | Test solution 4 | | |
|---|---|---|---|---|---|---|
| | Nominal conc. (ppm) | XRF result (ppm), $\bar{x} \pm s$ | XRF, recovery (%) | Nominal conc. (ppm) | XRF result (ppm) $\bar{x} \pm s$ | XRF, recovery (%) |
| Na | 100 | 76 ± 10 | 76.2 | 20 | 15 ± 7 | 76.0 |
| Mg | 100 | 93 ± 9 | 93.0 | 20 | 26 ± 3 | 130.2 |
| Si | 50 | 44.5 ± 0.8 | 89.0 | 10 | 10 ± 9 | 103.0 |
| P | 50 | 38 ± 2 | 76.6 | 10 | 7 ± 1 | 74.0 |
| S | 50 | 30 ± 2 | 59.9 | 10 | 5 ± 2 | 52.7 |
| Cl | 154 | 66 ± 6 | 42.9 | 30,8 | 0 | 0 |
| K | 100 | 69 ± 3 | 69.3 | 20 | 10 ± 2 | 50.8 |
| Ca | 50 | 35 ± 3 | 69.2 | 10 | 5 ± 2 | 48.7 |
| Mn | 20 | 15.8 ± 1.0 | 78.8 | 4 | 2.8 ± 0.2 | 70.0 |
| Fe | 20 | 11.9 ± 0.2 | 59.7 | 4 | 0 | 0 |

n = 3

The results for standard solutions showed low recoveries even with higher concentrations of test solution 2. For test solution 4, chlorine and iron were no longer detected, and the recoveries were low for all other elements except for Mg and Si. The Petro-Quant method was calibrated with mineral oil based standards, and it was optimised for oil samples. Therefore, measuring in heavier water matrix might have been one reason for low recoveries, although the matrix component was changed for result calculations. Also, the defined blank of the method was paraffin oil, not water. The other probable reason was the formation of bubbles, which led to incomplete cup bottom filling during the measurement. Keeping in mind that the method was built for completely different sample type, the results were after all on the right concentration range.

Since the empirical method was giving promising results for calibration and test measurements, it was decided that the Petro-Quant based method wouldn't be further developed at this point, and this project would focus on developing and testing an empirical method. Petro-Quant based method could be suitable for qualitative or semi-quantitative measurements, but most probably couldn't fulfil the requirements for the intended use.

# 12 Method based on empirical calibration

In addition to modifying and testing the Petro-Quant application, an empirical method based on new calibration standards was created and named “Wastewaters”. The method was built up using the SPECTRAplus software’s[48] Application Setup tool, where all the method settings were open for changes and which automatically created suggestions based on the information of standards used. The tool included the following steps: defining the new standard materials (i.e., the calibration standards) and the preparation of the specimens, setting the measurement method parameters, measuring the standard materials, constructing and computing the calibration curves, setting the correction terms and defining the result calculations and output.

## 12.1 Standard materials and specimen preparation

Calibration standards were prepared from aqueous ICP-OES standard solutions and salt solutions made with analysis grade salts. A mixed stock solution of NaCl, $Mg(NO_3)_2$ and $KNO_3$ salts was prepared so that the concentration of Na, Mg and K was 5000 mg $L^{-1}$ and concentrated $HNO_3$ was added to the solution so that the final $HNO_3$ concentration was 1 v-%. For other elements, 1000 mg $L^{-1}$ ICP-OES standards were used. The standards having over 200 ppm concentrations of P and S were prepared later when 10,000 mg $L^{-1}$ stock solutions were available. The concentrations of the prepared standards (as ppm) are listed in Table 4. Automatic pipette of 1-5 mL and 50 mL volumetric flasks were used for the preparation of multielement solutions.

Table 4 Concentrations (ppm) of the standard calibration solutions

| | Na | Cl | Mg | K | P | Si | S | Ca | Fe | Mn |
|---|---|---|---|---|---|---|---|---|---|---|
| Blank | 0 | 0 | 0 | 0 | 0 | 0 | 0 | 0 | 0 | 0 |
| STD1 | 20 | 31 | 20 | 20 | 20 | 20 | 40 | 10 | 10 | 10 |
| STD2 | 40 | 62 | 40 | 40 | 50 | 50 | 80 | 20 | 20 | 20 |
| STD3 | 80 | 123 | 80 | 80 | 80 | 80 | 120 | 30 | 30 | 30 |
| STD4 | 100 | 154 | 100 | 100 | 100 | 100 | 200 | 50 | 50 | 50 |
| STD5 | 150 | 231 | 150 | 150 | 120 | 120 | 0 | 80 | 80 | 80 |
| STD6 | 200 | 308 | 200 | 200 | 150 | 150 | 0 | 100 | 100 | 100 |
| STD7 | 300 | 462 | 300 | 300 | 200 | 200 | 0 | 120 | 120 | 120 |
| STD8 | 500 | 771 | 500 | 500 | 0 | 0 | 0 | 200 | 200 | 200 |
| STD9 | 800 | 1234 | 800 | 800 | 0 | 0 | 0 | 0 | 0 | 0 |
| STD10 | 1000 | 1542 | 1000 | 1000 | 0 | 0 | 0 | 0 | 0 | 0 |
| STD11 | 0 | 0 | 0 | 0 | 300 | 0 | 400 | 0 | 0 | 0 |
| STD12 | 0 | 0 | 0 | 0 | 500 | 0 | 800 | 0 | 0 | 0 |
| STD13 | 0 | 0 | 0 | 0 | 0 | 0 | 1200 | 0 | 0 | 0 |
| STD14 | 0 | 0 | 0 | 0 | 0 | 0 | 1500 | 0 | 0 | 0 |
| STD15 | 0 | 0 | 0 | 0 | 0 | 0 | 2000 | 0 | 0 | 0 |

The preparation setting for measured specimens was liquid, and no additive or contamination elements were listed in the software. All standards and samples were measured in liquid cups that had 4 µm Prolene foil. The amount of sample was set to 7 g, which was the same sample size that other frequently used methods have.

## 12.2 Measurement method parameters

The measurement method information and line parameters were defined in the MethodWizard part of the software. The software had a list of possible line settings for each element, having optimised properties for different concentration ranges (trace concentration, minor or major component). The lines were also categorised as high-sensitivity or high-resolution types depending on which property was desired. High-sensitivity lines had bigger collimator aperture, which lets more light through and increases both the analyte signal intensity and background

radiation coming to the detector. High-resolution lines had narrower collimator aperture, which gives a sharper analytical peak and lower background.

At first stage, multiple lines were selected for a few elements. Lines were compared by scan measurements, and the line giving enough sensitivity, sufficient resolution and smoother background was selected for each element. For Na, Mg, Si, P, Cl, K and Ca, high sensitivity lines optimised for trace concentrations were selected and for S, high-sensitivity line for minor concentrations. Sensitivity was preferred over resolution and background level for light elements (see Figure 23 for Mg). For Mn and Fe, high-resolution lines for trace concentrations seemed better than high-sensitivity lines, because of lower and simpler background, but still giving sufficient sensitivity (see Figure 24 for Fe).

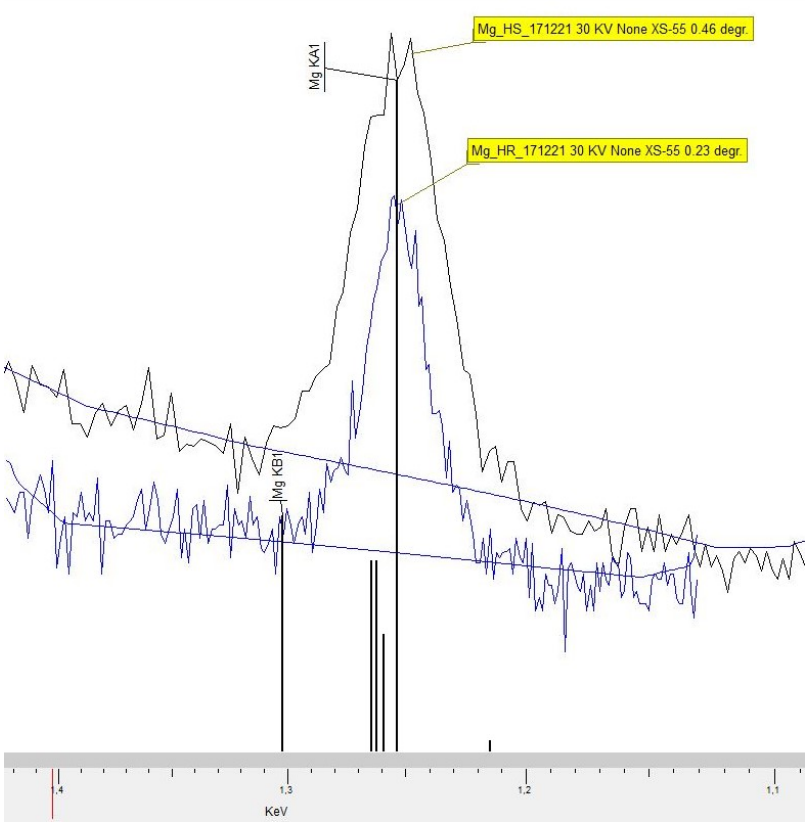


Figure 23 High-sensitivity (black) and high-resolution (blue) lines for Mg.

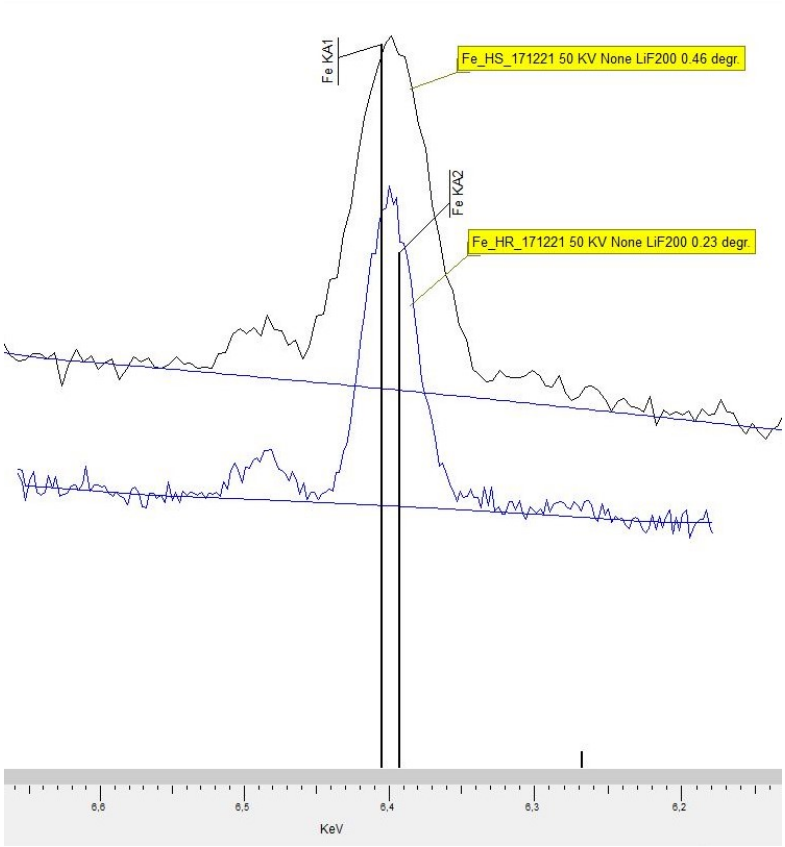


Figure 24 High-sensitivity (black) and high-resolution (blue) lines for Fe.

Scan measurements were also used to check if the peak position needed to be adjusted from the theoretical position, and to set 1-2 background measurement points for each line. The method used fixed position mode for both peak and background measurements, which allowed longer measurement times for each point and led to lower statistical error than scan mode measurement would. Measuring time optimization using statistical error limits (counting statistical error, CSE%) was not used for any line.

A longer measurement time of 100s was set for the lightest elements (Na, Mg, Si), whereas 30s was used for other lines. The total background measurement time was set equal to peak measurement time. Measurement order was defined to be from the lightest element to the heaviest ones. The total measurement time for this method was approximately 20 minutes. Main line parameters are listed in Table 5 and a more complete description of method parameters can be found in Appendix 3.

Table 5 Line parameters for Wastewaters method

| Analyte line | Tube current (mA) | Tube voltage (kV) | Crystal | Detector | Counting time peak/bkg |
|---|---|---|---|---|---|
| Na Kα1 | 33 | 30 | XS-55 | FC | 100s/100s |
| Mg Kα1 | 33 | 30 | XS-55 | FC | 100s/100s |
| Si Kα1 | 33 | 30 | PET | FC | 100s/100s |
| P Kα1 | 33 | 30 | PET | FC | 30s/30s |
| S Kα1 | 33 | 30 | PET | FC | 30s/30s |
| Cl Kα1 | 33 | 30 | PET | FC | 30s/30s |
| K Kα1 | 20 | 50 | LiF200 | FC | 30s/30s |
| Ca Kα1 | 20 | 50 | LiF200 | FC | 30s/30s |
| Mn Kα1 | 20 | 50 | LiF200 | SC | 30s/30s |
| Fe Kα1 | 20 | 50 | LiF200 | SC | 30s/30s |

FC = flow counter, SC = scintillation counter

## 12.3 Calibration parameters

After setting the method parameters and measuring the calibration standards, the calibration curves were computed by the software. The intensity of an analytical line was detected as kilo counts per second (kcps), and the software also calculated "XRF concentrations" for each standard, based on the other information in the calibration steps. The deviations between nominal and calculated concentrations indicated the quality of the calibration.

For each line, only the blank standard and the standard samples having that analyte were enabled for the calibration. Also, single standards were disabled from the calculation if they were clearly off the line. The calibrations were computed with net intensities, and the regressions were weighted by optimising the absolute error of the standards. This was done by minimising Equation (6) as

$$\sum_{i=1}^{n}\left(C_i^{chem} - C_i^{XRF}\right)^2 \quad (6)$$

where $C_i^{chem}$ refers to the nominal concentration of standard $i$ and $C_i^{XRF}$ to the computed concentration of the same standard.

The calibration software allows to easily test the effect of different correction terms. The use of absorption correction term didn't influence any of the lines, so this correction was not used. All analyte concentrations were low (ppm level) and therefore the absorption effects were negligible and did not need correction. The offset correction was used for Mg, Cl and Fe. This correction considers the offset term of the line equation and corrects the measured intensities with the offset value. Quadratic (second degree) term correction or peak overlay corrections were not used.

The software calculated a standard deviation value to indicate the quality of the regression. The standard deviation for the set of standard samples was estimated by Equation (7) as

$$\hat{\sigma}^2 = \frac{1}{n-1}\sum_{i=1}^{n}\left(C_i^{XRF} - C_i^{chem}\right)^2 \quad (7)$$

where again $C_i^{XRF}$ refers to the nominal concentration of standard $i$ and $C_i^{chem}$ to the computed concentration of the same standard.

The software also calculated a lower limit of detection (LLD) values for the analytical lines of each measured sample. LLD represented the smallest detectable concentration, and it was defined as the smallest net intensity that was above the signal fluctuation. LLD was calculated by Equation (8) as

$$LLD = \frac{3}{m}\sqrt{\frac{I_{Bkg}}{t}} \quad (8)$$

where $m$ is sensitivity (the slope of the calibration curve), $I_{Bkg}$ is the background intensity at the specific wavelength, and $t$ is the counting time for the background. LLD is specific for an element, and it also depends on the matrix and counting time.

For quantitative analysis, the definition of limit of detection (LOD) and limit of quantitation (LOQ) gives more practical use than the LLD value calculated by the software. Limit of detection is also defined as the concentration that gives a signal that is significantly different from the background. LOD is typically defined as blank sample intensity plus three times the standard deviation of the blank intensity.[44b)] When this value is placed in the equation of the calibration curve, and the blank intensity is approximated to be the same as the offset term of the equation, LOD can be calculated by Equation (9) as

$$LOD = \frac{3 \cdot s_b}{m} \tag{9}$$

where $s_b$ is the standard deviation of blank intensity and $m$ is the slope of the calibration curve.

For the Wastewaters method, $s_b$ was defined by measuring 10 replicates of ultrapure water as a blank sample. In addition to LOD, a limit of quantitation (LOQ) is commonly defined as the lowest concentration that can be measured with acceptable analytical accuracy and precision. LOQ is typically calculated similarly as LOD but by taking ten times the standard deviation of the blank signal.[44b)] The calculated limits of determination and quantitation for all elements are listed in Table 6, along with other calibration parameters.

Table 6 Calibration parameters for Wastewaters method

| Line | Calibration range (ppm) | Correlation coefficient $R^2$ | Standard deviation (ppm) | LLD (avg., ppm) | LOD (ppm) | LOQ (ppm) |
|---|---|---|---|---|---|---|
| Na Kα1 | 0-1000 | 0.9996 | 9 | 5.7 | 7.4 | 24.6 |
| Mg Kα1 | 0-1000 | 0.9999 | 3 | 2.6 | 3.6 | 12.2 |
| Si Kα1 | 0-200 | 0.9988 | 4 | 1.3 | 2.1 | 7.0 |
| P Kα1 | 0-500 | 0.9992 | 5 | 1.7 | 3.3 | 11.1 |
| S Kα1 | 0-2000 | 0.9996 | 15 | 1.2 | 2.7 | 9.1 |
| Cl Kα1 | 0-1234 | 0.9999 | 4 | 4.3 | 6.4 | 21.2 |
| K Kα1 | 0-1000 | 0.9996 | 7 | 1.3 | 3.1 | 10.5 |
| Ca Kα1 | 0-200 | 0.9993 | 2 | 1.3 | 2.1 | 7.0 |
| Mn Kα1 | 0-200 | 0.9995 | 2 | 0.7 | 1.0 | 3.4 |
| Fe Kα1 | 0-100 | 0.9983 | 2 | 0.7 | 1.3 | 4.3 |

Correlation coefficients over 0.990 indicated that the calibration was linear over the working range, which was expected as XRF is known to be very linear up to high concentrations. The calibration range was set to be wide (up to 200 or 1000 ppm for most elements), so that many types of aqueous process samples could be measured with the Wastewaters method. In case the analyte concentrations in the samples are in much lower concentration range, the calibration range could be narrowed using re-calibration or developing the method to improve accuracy at low concentrations.

Limits of quantitation were mostly on an expected level (around 10 ppm), as Na was known to be challenging and many other analytes have LOQ of around 10 ppm or less. The LOQ for Cl was over 20 ppm, which was higher than was hoped, as Cl concentration was relatively low in most samples. The calibration curve for K is shown as an example in Figure 25, and the complete calibration information is collected in Appendices 4-13.

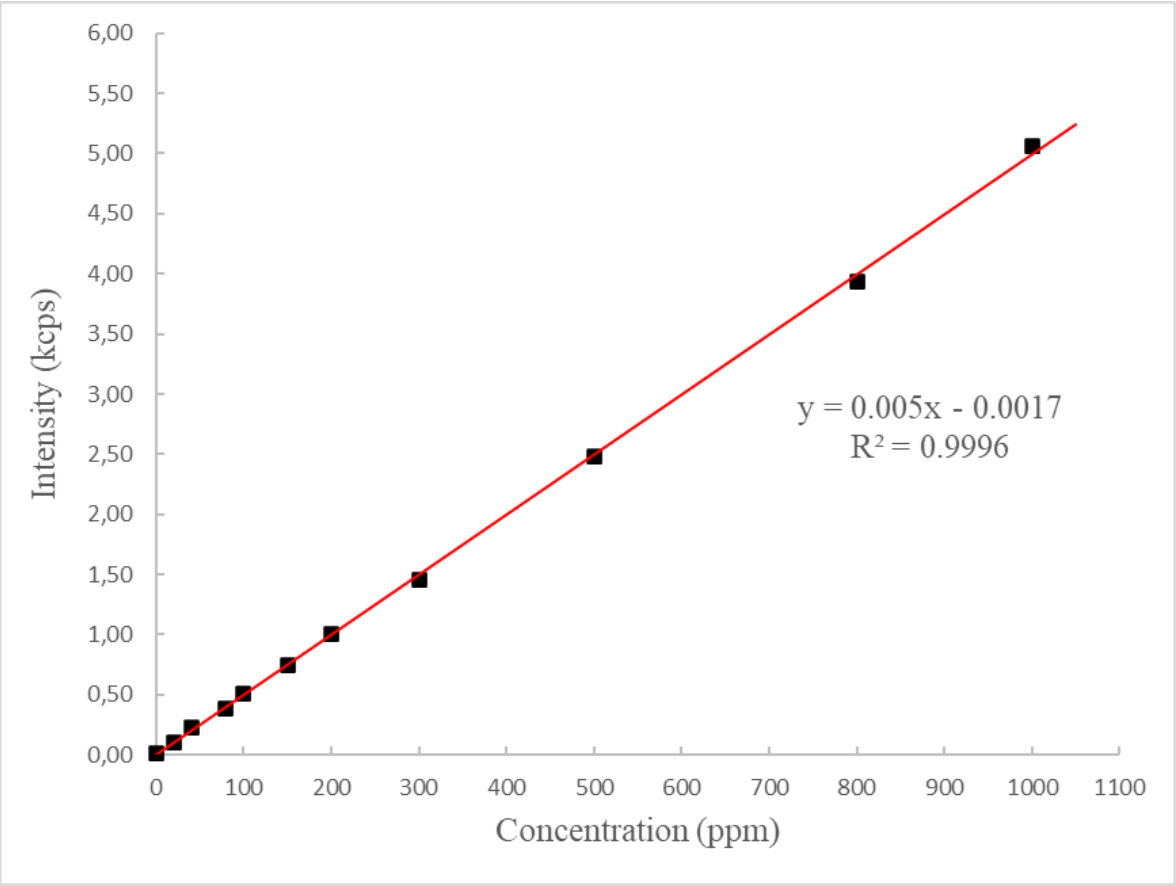


Figure 25 Calibration curve for K Kα1 line.

## 12.4 Other method settings

In the final steps of the application setup the result evaluation rules, and result display selections were defined. Water ($H_2O$) was set as the matrix compound, so that the sum of concentrations was balanced to 100%. Among the analytical lines, also a rhodium line measuring the inelastic Compton scattering was selected. The intensity of Compton scattering is generally high for light sample matrices (e.g., water or hydrocarbons) and the intensity depends on the average molar mass and density of the sample.[48] The software calculates a Compton ratio value, that is the ratio between measured and theoretical Compton value. Compton ratio over 100% indicates that the matrix is heavier that what was defined in the software, and the matrix used for calculations should be corrected. On the other hand, Compton ratio value below 100% indicates that the matrix is lighter than expected.

Defining the drift correction and quality control samples related to the method was also possible at this point. Drift correction samples are used to correct the intensity levels and calibration

from the changes in the instrument conditions, e.g., x-ray tube aging. Wastewaters method used four fused bead glass samples offered by the instrument manufacturer as drift correction specimens. Also, aqueous drift correction samples could be set, but these specimens need to be carefully planned and prepared so that drift corrections wouldn't give errors to calibration. Matrix-matched drift correction samples were not set during this work. Quality control specimens were not yet defined, but the quality assurance of the method should be planned in the future.

## 12.5 Method challenges

Few important challenges were noticed with the developed method, and although the results seemed promising, these challenges would need to be solved for the method to work optimally. Challenges were related to the calibration and its accuracy at low concentrations and to the earlier mentioned bubble formation during measurement of the standards.

### 12.5.1 Bubble formation

As was observed in the first scan measurements, the x-ray exposure and heating of sample created gas bubbles at the bottom of the sample cup. Between standard solution replicates the formation of bubbles was relatively repeatable. Due to dissolved organic matter and different surface tension in the wastewater samples, the formation of bubbles was different from the standard solutions in UP water. At the end of the 20 minutes measurement method, there were usually no bubbles in the sample solution, whereas standard solution cup had many relatively big bubbles (see Figure 26). The bubbles resulted in incomplete filling of the sample cup bottom, and as the measurement depth was only a few micrometres for most of the lines, they affected the measured result compared to a cup without bubbles.

Figure 26 Bubble formation in standard solution (left) and wastewater sample (right).

The samples were measured with two shorter methods (Cl method and Petro-Quant based method) to see if there was bubble formation at some point of the measurement. After a four-minute Cl method, large number of small bubbles were observed. After an eleven-minute Petro-Quant based method, the bubbles were typically on the edges of the cup and partly on the surface of the sample (see Figure 27). From these tests it could be concluded that bubbles were formed during the measurement in the samples as well, but they escaped the bottom of the cup before the end of the measurement.

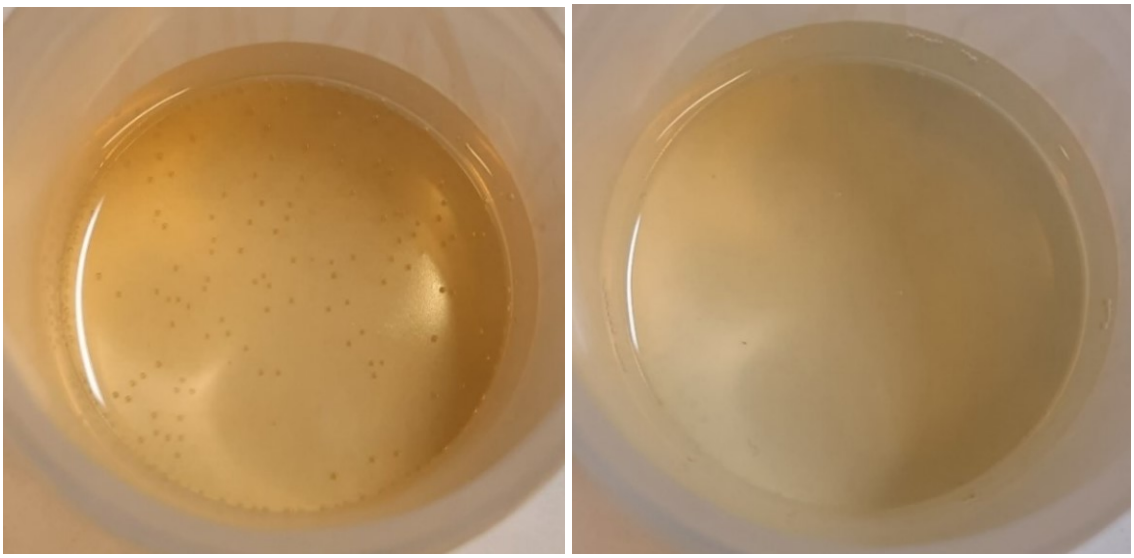

Figure 27 Bubble formation in wastewater samples during 4-minute method (left) and 11-minute method (right).

The bubbles are a result of dissolved gas emerging from the solution and therefore degassing of the liquid was tested. Degassing was performed with an ultrasonic bath (VWR USC 1200D) using the degassing function of the bath. The bath was heated to 40 °C, and full power (180 W) was used. A test solution having 46.2 ppm Na, 25 ppm Mg, Si, P, Cl and K, 500 ppm S and 10 ppm Ca, Mn and Fe was treated with degassing function for 15 minutes. A part of the sample was further treated with regular ultrasound for 10 minutes. The samples were measured right after treatment and again after cooling down to room temperature. Ultrasonic degassing gave only minor decrease in bubble formation during XRF measurements and the XRF results were close to reference sample results. The use of vacuum to speed up the ultrasonic degassing could be further tested for gas removal.

The addition of surfactant Triton X-100 (IUPAC name 2-[4-(2,4,4-trimethylpentan-2-yl)phenoxy]ethanol) was tested to lower the surface tension and reduce bubble formation in standard solutions. An aqueous solution of 1.0 v-% Triton X-100 was prepared for the foil tests. Further dilutions of 0.1 v-%, 0.05 v-% and 0.01 v-% were prepared for measurements. The triton-water mixture foamed in the flasks and sample cans, but no bubbles were transferred to the XRF measurement cup. After measurement, the 0.1 v-% solution had turned cloudy, but no bubbles were observed. Also, the 0.05 v-% solution had no bubbles at the end of the measurement, whereas 0.01 v-% solution had a few small bubbles. As there seemed not to be severe contamination with Triton X-100, the tests were repeated with standard solution. Two solutions having 46.2 ppm Na, 25 ppm Mg, Si, P, Cl and K, 500 ppm S and 10 ppm Ca, Mn and Fe were prepared, one without Triton and the other having 0.05% Triton. As was expected, the XRF results were bigger when Triton was added, because more sample volume was measured compared to cups having bubbles (see Table 7). Also, possible minor contamination from adding Triton could affect the results.

Table 7 XRF results for test solutions with and without Triton X-100

| Element | Nominal conc. (ppm) | XRF result (ppm), $\bar{x} \pm s$, no Triton | XRF result (ppm), $\bar{x} \pm s$, 0.05% Triton |
|---|---|---|---|
| Na | 46.2 | 34 ± 7 | 36 ± 10 |
| Mg | 25 | 27 ± 2 | 34 ± 3 |
| Si | 25 | 30 ± 1 | 37 ± 2 |
| P | 25 | 27 ± 2 | 33 ± 2 |
| S | 500 | 492 ± 7 | 607 ± 4 |
| Cl | 25 | 25 ± 3 | 39 ± 4 |
| K | 25 | 29 ± 2 | 32.9 ± 0.9 |
| Ca | 10 | 12 ± 1 | 13.4 ± 0.3 |
| Mn | 10 | 11.7 ± 0.3 | 12.3 ± 0.4 |
| Fe | 10 | 11 ± 1 | 13.3 ± 0.5 |

n = 3

When Triton was added to UP water, the solution remained clear during XRF measurement. Standard solution with Triton turned yellowish and cloudy during measurement, which indicated that some chemical reactions occurred between analytes and Triton (see Figure 28). The behaviour of Triton with single analytes and higher analyte concentrations than the ones tested here need to be further studied. Adding Triton to calibration standards results in matrix difference between standards and samples, and the significance of the difference need to be tested to see if Triton can be added only to standard solutions and not to wastewater samples that already have dissolved organic matter which can reduce surface tension.

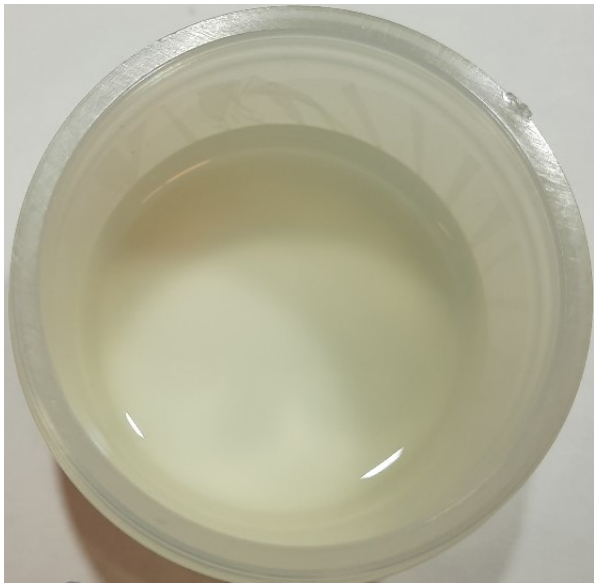

Figure 28 Standard solution with 0.05% Triton X-100 after XRF measurement.

### 12.5.2 Blank sample challenges

When UP water was measured as blank sample with the method, some net intensity was detected for several analytes, although visible peaks were not observed in the spectrum. The elements that required the use of offset correction in calibration gave the greatest intensities for UP-water (e.g., 0.207 kcps for Cl and 0.767 kcps for Fe). As calculated concentrations, the typical results for blank sample were around 10 ppm S, 5 ppm Si and 1-3 ppm P, Cl, K, Ca and Fe. As sulphur is present in large concentrations (e.g., 1000 ppm), inaccuracy at low concentrations was not a severe issue. On the contrary, low concentrations of Si (e.g., 10-30 ppm) would need to be determined accurately.

The used UP-water was expected to be pure enough, but as XRF is a sensitive method, Bruker's technical support advised that a completely pure water sample giving zero intensities would be needed as calibration blank sample. Also, different options and settings in the calibration setup should be further studied so that the calculated results for blank sample would be zero, even though minor net intensity would be detected (for some elements the sloping background and use of only one background correction point results in small net intensity even without a visible peak).

Possible contaminations should also be further investigated to improve trueness and accuracy at low concentrations. The used Prolene foils have P, Ca and Fe as typical impurities at ppm level. For Cl, contamination from other standards was considered as a possibility, and pure ion chromatography standards could be used for further testing. For Si, contamination from laboratory glassware was suspected. To test this, plastic sample cans were washed with 1%

$HNO_3$ solution overnight, and UP water was sampled straight from the water machine to the clean plastic cups. Similar concentrations were still measured, so the effect of contamination from glassware can be excluded. Si contamination from dust in sample cups or foils was considered as a possibility, although the measured intensity for Si remained relatively low and constant. Minor Si contamination is typical in many cases since Si is present in all over laboratory environment.

The offset correction was tested for Si, and it resulted in decrease in Si result (blank sample Si from 8 ppm to 2 ppm and 25 ppm standard solution from 30 ppm to 26 ppm). Offset is a powerful correction tool, and it can be used when the calibration blank is not giving zero intensities, but the primary way is to find a pure enough blank sample. Also, weighing the calibration curve and limiting the measurement range to lower concentrations could improve the measurement accuracy close to zero.

# 13 Test measurements for Wastewaters method

The wastewaters method was tested with multiple sample sets to see if the method would give results with sufficient accuracy and precision. Systematic error (bias) and random error (deviation of the results) together describe the overall uncertainty related to the measurement. The challenges related to blank sample intensities and bubble formation were observed during the tests as these issues were not solved prior to the test measurements or in between sample sets, so the results can be compared. The test measurements were planned so that they would give answers to the general method validation questions:

- Does the method give results close to the true or expected value?
- Does the method give similar results to aliquots of same sample?
- How sensitive is the method for changes in measurement conditions?
- Are sensitivity and measurement range sufficient for the purpose?

## 13.1 Trueness tests

Trueness tests aimed to prove that the results the method gave were close to the true or known value. The difference between expected (true) and measured value is the bias related to the measurement. Test measurements were performed with standard solutions of known concentrations, as well as with samples with standard additions. The XRF results were also compared to ICP-OES results.

### 13.1.1 Recovery tests

Certified reference materials corresponding to sample matrix were not available, and therefore the method was tested with standard solutions of known concentrations. Standard solutions were prepared in UP water from ICP-OES standard solutions or salt solutions. The accuracy is represented as recovery percentage of expected value, which was calculated by Equation (*5*).

The method was tested with two standard solutions. The concentrations of test solution 5 were close to XRF method quantitation limits, and the concentrations of test solution 6 were set to a level where XRF method should already perform well. The same solutions were also measured for comparison with ICP-OES. With ICP-OES, the recovery results were mainly between 95-105%. The results from the tests measurements are represented in Table 8.

Table 8 XRF results and recoveries for test solutions 5 and 6. Result as average ± standard deviation

| | Test solution 5 | | | Test solution 6 | | |
|---|---|---|---|---|---|---|
| | Nominal conc. (ppm) | XRF result (ppm), $\bar{x} \pm s$ | XRF, recovery (%) | Nominal conc. (ppm) | XRF result (ppm), $\bar{x} \pm s$ | XRF, recovery (%) |
| Na | 31.5 | 20 ± 11 * | 64.9 | 66.2 | 56 ± 5 | 84.2 |
| Mg | 30 | 29 ± 3 | 95.0 | 50 | 53 ± 5 | 105.4 |
| Si | 20 | 27 ± 3 | 137.3 | 50 | 58 ± 5 | 116.4 |
| P | 10 * | 13 ± 2 | 126.2 | 25 | 27 ± 3 | 107.2 |
| S | 10 | 18 ± 2 | 182.2 | 1000 | 950 ± 72 | 95.4 |
| Cl | 10 * | 11 ± 7 * | 105.2 | 25 | 26 ± 8 | 103.2 |
| K | 10 | 12.7 ± 0.8 | 126.8 | 25 | 28 ± 2 | 111.4 |
| Ca | 5 * | 6.8 ± 1.0 * | 135.7 | 15 | 17.2 ± 0.5 | 114.8 |
| Mn | 5 | 5.6 ± 0.8 | 112.7 | 15 | 15.8 ± 1.0 | 105.6 |
| Fe | 5 | 6.4 ± 0.5 | 128.0 | 15 | 14.7 ± 1.0 | 98.1 |

n = 6

* Value under limit of quantitation

The recoveries in XRF measurements were generally close to 100%, except for sodium. As was seen during the scan measurements, the peak for sodium was extremely small even for the solution containing 100 ppm Na, and measuring low concentrations was expected to be challenging. For test solution 6 with higher concentrations the recoveries were closer to 100% than for test solution 5, as the concentrations were well above LOQ. Also, the measured concentration for silicon and sulphur was higher than expected at 10 ppm level. Overall, the results as ppm's are sufficient when considering the challenges and possible limitations related to the XRF method. The measurement data is collected in Appendix 14.

### 13.1.2 Comparisons between XRF and ICP-OES results

ICP-OES method was daily used in UPM Research Center laboratories to measure the type of aqueous process samples that would be measured with the developed XRF method. Therefore, the results from XRF method were compared to ICP-OES results. The technical and physical backgrounds of the methods are very different, and the differences in sample introduction, excitation and detection need to be considered when comparing the results.

The results for test solutions 5 and 6 from both analytical methods were compared using students' t-test. Calculations were done in excel, and t-test assuming equal or unequal variances was selected based on f-test results. With higher concentrations, the results were closer to each other, and the difference was significant for only Na, Si, Ca and Fe at P = 0.05 level. With lower concentrations the difference was insignificant only for Mg, Cl and Mn, and all other analytes showed statistically significant difference between the two techniques.

Samples 22-00430, 22-00433, 22-00434 and 22-00435 were measured with both methods for comparison, and the results for 22-00430 and 22-00434 are shown in Table 9 and measurement data is collected in Appendix 15. Three replicates were measured with both XRF and ICP-OES. Sample 22-00430 was filtrated with 0.45 µm syringe filter before introducing the sample to the ICP-OES instrument. With ICP-OES, all samples were measured in 5% $HNO_3$ matrix, and if needed, the samples were also measured after being diluted 10-fold. Chlorine concentration was measured as chloride ions with ion chromatography.

Table 9 Comparison of XRF and ICP-OES results (ppm) for two wastewater samples. Result as average ± standard deviation

| | 22-00430 | | 22-00434 | |
|---|---|---|---|---|
| | XRF (ppm), $\bar{x} \pm s$ | ICP-OES (ppm), $\bar{x} \pm s$ | XRF (ppm), $\bar{x} \pm s$ | ICP-OES (ppm), $\bar{x} \pm s$ |
| Na | 43 ± 15 | 54.0 ± 0.8 | 8 ± 3 * | 19.80 ± 0.07 |
| Mg | 8 ± 4 * | 1.113 ± 0.005 | 6.7 ± 0.9 * | 0.489 ± 0.003 |
| Si | 12 ± 5 * | 2.78 ± 0.03 | 10.7 ± 0.7 * | 4.26 ± 0.03 |
| P | 55 ± 2 | 45.6 ± 0.6 | 64 ± 2 | 52.2 ± 0.2 |
| S | 850 ± 15 | 179 ± 2 | 2360 ± 17 | 1396 ± 3 |
| Cl ** | < LOD | 0.80 ± 0.01 * | < LOD | 0.59 ± 0.03 * |
| K | 12.5 ± 0.5 | 8.79 ± 0.03 | 9.4 ± 0.6 * | 6.725 ± 0.003 |
| Ca | 3.2 ± 0.3 * | 2.295 ± 0.007 | < LOD | 0.19 ± 0.02 |
| Mn | < LOD | 0.2567 ± 0.0006 | <LOD | 0.10000 ± 0.00006 |
| Fe | 2.1 ± 0.3 * | 0.109 ± 0.003 | 2.2 ± 0.5 * | 0.413 ± 0.002 |

n = 3

* Result under limit of quantitation

** Cl concentration measured with IC instead of ICP-OES

Overall, the XRF and ICP-OES results were on the same concentration ranges, but XRF results were generally higher than ICP-OES results, except for sodium that already showed lower recoveries with standard solutions. For P, K and Ca, if detectable, the results were relatively close to each other. Unfortunately, few XRF results were below quantitation or detection limits, which made the comparison difficult.

On the other hand, sulphur results were on a significantly different level, XRF giving much greater concentrations. The reason for this difference was somewhat unclear, and more tests are needed with both methods to understand if the difference is related to the methods or the sample behaviour. (e.g., XRF scan measurements of S in samples, standard additions of S to XRF samples and measuring samples prepared to ICP-OES also with XRF). If possible, a third method could also be used for comparison. The difference between results was tested with students' t-test, and as can be seen from Table 10, the difference was significant for many analytes (values under $t_{critical}$ bolded).

Table 10 Results for t-test comparing XRF and ICP-OES results for samples 22-00430 and 22-0434

| Sample | 22-00430 | 22-00434 |
|---|---|---|
| | \|t\| | \|t\| |
| Na | **1,31** | 6,81 |
| Mg | **3,6** | 13,1 |
| Si | **3,81** | 17,2 |
| P | 8,77 | 11,1 |
| S | 79,5 | 97 |
| Cl | **3,69 *** | 5,75 * |
| K | 14,7 | 8,31 |
| Ca | 7,03 | **1,46 *** |
| Mn | **2,4 *** | **1,51 *** |
| Fe | 11,1 | 7,57 |

$t_{critical(2)}$ = 4,30 for P = 0,05

* XRF result under LOD

Also, two solutions from the standard addition tests of sample 22-00435 were measured with ICP-OES. The additions were 26,5 ppm Na and 10 ppm Mg, Cl and K for addition-1 and 20 ppm Si, 50 ppm P and 10 ppm Ca, Mn and Fe for addition-5. The standard addition samples

were prepared so that wastewater made up 85% of the final sample volume. After standard addition, the analyte concentrations were on a level were XRF should perform well but the sample matrix was still similar compared to original samples. The same trend between methods could be seen with spiked samples as well: XRF results were slightly higher than ICP-OES results (except for Na). Silicon results were closer to each other after standard addition, but the difference remained similar with other analytes. Comparison of results is shown in Table 11 and measurement data is collected in Appendix 16.

Table 11 XRF and ICP-OES results (ppm) for two standard addition samples of 22-00435, result as average ± standard deviation

| | 22-00435 addition-1 | | 22-00435 addition-5 | |
|---|---|---|---|---|
| | XRF (ppm), $\bar{x} \pm s$ | ICP (ppm), $\bar{x} \pm s$ | XRF (ppm), $\bar{x} \pm s$ | ICP (ppm), $\bar{x} \pm s$ |
| Na | 40 ± 6 | 55.4 ± 0.4 | 11 ± 4 * | 28.0 ± 0.3 |
| Mg | 15 ± 3 | 10.26 ± 0.01 | 6 ± 3 * | 0.734 ± 0.003 |
| Si | 13 ± 2 | 5.6 ± 0.3 | 36.0 ± 0.7 | 33.5 ± 0.2 |
| P | 86 ± 0,8 | 72.1 ± 0.1 | 144 ± 2 | 123.3 ± 0.5 |
| S | 2108 ± 7 | 1105 ± 6 | 2140 ± 12 | 1105 ± 5 |
| Cl ** | 18 ± 4 * | 10.2 ± 0.3 | < LOD | 0.57 ± 0.02 * |
| K | 25.8 ± 0.3 | 19.7 ± 0.2 | 13 ± 2 | 9.59 ± 0.07 |
| Ca | < LOD | 0.25 ± 0.04 | 12.8 ± 0.4 | 10.140 ± 0.009 |
| Mn | < LOD | 0.131 ± 0.002 | 12.6 ± 0.3 | 10.12 ± 0.03 |
| Fe | 2.5 ± 0.1 * | 0.6410 ± 0.0006 | 15.1 ± 0.3 | 11.090 ± 0.006 |

n = 3

* Result under limit of quantitation

** Cl concentration measured with IC instead of ICP-OES

One explanation for bigger XRF results may be linked to the different bubble formation and behaviour between standard solutions and wastewater samples. Bubbles seemed to be smaller in samples than in standards, and they escaped the cup bottom during the measurement. Therefore, more sample area was measured compared to specimens where the bubbles covered significant parts of the cup bottom. More fluorescent radiation could then be generated and detected, which could lead to greater results. The method was calibrated with solutions that create bubbles, which could lead to positive systematic error for samples that have less bubbles.

The sample matrix was different in standard solutions and samples, since the standards were composed only of analytes as salts or pure elements, nitric acid and UP water, whereas samples had a large variety of different compounds as dissolved organic matter among others. Organic compounds could affect XRF result by changing the average molecular mass of the matrix and through that, the absorption efficiency towards fluorescent radiation. There was a minor decrease in the Compton values compared to standard solutions, which could indicate a lighter matrix. The change was small, but its effect would be towards lower absorption and greater detected intensity. On the other hand, volatile organic compounds are likely to enter the plasma in ICP-OES and could possibly lower plasma energy and interfere the excitement of analytes or give rise to the measurement background.

The chemical orientation of analytes also affects different methods in different ways. Ion chromatography measures only chlorine as inorganic chloride, and any possibly present organic chlorine is excluded from the analysis. XRF, on the other hand, measures signal from inner shell electron transitions, which isn't sensitive to the chemical orientation or bonding of the atoms. The distribution of the analytes in the XRF measurement cup is relevant, when the analysis depth is low, and only the signal from bottom layers reaches the detector. With ICP-OES, the matrix differences between standard solution and sample may interfere the measurement, if e.g., sample's physical properties, plasma temperature or the number of electrons in plasma are changed. Analyte removal in the additional filtrations for ICP-OES and IC and possible precipitation during XRF measurement could also increase the difference between methods.

### 13.1.3 Standard addition tests

XRF method was also tested by standard addition tests, where a series of samples with added analyte concentrations were prepared and measured. Sample 22-00435 was chosen for the standard addition tests, and the spiked samples were prepared so that 85 mL of wastewater was measured with a graduated cylinder to volumetric flask and after adding the standard solutions with an automatic pipette, the sample was made up to 100 mL with UP water. The wastewater sample made up to 85% of the matrix in all the spiked samples. When calculating the recovery percentages in Table 12 according to Equation (5), the expected concentration $\mu$ was calculated as 0.85 times the analyte concentration in original sample plus the added concentration of standard. Measurement data is collected in Appendix 17.

Table 12 Recoveries for standard addition samples of 22-00435

| Element | Addition (ppm) | Recovery (%) | Element | Addition (ppm) | Recovery (%) |
|---|---|---|---|---|---|
| Na | 26,5 | 80,5 | Cl | 10 | 129,1 |
| | 53,0 | 89,8 | | 20 | 136,9 |
| | 83 | 92,9 | | 50 | 124,2 |
| Mg | 10 | 105,2 | K | 10 | 112,0 |
| | 20 | 111,9 | | 20 | 114,3 |
| | 50 | 105,3 | | 50 | 117,5 |
| Si | 10 | 101,3 | Ca | 10 | 123,1 |
| | 20 | 109,2 | | 20 | 124,2 |
| | 50 | 109,9 | | 50 | 122,0 |
| P | 20 | 105,0 | Mn | 10 | 122,2 |
| | 50 | 105,6 | | 20 | 120,5 |
| | 100 | 112,5 | Fe | 10 | 126,9 |
| | | | | 20 | 124,4 |

Overall, the recoveries at 100-120% level were sufficient. The recovery for sodium was closer to 100% as the measured concentration increased towards 100 ppm. Mg, Si and P were in line with the expected values, as the recovery was between 100% and 113%. Standard additions led to overestimation of chlorine results, and similar results were obtained both in standard addition tests for sample 22-00435 and later in the spiking tests for samples 22-00430 and 22-00434. With Ca, Mn and Fe the concentration of the original sample was low, and the standard additions gave minor overestimation in the results. Similar tendency in the recoveries was obtained also with samples 22-00430 and 22-00434, when the standard addition was 5 ppm for Mn and Fe.

High recoveries in the standard addition tests may again be linked to the bubble formation properties. The method was calibrated in a bubble-forming matrix, and a standard addition was made to a sample matrix that formed less bubbles, thus giving overestimation of the concentration of some elements. The effect seemed to be important for heavier elements that were measured later in the method when the bubble difference was the greatest. The overestimation of Cl results may not be explained with only bubble formation, and Cl contamination from reagents was suspected. The addition tests could be repeated with certified Cl standard meant for IC, and more comparisons between XRF and IC methods should be run.

Overall, the accuracy of low Cl concentrations (up to 50 ppm) with XRF method was poor in many of the tests.

## 13.2 Precision tests

If the sample is homogenous and pretreatment is remained simple and constant, the variance in XRF measurement arise mainly from the measurement itself. Liquid samples need to be mixed well to make sure that the measured specimen is representative of the original sample. XRF method is typically stable and has low variance when large concentrations (percentage level) or heavy elements are measured. For the developed method, the water matrix gave high background, analytes were relatively light elements, and the measured intensities were relatively low, and therefore the variance of the results was expected to be significant. In routine measurements only one replicate measurement would usually be performed, which makes it crucial to know the typical variance related to the analysis.

Inter-laboratory tests for reproducibility were not possible, so the tests focused on instrument and intra-assay precision. Series of multiple replicate measurement were measured with XRF to estimate the variance and random error between measurements. Precision tests were repeated with standard solutions and spiked samples, and six replicates were measured in these series. Based on the ICP-OES and IC measurements for three or six replicates, the variance in these methods was relatively low. The variances of XRF results were compared to ICP-OES and IC, and according to the z-test results (P = 0.05), the variance in the XRF method was generally much greater than in the ICP-OES or IC methods.

Test solutions 5 and 6 were measured as a series of six replicates, and the average and standard deviation of the results were calculated for each element in excel. Relative standard deviation (RSD%) gives the standard deviation of the results related to the average of the results, which makes the comparison of different measurement sets possible. The relative standard deviation is calculated by Equation (10) as

$$RSD\% = \frac{s}{\bar{x}} * 100\% \tag{10}$$

where $s$ is the standard deviation and $\bar{x}$ is the average of the results. For test solutions 5 and 6, the standard deviation was relatively smaller when the analyte concentration was increased (see Table 13 and measurement data in Appendix 14). Bubble formation in sample cups may have

increased the deviation between replicate XRF measurements. The RSD% for chlorine was higher than expected, which again indicated that the method was not working optimally for low Cl concentrations.

Table 13 Relative standard deviation (RSD%) in XRF measurements for test solutions 5 and 6

| | Test solution 5 | | Test solution 6 | |
|---|---|---|---|---|
| | Nominal conc. (ppm) | RSD% | Nominal conc. (ppm) | RSD% |
| Na | 31.5 | 50.3 | 66.2 | 7.9 |
| Mg | 30 | 10.6 | 50 | 9.5 |
| Si | 20 | 7.7 | 50 | 7.7 |
| P | 10 * | 9.4 | 25 | 9.5 |
| S | 10 | 11.4 | 1000 | 7.5 |
| Cl | 10 * | 61.8 | 25 | 28.0 |
| K | 10 * | 5.8 | 25 | 5.7 |
| Ca | 5 * | 14.5 | 15 | 2.8 |
| Mn | 5 | 13.1 | 15 | 5.8 |
| Fe | 5 | 7.3 | 15 | 6.8 |

n = 6

* Concentration under limit of quantitation

The samples 22-00430 and 22-00434 were measured with XRF after spiking with 10ppm Na, Mg and K, 15.4 ppm Cl and 5 ppm Mn and Fe. Spiking increased the measured analyte concentrations close to or above quantitation limit, which made the measurement more reliable. Wastewater sample made up to 98% of the final sample volume. The spiked samples were measured six times in total, three replicates during one day and three more during the following day. The average concentrations and RSD% of measured analytes are listed in Table 14 and the measurement data is collected in Appendix 18.

Table 14 Relative standard deviations for two wastewater samples

| | 22-00430, spiked | | 22-00434, spiked | |
|---|---|---|---|---|
| | Result, average (ppm) | RSD% | Result, average (ppm) | RSD% |
| Na | 49.4 | 15.0 | 16.2 * | 46.2 |
| Mg | 16.2 | 7.8 | 15.7 | 8.4 |
| Si | 10.9 | 16.0 | 10.9 | 5.9 |
| P | 53.3 | 2.0 | 62.0 | 2.4 |
| S | 729.1 | 1.5 | 2237.6 | 0.5 |
| Cl | 25.9 | 9.1 | 26.0 | 10.1 |
| K | 24.4 | 2.6 | 21.2 | 2.9 |
| Ca | 4.2* | 14.5 | < LOD | - |
| Mn | 7.0 | 6.0 | 6.6 | 2.8 |
| Fe | 8.9 | 4.8 | 8.0 | 5.4 |

n = 6

* Result under limit of quantitation

For many analytes, the RSD% values were smaller with samples than with test solutions, which indicated better precision. The lack of air bubbles may be one reason for lower variance between replicate measurements. The RSD% values of chlorine results were smaller for samples than they were for standard solutions, but together with high LOQ, the Cl measurement did not work optimally. The measured concentrations were close to each other between the two days, but more tests should be run to demonstrate the day-to-day and long-term stability. After all, repeatability between days indicated good stability of the method, which is one great advantage in x-ray fluorescence spectrometry.

## 13.3 Method robustness tests

The effect of increasing sulphur or nitric acid concentration was tested to determine the robustness of the method towards these parameters. ICP-OES standards and the other used stock solutions had 1-3% $HNO_3$, so the final concentration of $HNO_3$ in standard solution varied from about 0.1% to approximately a maximum of 1.5%. The effect of nitric acid was tested by measuring similar standard solutions of which the other had no $HNO_3$ added and the other had

5 v-% $HNO_3$ concentration. The addition of $HNO_3$ increased the total oxygen concentration of the matrix and through that, increased the average molar mass of the matrix and may have changed the absorption properties. The results were compared with t-test, and no significant difference in analyte concentrations was observed within P = 0.05 level. Statistically significant increase was although observed in the percentage value describing Compton scattering, which indicates that the matrix became heavier.

In the process samples other element concentrations are typically low (under 500 ppm), but in some trial points the sulphur concentration can reach thousands of ppm's. Therefore, the effect of increased sulphur concentration to the result of other analytes was tested. For two similar test solutions having either 0 ppm S or 2000 ppm S, no significant difference (P = 0.05) was observed. However, the effect of much higher (e.g., 10,000 ppm) sulphur concentration would need to be confirmed in the future. Acid additions (both $HNO_3$ and $H_2SO_4$) to the wastewater samples and their effect to XRF results would need to be tested as well.

Two spiked wastewater samples of 22-00430 and 22-00434 were also measured in different temperatures to test the effect of sample temperature to XRF results. Three replicates of the sample were measured at approximately 5 °C (fridge temperature) and other three replicates in 40 °C (heated in heating cabinet). Based on the results, the sample temperature did not have a notable effect on XRF results. After measurement, small bubbles at the cup edges were observed with many specimens in all temperatures. Since the aqueous samples tended to evaporate during weighing already at 40 °C, it is recommended to measure samples in room temperature.

## 13.4 Comments on method validation

The test measurements were planned so that initial comments on method performance and fitness could be stated, although complete method validation was not yet performed, and more tests are required to do that. The developed method was selective, since no spectral overlapping was expected or observed, and the matrix effects seemed negligible. More tests are needed for Cl and S determination to understand the challenges related to accuracy, precision and difference to ICP-OES results.

The calibration was linear over a wide concentration range, but the calibration range could be further adjusted to fit the actual measurement range and to improve accuracy at low concentrations. Limits of determination and quantitation were mostly on the expected ranges,

as all elements, except for Na and Cl, could be measured from concentration as low as 10 ppm. The sample concentrations may sometimes fall under LOQ with Mg, Cl, Ca and Mn, but the result could then be confirmed with ICP-OES if accurate concentration is required. The measurement of Cl should be further optimised, as a LOQ around 10 ppm would be more sufficient than the present LOQ of 21 ppm.

Overall, the XRF results were close to the expected values. Matrix-matched certified reference materials were not available, so the trueness estimation was based on measuring standard additions and comparing the results to ones obtained with ICP-OES. Since the sample matrix is complex, also ICP-OES has its challenges, and the results can't be used as "true values". The determination of sodium was challenging for concentrations under 100 ppm, as the recoveries were low and variance relatively high. For other elements, the result was typically slightly overestimated, compared to ICP-OES, which may be corrected if the method is re-calibrated without bubble formation in standard solutions. However, it was concluded that the results obtained using the developed method were good enough for monitoring the processes and following trends rather than for monitoring individual concentrations.

Variance between replicate measurements was higher than with ICP-OES, but as the sample type and concentration range was known to be challenging for the technique, higher variation could be accepted. It is important that the results are interpreted with the information of the method limitations, and the typical variance of the results needs to be considered when conclusions are drawn based on the results. Sodium and chlorine seemed to have significant variance at least up to 100 ppm level, and more tests and optimisation are required. For other elements, the deviation of the results was in control.

The method seemed to be robust for small changes in temperature and acid concentrations. Also, the results from sample matrix (that is different compared to calibration matrix) were good, which indicated that the method would work for different sample types of varying pH and organic matter. The process samples can vary a lot, depending on the process feed and parameters, and all sample properties are not well known. Therefore, the method should be further tested with different sample types to identify possible limitations for certain matrix properties that could interfere the measurement.

Uncertainty related to the method is a combination of systematic error (bias) and random error (deviation of the results). Proper estimation of method uncertainty needs more results, and the estimation of bias was challenging since certified reference materials were not available. Repeating measurements for a specified quality control sample would give data for uncertainty

estimation and help to follow possible drift in the method. Uncertainty must be calculated separately for each element, and according to the results from this work, it will be greater for Na and Cl and smaller for e.g., K, Ca and Fe. As the samples are very diverse, defining one specific uncertainty value may not be sufficient, and it's important that everyone interpreting and using the results understand the nature and limitations of the method.

Overall, the developed method meets the requirements that were set at the beginning of the work, and it is well fit for purpose. With this method, the aqueous process samples can be analysed directly as liquids, and the results are available for process control soon after sampling. The method has better accuracy than was originally expected, and the measurement of aqueous samples with XRF was proved to be more than a coarse indication of concentrations. Further method development is still needed to improve the accuracy of the results, but the method was accepted for use as it was at the end of this project.

# 14 Sample pretreatment tests

After representative sampling the samples usually need handling or pretreatment in the laboratory before introducing to the instrument. In general, sample handling should be kept as simple as possible to avoid errors and contamination. The aqueous samples to be analysed with the developed method may contain oil and particles, but as the dissolved elements are the main interest, they can be removed from the samples if needed. The aim of these pretreatment tests was to investigate the effect of different pretreatment procedures to sample properties and XRF results. Another goal was to set general guidelines for sample handling, so that the samples would always be pretreated according to same instructions.

Whereas ICP-OES sample introduction system is sensitive for particles and gets easily dirty, during XRF measurement the sample stays in the disposable sample cup and has no contact with the instrument. Problems with XRF may arise from separation and settling of the sample in the sample cup, since the analysis depth is extremely low (only a few micrometres for most of the analytes) and intensity is recorded only from the bottom layer of the sample. If oil separation takes place during measurement, an oil phase would usually form on top of the aqueous phase which should not disturb the measurement. The measured analytes are expected to occur mostly as ions, and ions would stay rather in the acidic aqueous phase than move to the organic phase. On the other hand, particles settling in the cup bottom can have dramatic

effects in the XRF results, as the solid settling matter is overrepresented in the measurement. Also, possible bubble formation can affect the results, as presented earlier.

Compared to the calibration standards, one big difference in the sample matrix is the amount of organic matter. Some aqueous samples form relatively stable emulsified systems, and the others are clear after separating the oil phase, but have some dissolved organics still left in them. Carbon in the sample matrix decreases the average molar mass of matrix, which can change the absorption and scattering properties. On the other hand, sample matrix doesn't have nitric acid, but the standards do, although the concentration of $HNO_3$ in standards is relatively low.

## 14.1 Pretreatment procedures and samples

Pretreatments selected for the tests were separation in a separating funnel, centrifugation and filtration. These pretreatments were considered easy and fast ways of separating possible solids or oil phases from the aqueous phases. Also, these pretreatments were commonly used for other samples in the laboratory, so they would be easily adapted by the operators and laboratory technicians. Preconcentration procedures were not tested, since the aim of the work was to test if aqueous process samples could be measured simply as liquid.

Samples for pretreatment tests were collected from oil pretreatment process at the UPM Biorefinery Development Center in Lappeenranta during February and March 2022. Sample handling and XRF measurements were performed during the few following days after sampling. Sample canisters of 0.5 – 2 L were mixed well by hand for approximately 30 seconds before pouring subsamples for reference measurements and pretreatment tests. The reference sample without any pretreatment was measured with XRF as soon as the sample had cooled to room temperature.

Total of four samples were thoroughly tested. Two of the samples represented the emulsion type samples, named 22-02119 and 22-02255. The process parameters were then changed, and the other two samples represented the sample type that has clear aqueous phase, named 22-03363 and 22-03412. The two sample types had different properties other than their appearance. The pH was 3.1 for emulsion-type samples and 1.3 – 1.4 for clear-type samples and TOC was around 17,000 mg $L^{-1}$ and around 2000 mg $L^{-1}$, respectively. The emulsion-type samples were determined to have over 26,000 mg $L^{-1}$ suspended solids (glass fibre filtration Whatman GF/A 1,6 µm), whereas the amount was only around 150-300 mg $L^{-1}$ for clear-type samples. Overall, the emulsion-type samples had greater amounts of suspended solids and organic matter,

whereas clear-type samples were highly acidic, and the organic matter was separated from the aqueous phase more efficiently. All samples were also measured with ICP-OES and IC as routine process samples, and the results can be used for comparison.

### 14.1.1 Separating in a separating funnel

Approximately 100 ml of sample was placed in two separating funnels. One funnel was left to stay in room temperature and the other was placed in a fridge at around 5 °C. The funnels were checked and photographed after 30 minutes, 1 hour, 2 hours and 3 hours. The funnels were left to stay overnight, and the main aqueous phase was separated the next morning.

With emulsified samples, the main phase remained as an emulsion, and only a small amount of darker matter was separated in the surface. In the funnel that was placed in fridge, the top phase seemed to be oily (see Figure 29). Cooling of the glassware and plastic tap resulted in minor leakage in the funnel that was placed in fridge. With the clear samples, no oil phase was separated in the surface, but some organic matter was separated at the bottom of the funnel and on the glass surface (see Figure 30). With this sample type, it is also typical to have a clear oil phase separating in top of the aqueous phase.

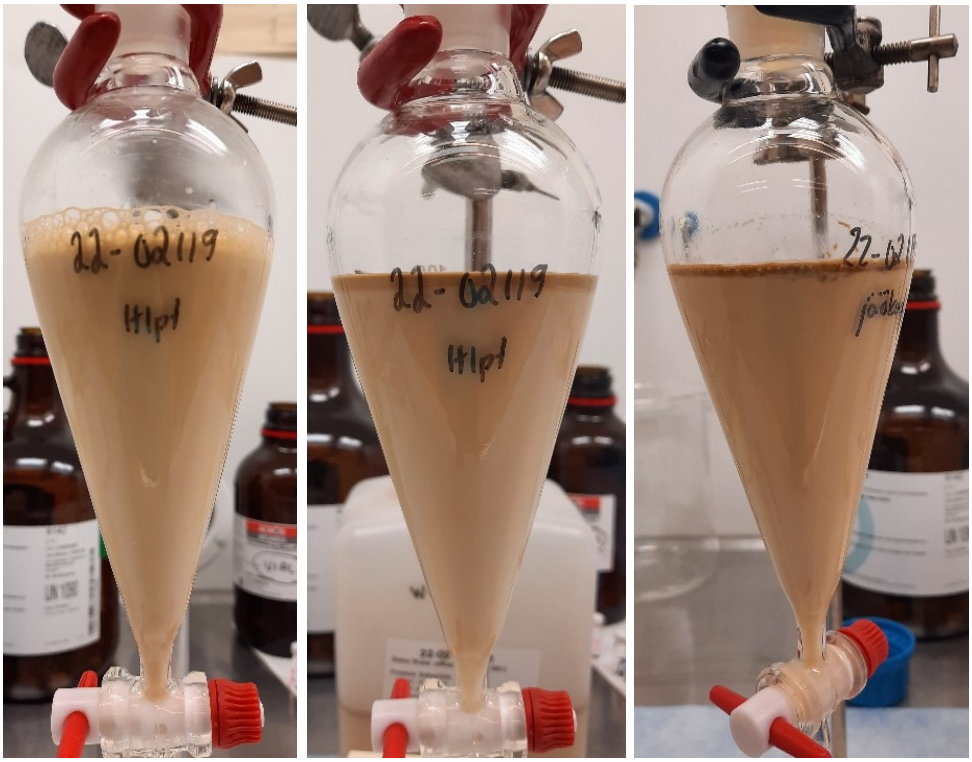


Figure 29 Sample 22-02119 before separation (left), and after overnight separation in room temperature (middle) and fridge (right).

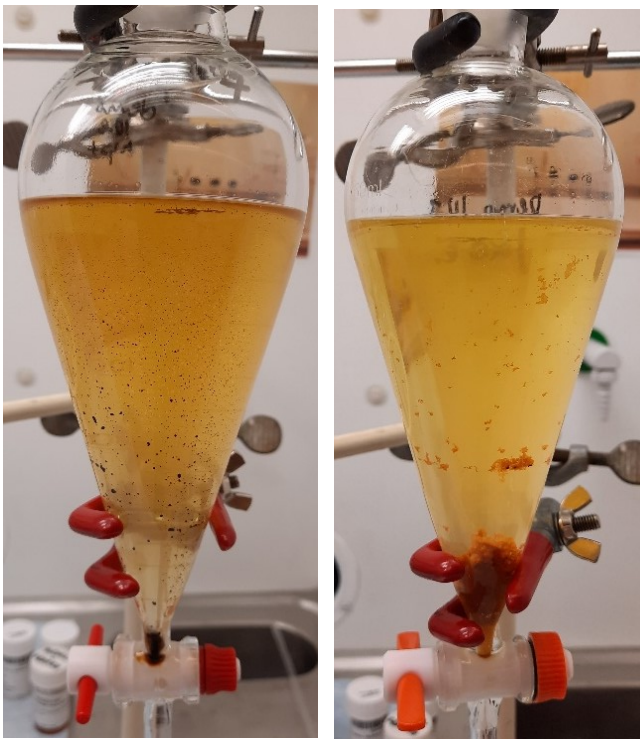

Figure 30 Sample 22-03412 after overnight separation in room temperature (left) and fridge (right).

After separation the aqueous phase was mixed well before measurements. The cooled sample was let to warm up to room temperature before XRF measurements. For the emulsified samples, the separation continued in sample cans and bottles, and a new darker top phase was formed after a few hours. Samples in room temperature were possible to re-mix, but after storing in fridge, the newly separated phases were difficult to mix. Pretreated clear-type samples didn't have further separation during storage.

Since the physical separation of the samples was different depending on the separation temperature, a specific storage temperature and procedure should be agreed for the aqueous samples, if the samples need to be stored before XRF analysis. Long-term stability of the samples should also be checked to define the maximum storage time.

### 14.1.2 Centrifugation

Centrifugation was also tested for separating possible phases in the samples. The rotational forces in centrifugation give more efficient phase separation, and if the sample has some heavier particles, it would be observed at the bottom of the centrifugation tube. Samples of 30-40 mL were poured into 50 mL centrifugation tubes, and the tubes were centrifuged at 2500 rounds per minute for 15 minutes. After centrifugation, the main phase was sampled carefully with a

pipette from tubes. For the emulsion-type samples, the emulsion was remained after the centrifugation, and a small amount of darker, oily matter was separated in the top (see Figure 31). There was no bottom phase containing solids. With clear samples, some organic matter was separated to the tube surface and the solution had lighter colour after centrifugation. Solid bottom phase was not observed for these samples, which indicated that settling during XRF measurements shouldn't happen.

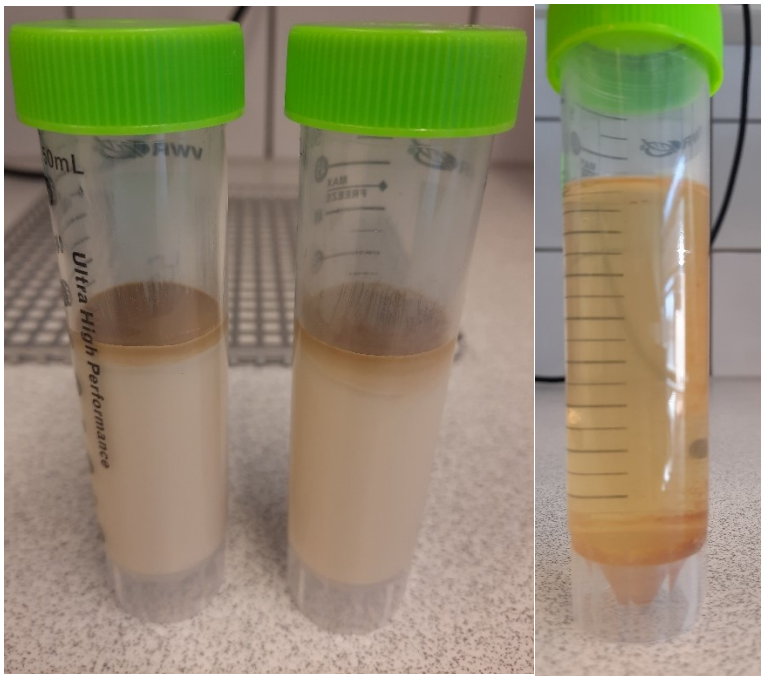


Figure 31 Samples 22-02255 (left, two replicates) and 22-03412 (right) after centrifugation.

### 14.1.3 Filtration

Filtration was tested with blue ribbon filter paper (Schleicher & Schuell 589/3, < 2 µm). Filtrations were performed with a Büchner funnel and a mild vacuum with filtering flask. With a higher vacuum, the emulsion-type sample foamed. A sample of 100-200 mL was poured on the filter paper moistened with UP water. With emulsion-type samples, no solids or oil were clearly left on the filter paper, and the emulsion remained after the procedure. With clear-type samples, some organic matter was left on the filter paper, and the sample had lighter colour after filtration (see Figure 32).

Figure 32 Filter paper after filtration of sample 22-03363.

## 14.2 XRF results from pretreatment test

The pretreated samples were measured with XRF to see the effect of the pretreatment on the measured analyte concentrations. All samples were measured with the Wastewaters method at room temperature. For each trial point, two replicate measurements were done. In most cases, the difference between replicate results was small. The same process samples were also measured with ICP-OES as routine samples a few days later, and the XRF results were compared to those results. For ICP-OES, the emulsion-type samples were filtrated with black ribbon paper and 0.45 µm PET syringe filter, whereas clear-type samples were filtrated with only black ribbon paper.

### 14.2.1 Emulsion-type samples

For the emulsion-type samples 22-02119 and 22-02255 the effect of pretreatment was not significant. Separation in a funnel or by centrifugation didn't clearly increase or decrease the result of any analytes. The concentration of S had minor decrease after pretreatments, the largest change being 16% for sample 22-02255. Comparison of XRF results after pretreatments is shown in Figure 33 for sample 22-02255 and the measurement data is collected in Appendix 19.

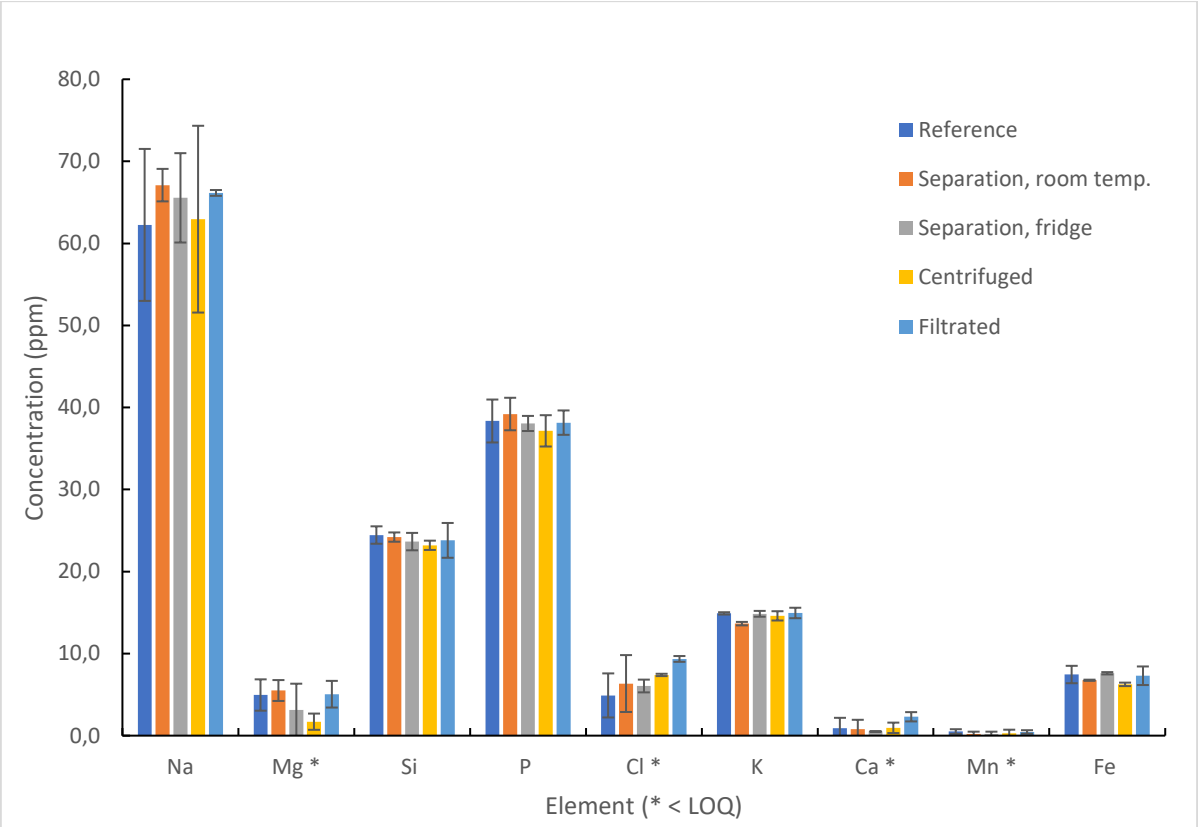


Figure 33 Pretreatment results for sample 22-02255, $\bar{x} \pm s$ (n = 2).

The difference to ICP-OES results was similar to previous comparisons between the methods. ICP-OES gave slightly bigger result for Na, and for Si, P, K and Fe the ICP-OES result was generally smaller than XRF result. XRF gave small concentration for Mg and Ca, whereas ICP-OES result was practically zero. IC result for chloride ion was around 1 ppm for samples 22-02119 and 22-02255, whereas Wastewater method gave around 5-9 ppm. Cl results from the element specific XRF method were 1.7 ppm and 2.8 ppm, respectively, which was in between the IC and Wastewaters method results.

After the XRF measurements of 22-02119 and 22-02255, the specimens of reference sample, separated samples and filtrated sample had an oily layer on the surface (see Figure 34). Similar oily layer was not observed with centrifuged samples, which indicated that centrifugation was more efficient in separating the oil from the aqueous phase than the other procedures. Also, the Compton value was slightly increased for the centrifuged samples, which indicated heavier matrix compared to reference sample and was most probably related to the removal of organic matter. Bubbles were not observed with emulsion-type samples.

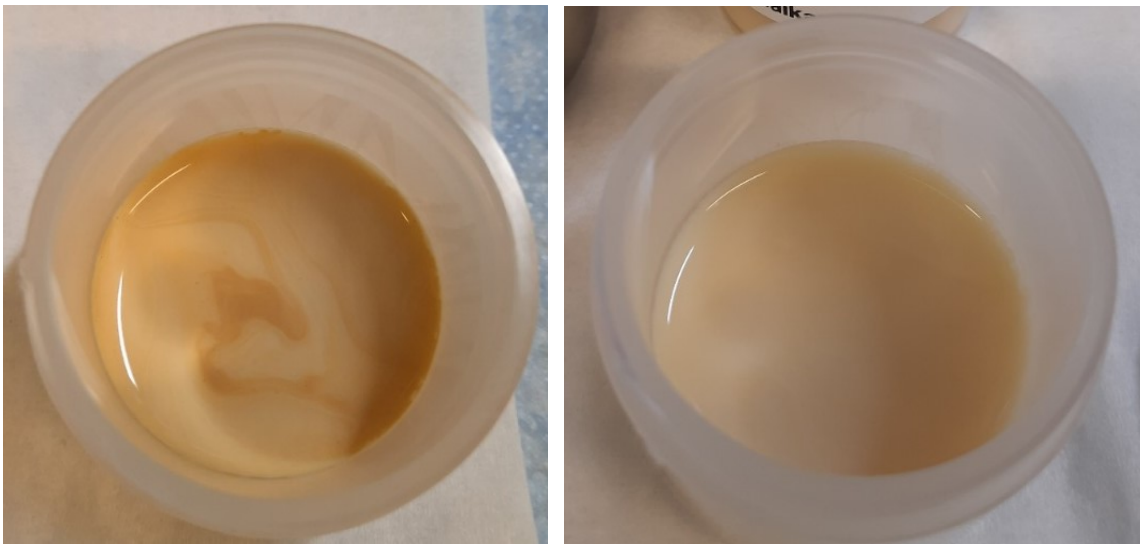

Figure 34 Reference sample (left) and centrifuged sample (right) specimens of emulsion-type sample 22-02255 after XRF measurement.

### 14.2.2 Clear-type samples

For the samples 22-03363 and 22-03412 that had clear aqueous phase the effect of pretreatments was also small. Although the samples looked different after pretreatments (filtrated and centrifuged samples had lighter colour), the XRF results were similar for each testing point. The result of Na, Si, P, Cl, K and Fe remained within the analytical error, whereas Mg, Cl, Ca and Mn were under limit of quantitation and had great variance. Comparison of XRF results after pretreatments is shown in Figure 35 for sample 22-03412 and the measurement data is collected in Appendix 20.

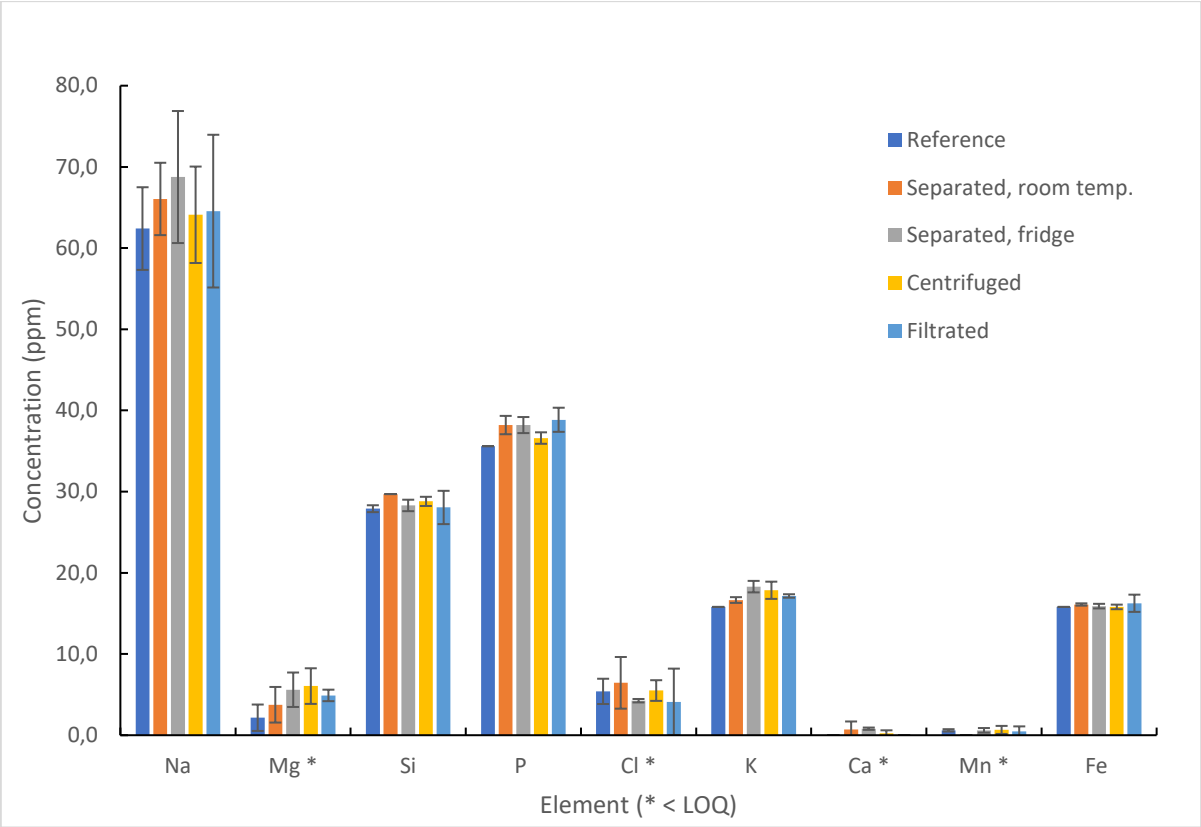


Figure 35 Pretreatment results for sample 22-03412, $\bar{x} \pm s$ (n = 2).

Although the result of other analytes remained practically unchanged after pretreatments, the result for sulphur significantly decreased for the clear-type samples. Compared to the reference measurement run right after sampling, the result for sulphur was decreased after pretreatments approximately 36% for sample 22-03363 and approximately 31% for sample 22-03412. The difference between the pretreatments was small (see Figure 36). The reference sample was measured again after a few hours ("Afternoon measurement"), as the subsample can had been left in room temperature. Separation of the reference sample was observed during the day, and the separated matter wasn't anymore miscible in the sample. The sulphur result was decreased by over 20% compared to reference measurement. The results indicated that the organic matter separated from the clear-type samples included sulphur compounds. If accurate results for sulphur are needed for this sample type, the issue must be further studied to understand these phenomena better.

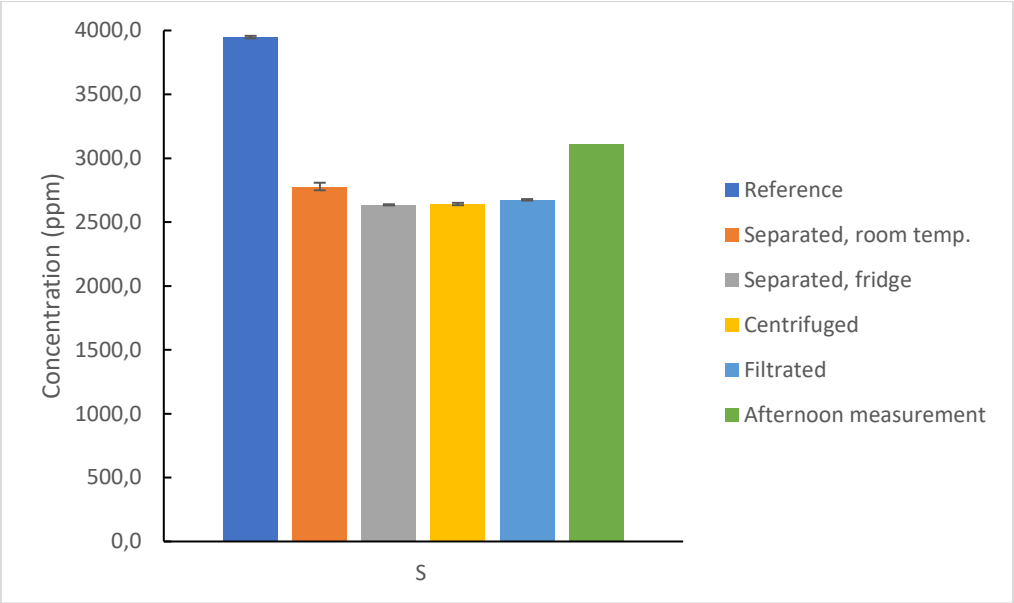


Figure 36 S result, sample 22-03412, $\bar{x} \pm s$ (n = 2).

When the results were compared to ICP-OES results, the observations were similar than before: Na result was smaller with XRF, and Si, P, K and Fe results larger, but overall, the results were close to each other. The difference in S results was again present, ICP-OES giving approximately 1480 ppm S. For sample 22-03363 the Cl result was similar with both XRF methods (4.3 and 4.4 ppm), whereas for sample 22-03412 the chlorine method gave 0 ppm. IC result was under 1 ppm for both samples.

Clear samples appeared slightly cloudy after XRF measurement but there was no clear oil separation. Single bubbles were observed in a few measurement cups. Compton values were slightly bigger for all pretreated samples, but the difference to reference sample was only around one percentage point. Pretreated samples had slightly lighter colour, but other differences to reference or between trial points were not observed.

## 14.3 Suggestions for sample pretreatment and storage

Overall, the effect of pretreatments on the XRF results was small with both sample types, excluding the sulphur results for clear-type samples. More sample types of e.g., different process feeds or oil content should be tested in a similar manner. As a general guidance, clearly and easily separating oil phases should be removed from the aqueous samples, as soon as possible after sampling. Emulsified samples don’t need separation before XRF measurement if

the measurement is performed soon after sampling. All samples should be measured in room temperature.

All samples should preferably be measured soon after sampling, as the physical composition of samples can change during storage. For short periods of time (e.g., overnight) the samples can be stored in room temperatures, since they seemed to be more difficult to mix after storing in fridge, but long-term storage must be done in cold as is suggested for water samples in general. Preservation with acid addition is not needed, since the samples already have low pH. The long-term stability of the samples needs to be further tested to define the maximum storage time. After storage, separation in a funnel or filtration with coarse paper to remove small amounts of oil or solids is recommended, since based on the results it does not seem to have significant effect on the XRF results.

# 15 Summary and conclusions

When aqueous samples are to be analysed, atomic absorption and emission techniques are the typical selection for elemental analysis. ICP-OES and ICP-MS techniques are sensitive and accurate methods for multi-elemental analysis, but challenges arise from reproducible sample introduction and matrix interferences when the sample background becomes complex.

XRF techniques have been more typically used for solid samples, but applications for liquid sample analysis do exist. The instruments are very stable and have high dynamic range, but sensitivity for low concentrations may be insufficient for some applications. According to the covered references, aqueous sample measurements with XRF are possible, but might face severe challenges. Fluorescence yield is higher for heavier elements and relatively poor for light elements, and a liquid matrix typically results in high scattering background.

Chemical matrix effects due to absorption of the radiation and secondary enhancement of analytes are typical for XRF analysis of higher concentrations, and several mathematical models have been developed for correcting the effects. In trace analysis, the counting time for analytical lines is increased to achieve sufficient accuracy, whereas inter-elemental matrix effects typically become negligible.

Liquid samples are measured in special sample cups, and the primary beam and fluorescent radiation need to pass the sample support foil that absorbs low energy fractions of the radiation.

Most publications apply preconcentration techniques for aqueous samples to improve sensitivity, and procedures leading to thin, solid specimens are preferred.

In the experimental part of the work, aqueous process sample measurements with WDXRF instrument were examined. The project included the development of a new measurement method, evaluation of method performance and tests for sample pretreatment. As a fast and easy-to-use method was preferred, direct liquid phase measurement without time-consuming preconcentration procedures was developed.

The XRF method was calibrated with aqueous standard solutions prepared from ICP-OES standards and salt solutions. Method performance was tested by measuring standard solutions, spiked samples, standard addition series and replicate sample series. The XRF results were also compared to ICP-OES and IC results. For fresh process samples, funnel separation, filtration and centrifugation were tested as sample pretreatments.

The calibrations were linear throughout the desired concentration ranges, and correlation coefficients were typically over 0.999. The limits of quantitation were on a sufficient range, or even better than expected, as most elements could be measured from around 10 ppm level. The addition of Triton X-100 in UP-water reduced bubble formation noticed during measurements of calibration standards and could provide a way to obtain calibration without bubbles.

The results from XRF measurements were generally higher than ICP-OES results for the same samples. As the techniques are very different, some difference in results was expected, but overall, the XRF and ICP-OES results seemed to be in good agreement. The standard addition recoveries were on a good range but mostly slightly over 100%. In XRF, the bubble difference between calibration standards and samples gave a logical reason for slight overestimation of concentrations.

XRF results also had higher variance, which was expected, as the matrix, analytes and concentration ranges were known to be challenging for the technique. Relative standard deviation was mainly under 10%, but Na and Cl showed higher variance. The typical variance needs to be considered if conclusions are drawn based on single measurement results. As expected, the day-to-day stability of XRF seemed good.

Based on the theory and preliminary tests, the measurement of low sodium concentrations was expected to be challenging. Based on the tests, Na concentration is slightly underestimated up to 100 ppm level. Variation in the results remain remarkable also above LOQ level, and single results need to be interpreted with caution.

The measured sulphur concentrations in the wastewater samples are typically high (hundreds or thousands of ppm), and minor inaccuracy at low concentrations was not considered a problem. The results for standard solutions were accurate with both methods, but for the wastewater samples, XRF gave significantly bigger S result compared to ICP-OES. More tests are needed to understand the origin of this difference, but most probably it's linked to sample properties and behaviour rather than problems in either measurement method.

The results for chlorine measurements didn't completely fulfil the expectations, as LOQ was over 20 ppm and variance between results was high. Also, the standard additions were overestimated. More tests and comparison to IC and to the element specific XRF method are needed, and improvements by changes in measurement parameters and calibration can be searched.

The method seemed to be robust for small changes in sample temperature and acid concentrations. Reasonable results were obtained for two very different sample types, which both had a clear matrix difference compared to the calibration standards. Also, the tested pretreatments had negligible effect in the XRF results, even though the sample properties were clearly changed. Overall, the method seemed to tolerate changes in sample properties well, but more tests are needed to set the limits for reliable measurement conditions.

The method was calibrated in UP-water matrix and not a specific sample matrix that would possibly limit the use of method to that one sample type. The aqueous process samples can be very versatile, depending on the process itself, process feeds and products and operating conditions. More tests need to be run with different sample types, but based on the results it seems that the method could be used for a variety of different aqueous process samples.

Overall, the goals set for the work were met. Despite the few challenges, measuring aqueous process samples with WDXRF was proven to be possible, and the results were in line with ICP-OES results. The developed method was taken into use at the Research Center laboratory and method development will continue after this work. More test measurements are needed to evaluate method uncertainty and complete the method validation. Quality control routines for the developed method will also be set in the future. Similar methods can be developed for measuring element concentrations in various aqueous process samples (e.g., elements indicating corrosion).

# Appendix

# Bibliography


1. Marguí, E. and van Grieken, R., *X-Ray Fluorescence Spectrometry and Related Techniques : An Introduction,* Momentum Press, New York, 2013. a) p. 1-32, b) p. 33-59, c) p. 61-71, d) p. 73-87, e) p. 121-127
2. Brown, R. J. C. and Milton, M. J. T., Analytical techniques for trace element analysis: An overview, *TrAC - Trends Anal. Chem.*, **2005**, *24*, 266–274.
3. Brouwer, P., *Theory of XRF - Getting acquainted with the principles,* 5th edition, Malvern Panalytical, Almelo, 2018.
4. van der Jagt, H. and Reijnders, H. F., Water analysis – Overview, in Worsfold, P.; Townshend, A. and Poole, C. (eds.), *Encyclopedia of analytical science*, 2nd edition, Elsevier Academic Press, Amsterdam and Boston, 2005, VOL. 9, 234–252.
5. Guerra, R., Water analysis - Industrial Effluents, in Worsfold, P.; Townshend, A. and Poole, C. (eds.), *Encyclopedia of analytical science*, 2nd edition, Elsevier Academic Press, Amsterdam and Boston, 2005, VOL. 9, 289–299.
6. ISO 5667-3:2018 Water quality — Sampling — Part 3: Preservation and handling of water samples. (2018).
7. Baird, R. B.; Eaton, A. D. and Rice, E. W. *Standard Methods for the Examination of Water and Wastewater*, 23rd edition, American Public Health Association, Washington D.C., 2017.
8. Ivanova, E. H., Atomic Absorption Spectrometry: Principles and Instrumentation, in Worsfold, P.; Townshend, A. and Poole, C. (eds.), *Encyclopedia of analytical science*, 2nd edition, Elsevier Academic Press, Amsterdam and Boston, 2005, VOL. 9,, 149–156.
9. Skoog, D. A.; Holler, F. J. and Nieman, T. A., *Principles of instrumental analysis*, 5th edition, Saunders College Publishing, Orlando, 1998. a) p. 192-205, b) p. 206-229, c) p. 230-252, d) p. 253-271
10. Twyman, R. M., Atomic Emission Spectrometry: Principles and Instrumentation, in Worsfold, P.; Townshend, A. and Poole, C. (eds.), *Encyclopedia of analytical science*, 2nd edition, Elsevier Academic Press, Amsterdam and Boston, 2005, VOL. 9, 190–193.
11. Nölte, J., *ICP Emission Spectrometry - a Practical Guide,* Wiley-VCH Verlag GmbH & Co. KGaA, Weinheim, 2003. p. 107, 146-153, 221
12. *Introduction to X-Ray Fluorescence Analysis*, Bruker AXS GmbH, Karlsruhe, 2016.

13. Marguí, E.; Zawisza, B. and Sitko, R., Trace and ultratrace analysis of liquid samples by X-ray fluorescence spectrometry, *TrAC - Trends Anal. Chem.*, **2014**, *53*, 73–83.
14. Webinar "Liquid analysis with XRF: Increased analysis sensitivity and safety for liquids", Shaffer, C. R., Thermo Fisher Scientific, https://players.brightcove.net/665001591001/default_default/index.html?videoId=5192696204001 (01.12.2021).
15. Mitä säteily on? Säteilyturvakeskus (STUK), https://www.stuk.fi/aiheet/mita-sateily-on (09.12.2021).
16. Säteilylaki 859/2018, FINLEX, https://www.finlex.fi/fi/laki/alkup/2018/20180859#Lidm45237817224640. (09.12.2021)
17. Jenkins, R.; Gould, R. W. and Gedcke, D., *Quantitative X-ray Spectrometry*, 2nd edition, Marcel Dekker Inc., New York, 1995. a) p.322-343 b) p. 344-387 c) p. 388-428
18. Mantler, M.; Willis, J.P.; Lachance, G.R.; Vrebos, B.A.R.; Mauser, K.-E.; Kawahara, N.; Rousseau, R.M. and Brouwer, P.N., Chapter 5. Quantitative analysis, in Beckhoff, B.; Kanngieser, B.; Langhoff, N.; Wedell, R. and Wolff, H. (eds.), *Handbook of Practical X-ray Fluorescence Analysis*, Springer, Berlin, Heidelberg and New York, 2006, 309–410.
19. Rousseau, R. M., Corrections for matrix effects in X-ray fluorescence analysis-A tutorial, *Spectrochim. Acta - Part B At. Spectrosc.*, **2006**, *61*, 759–777.
20. Solazzi, M. J., Disposable XRF Sample Cups and Thin-film Sample Supports for X-Ray Fluorescence Analysis, Chemplex Industries Inc., Reprinted from *American Laboratory*, **1984**, *16*, 72–78.
21. Moriyama, T. and Morikawa, A., Sample preparation for X-ray fluorescence analysis - VII. Liquid sample, *Rigaku Journal*, **2017**, *33*, 24–29.
22. Injuk, J.; Van Grieken, R.; Blank, A.; Eksperiandova, L. and Buhrke, V., Chapter 6. Specimen preparation, in Beckhoff, B.; Kanngieser, B.; Langhoff, N.; Wedell, R. and Wolff, H. (eds.), *Handbook of Practical X-ray Fluorescence Analysis*, Springer, Berlin, Heidelberg and New York, 2006, 411–432.
23. Elemental Analysis, Rigaku Corporation, https://www.rigaku.com/applications/elemental-analysis (22.04.2022).

24. Contaminants in Water, Bruker AXS GmbH, https://www.bruker.com/en/applications/detection-and-environmental/environmental/water-analysis-environmental/contaminants-in-water.html (22.04.2022).
25. Shaffer, C. R., Analysis of Aqueous Acid Solutions with Thermo Scientific ARL OPTIM'X WDXRF Sequential Spectrometer, *Thermo Fisher Scientific*, 2013.
26. Lerner, N.; Sedgi, I.; Chernia, Z. and Zeiri, O., Rapid direct determination of tin in beverages using energy dispersive X-ray fluorescence, *Talanta*, **2019**, *199*, 662–666.
27. Pashkova, G. V.; Smagunova, A. N. and Finkelshtein, A. L., X-ray fluorescence analysis of milk and dairy products: A review, *TrAC - Trends Anal. Chem*., **2018**, *106*, 183–189.
28. Rinaldoni, A. N.; Campderrós, M. E.; Pérez Padilla, A.; Perino, E. and Fernández, J. E., Analytical determinations of minerals content by XRF, ICP and EEA in ultrafiltered milk and yoghurt, *Lat. Am. Appl. Res*., **2009**, *39*.
29. Van Grieken, R., Preconcentration Methods for the Analysis of Water by X-Ray Spectrometric Techniques, *Anal. Chim. Acta*, **1982**, *143*, 3–34.
30. McNaught, A. D.; Wilkinson, A. and Chalk, S. J., Compendium of Chemical Terminology (the 'Gold Book'), International Union of Pure and Applied Chemistry (IUPAC), Blackwell Scientific Publications, 1997.
31. Marguí, E.; Van Grieken, R.; Fontàs, C.; Hidalgo, M. and Queralt, I., Preconcentration methods for the analysis of liquid samples by X-ray fluorescence techniques, *Appl. Spectrosc. Rev*., **2010**, *45*, 179–205.
32. Eksperiandova, L. P.; Blank, A. B. and Makarovskaya, Y. N., Analysis of waste water by x-ray fluorescence spectrometry, *X-Ray Spectrom*., **2002**, *31*, 259–263.
33. Zhang, N.; Li, T.; Meng, Z.; Wang, C.; Ke, L. and Feng, Y., X-ray fluorescence spectrometry analysis for minerals with agaron gel for sample preparation, *Microchem. J.,* **2009**, *91*, 59–62.
34. Gonzalez-Fernandez, O.; Margui, E. and Queralt, I., Multielemental analysis of dried residue from metal-bearing waters by wavelength dispersive X-ray fluorescence spectrometry, *Spectrochim. Acta - Part B At. Spectrosc*., **2009**, *64*, 184–190.
35. Uemura, S. and Moriyama, T., Water analysis by X-ray fluorescence spectrometry using UltraCarry, *Rigaku Journal*, **2020**, *36 (2)*, 25–30.
36. Rathod, T. D.; Tiwari, M.; Maity, S.; Sahu, S. K. and Pandit, G. G., Multi-element detection in sea water using preconcentration procedure and EDXRF technique, *Appl. Radiat. Isot*., **2018**, *135*, 57–60.

37. Inui, T.; Abe, W.; Kitano, M. and Nakamura, T., Determination of Cr(III) and Cr(VI) in water by wavelength-dispersive X-ray fluorescence spectrometry after preconcentration with an ion-exchange resin disk, *X-Ray Spectrom*, **2011**, *40*, 301–305.
38. Marguí, E.; Hidalgo, M.; Queralt, I.; Van Meel, K. and Fontàs, C., Analytical capabilities of laboratory, benchtop and handheld X-ray fluorescence systems for detection of metals in aqueous samples pre-concentrated with solid-phase extraction disks, *Spectrochim. Acta - Part B At. Spectrosc*., **2012**, *67*, 17–23.
39. Zawisza, B.; Skorek, R.; Stankiewicz, G. and Sitko, R., Carbon nanotubes as a solid sorbent for the preconcentration of Cr, Mn, Fe, Co, Ni, Cu, Zn and Pb prior to wavelength-dispersive X-ray fluorescence spectrometry, *Talanta*, **2012**, *99*, 918-923.
40. Marguí, E.; Zawisza, B.; Skorek, R.; Theato, T.; Queralt, I.; Hidalgo, M. and Sitko, R., Analytical possibilities of different X-ray fluorescence systems for determination of trace elements in aqueous samples pre-concentrated with carbon nanotubes, *Spectrochim. Acta - Part B At. Spectrosc*., **2013**, *88*, 192–197.
41. Örnemark, U. and Magnusson, B. (eds.), Eurachem Guide: The Fitness for Purpose of Analytical Methods - A Laboratory Guide to Method Validation and Related Topics, 2nd edition, Eurachem, 2014.
42. Ehder, T. (eds), Kemian metrologian opas, Metrologian neuvottelukunta, 2005.
43. Hägg, M. (eds), Validoinnin suunnittelun opas, VTT Technology 276, 2016.
44. Miller, J. N. and Miller, J. C., Statistics and Chemometrics for Analytical Chemistry, 6th edition, Pearson Education Limited, Harlow, 2010. a) p. 78-89, b) p. 124-127
45. Magnusson, B.; Näykki, T.; Hovind, H.; Krysell, M. and Sahlin, E., Handbook for Calculation of Measurement Uncertainty in Environmental Laboratories, 4th edition, Nordtest Report TR 537, Nordtest, 2017.
46. Ellison, S. L. R. and Williams, A., Eurachem / CITAC Guide CG4: Quantifying Uncertainty in Analytical Measurements, 3rd edition, Eurachem, 2012.
47. Hovind, H.; Magnusson, B.; Krysell, M.; Lund, U. and Mäkinen, I., NORDTEST Technical report TR569: Internal quality control, Nordtest, Nordic Innovation Centre, 2006.
48. SPECTRAplus User Manual, Bruker AXS GmbH, 2013.

APPENDIX 1

| Measurement method parameters for PETRO-QUANT2 Oil-short_aqueous method | | | | | | | | | | |
|---|---|---|---|---|---|---|---|---|---|---|
| Analyte line | Tube current (mA) | Tube voltage (kV) | Filter | Collimator (°) | Crystal, 2d (nm) | Detector | Peak position (2θ) | Background positions (2θ) | Counting time (peak/background points) | LLD rule |
| Na Kα1 (Trace) | 50 | 20 | none | 0.46 | XS-55 2d=5.5 | FC | 25.108 | 19.115 / 23.357 / 26.950 / 29.445 | 100s / 10s per point | LLD 10ppm |
| Mg Kα1 (Trace) | 50 | 20 | none | 0.46 | XS-55 2d=5.5 | FC | 20.763 | 19.115 / 23.357 / 26.950 / 29.225 | 100s / 10s per point | LLD 10ppm |
| Si Kα1 (Trace) | 50 | 20 | none | 0.46 | PET 2d=0.874 | FC | 109.012 | 111.0 | 20s / 6s | LLD 1ppm |
| P Kα1 (Trace) | 50 | 20 | none | 0.46 | XS-Ge-C 2d=0.653 | FC | 141.017 | 147.4 | 20s / 6s | LLD 1ppm |
| S Kα1 (Trace) | 50 | 20 | none | 0.46 | XS-Ge-C 2d=0.653 | FC | 110.751 | 115.0 | 20s / 6s | LLD 1ppm |
| S Kα1 (Minor) | 50 | 20 | Al | 0.46 | XS-Ge-C 2d=0.653 | FC | 110.741 | 116.0 | 20s / 6s | LLD 100ppm |
| S Kα1 (ALT-Minor) | 50 | 20 | Al | 0.46 | XS-Ge-C 2d=0.653 | FC | 110.669 | 116.0 | 20s / 6s | LLD 1ppm |
| Cl Kα1 (Trace) | 50 | 20 | none | 0.46 | XS-Ge-C 2d=0.653 | FC | 92.789 | 96.3 | 20s / 6s | LLD 1ppm |
| Cl Kα1 (Minor) | 50 | 20 | Al | 0.46 | XS-Ge-C 2d=0.653 | FC | 92.794 | 96.3 | 20s / 6s | LLD 100ppm |
| K Kα1 (Trace) | 20 | 50 | none | 0.46 | LiF200 2d=0.403 | FC | 136.642 | 141.2 | 20s / 6s | LLD 1ppm |
| Ca Kα1 (Trace) | 20 | 50 | none | 0.46 | LiF200 2d=0.403 | FC | 113.105 | 108.0 / 123.5 / 131.0 | 20s / 6s per point | LLD 1ppm |
| Mn Kα1 (Trace) | 20 | 50 | none | 0.46 | LiF200 2d=0.403 | FC | 62.992 | 60.5 / 66.5 /74.5 | 20s / 6s per point | LLD 1ppm |
| Fe Kα1 (Trace) | 20 | 50 | none | 0.46 | LiF200 2d=0.403 | SC | 57.541 | 54.500 / 59.750 | 20s / 6s per point | LLD 1ppm |
| Rh Kα1 Compton | 10 | 50 | Al | 0.23 | LiF2002d=0.403 | SC | 18.564 | 14.5 / 21.0 /24.5 | Scan 30s | - |
| FC = flow counter<br>SC = scintillation counter<br>LLD = lower limit of detection | | | | | | | | | | |

APPENDIX 2

| XRF results for test solution 2 and 4. Petro-Quant based method | | | | | | | | | | | | | |
|---|---|---|---|---|---|---|---|---|---|---|---|---|---|
| Sample Name | Measurement Finished | Measurement method | Na | Mg | Si | P | S | Cl | K | Ca | Mn | Fe | Compton (%) |
| testiliuos2_PQ_3 | 29.12.2021 13.46 | PETRO-QUANT2-Oil-short_aqueous | 70.3 | 100.5 | 43.8 | 40.6 | 31.9 | 70.9 | 72.6 | 37.1 | 16.6 | 11.8 | 100.63 |
| testiliuos2_PQ_2 | 29.12.2021 13.32 | PETRO-QUANT2-Oil-short_aqueous | 70.7 | 83.8 | 44.4 | 36.6 | 28 | 59.4 | 66.8 | 32.6 | 14.7 | 11.9 | 100.69 |
| testiliuos2_PQ_1 | 29.12.2021 13.17 | PETRO-QUANT2-Oil-short_aqueous | 87.7 | 94.6 | 45.3 | 37.7 | 29.9 | 67.9 | 68.4 | 34.1 | 16 | 12.1 | 101.91 |
| testiliuos4_PQ_3 | 30.12.2021 9.02 | PETRO-QUANT2-Oil-short_aqueous | 21.7 | 23.8 | 19.5 | 8.3 | 7.4 | 0 | 11.6 | 6 | 2.7 | 0 | 100.02 |
| testiliuos4_PQ_2 | 30.12.2021 8.33 | PETRO-QUANT2-Oil-short_aqueous | 8 | 29.5 | 1.9 | 7.6 | 3.6 | 0 | 11 | 3.5 | 2.7 | 0 | 100.41 |
| testiliuos4_PQ_1 | 30.12.2021 8.20 | PETRO-QUANT2-Oil-short_aqueous | 15.9 | 24.8 | 9.5 | 6.3 | 4.8 | 0 | 7.9 | 5.1 | 3 | 0 | 103.16 |

APPENDIX 3

| Measurement method parameters for Wastewaters method | | | | | | | | | | |
|---|---|---|---|---|---|---|---|---|---|---|
| Analyte line | Tube current (mA) | Tube voltage (kV) | Filter | Collimator (°) | Crystal, 2d (nm) | Detector | Peak position (2θ) | Background positions (2θ) | Counting time peak/background | LLD rule |
| Na Kα1 | 33 | 30 | none | 0.46 | XS-55 2d=5.5 | FC | 25.018 | 23.322 / 26.851 | 100s/100s | LLD 10ppm |
| Mg Kα1 | 33 | 30 | none | 0.46 | XS-55 2d=5.5 | FC | 20.752 | 22.639 | 100s/100s | LLD 10ppm |
| Si Kα1 | 33 | 30 | none | 0.46 | PET 2d=0.874 | FC | 109.033 | 105.327 / 111.995 | 100s/100s | LLD 10ppm |
| PKα1 | 33 | 30 | none | 0.46 | PET 2d=0.874 | FC | 89.395 | 92.022 | 30s/30s | LLD 3ppm |
| S Kα1 | 33 | 30 | none | 0.46 | PET 2d=0.874 | FC | 75.747 | 79.275 | 30s/30s | LLD 10ppm |
| Cl Kα1 | 33 | 30 | none | 0.46 | PET 2d=0.874 | FC | 65.411 | 66.638 | 30s/30s | LLD 3ppm |
| K Kα1 | 20 | 50 | none | 0.46 | LiF200 2d=0.403 | FC | 136.664 | 139.538 | 30s/30s | LLD 3ppm |
| Ca Kα1 | 20 | 50 | none | 0.46 | LiF200 2d=0.403 | FC | 113.084 | 110.491 / 116.032 | 30s/30s | LLD 3ppm |
| Mn Kα1 | 20 | 50 | none | 0.23 | LiF200 2d=0.403 | SC | 62.968 | 61.834 / 64.096 | 30s/30s | LLD 3ppm |
| Fe Kα1 | 20 | 50 | none | 0.23 | LiF200 2d=0.403 | SC | 57.533 | 58.758 | 30s/30s | LLD 3ppm |
| FC = flow counter<br>SC = scintillation counter<br>LLD = lower limit of detection | | | | | | | | | | |

APPENDIX 4

## Na KA1-HS-Tr/Wastewaters_151221
## Wastewaters_151221.evm

Abridged calibration data for line Na KA1-HS-Tr/Wastewaters_151221
S/N 215396, Mask: 34 mm, Mode: Helium,  30 kV , 33 mA, Filter: None, Be: 75µm
Crystal (nominal): 2d = 55,1 Ao, Collimator aperture (nominal) = 0,46 degrees
Detector: flow counter LLD = 50, ULD = 150 % of nominal peak.
Adjusted peak at 25,018 degrees 2-theta, Wavelength = 11,91 Ao
Background  1 at 23,322 degrees 2-theta, weight 0,5196
Background  2 at 26,851 degrees 2-theta, weight 0,4804
Calibration data for compound Na in original sample
Absorption correction: None
Intensity model: net intensity
Minimization target: absolute error,  11 standards from 0 PPM  to 1000 PPM
Standard deviation: 9 PPM
Squared correlation coefficient: 0,999559
Slope: 0,2696 %/kcps / Sensitivity: 3,709 kcps/% (Adjustable by regression)

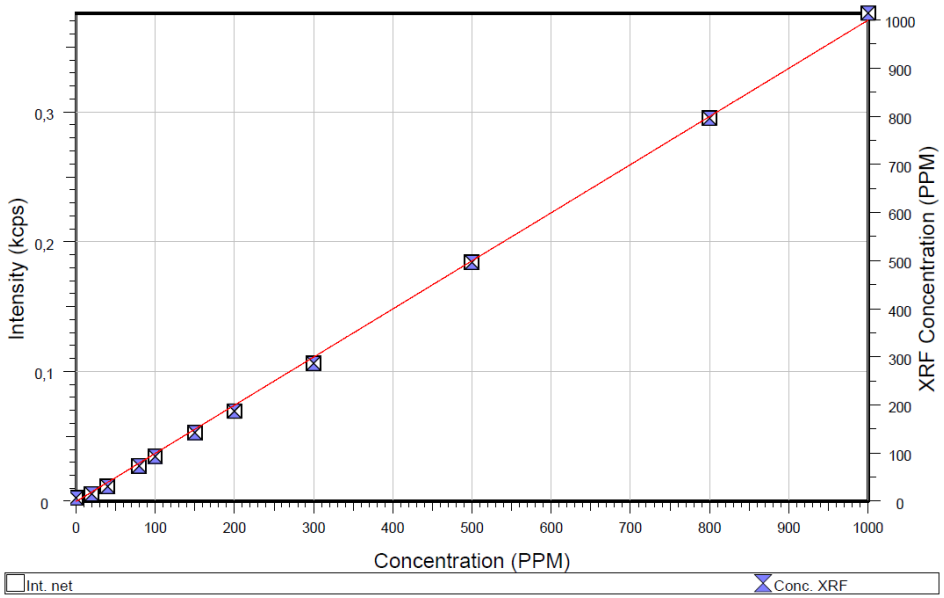


## Na KA1-HS-Tr/Wastewaters_151221
## Wastewaters_151221.evm

| # | Name | Net. Int. | Chem.Conc. | XRF.Conc. | Abs.Dev. | Rel.Dev. | LLD(PPM) |
|---|---|---|---|---|---|---|---|
| 11 | Wastewater_Blank | 0,0026 | Trace | 6,9 | 6,9 | | 5,5 |
| 1 | Wastewater_STD1 | 0,0057 | 20,0 | 15,5 | -4,5 | -22,729 | 5,5 |
| 2 | Wastewater_STD2 | 0,0114 | 40,0 | 30,7 | -9,3 | -23,339 | 5,5 |
| 3 | Wastewater_STD3 | 0,0272 | 80,0 | 73,3 | -6,7 | -8,427 | 5,6 |
| 4 | Wastewater_STD4 | 0,0345 | 100,0 | 92,9 | -7,1 | -7,091 | 5,7 |
| 5 | Wastewater_STD5 | 0,0529 | 150,0 | 142,5 | -7,5 | -4,999 | 5,6 |
| 6 | Wastewater_STD6 | 0,0694 | 200,0 | 187,1 | -12,9 | -6,465 | 5,7 |
| 7 | Wastewater_STD7 | 0,1062 | 300,0 | 286,2 | -13,8 | -4,586 | 5,8 |
| 8 | Wastewater_STD8 | 0,1841 | 500,0 | 496,4 | -3,6 | -0,727 | 5,8 |
| 9 | Wastewater_STD9 | 0,2952 | 800,0 | 795,8 | -4,2 | -0,529 | 5,8 |
| 10 | Wastewater_STD10 | 0,3761 | 1000,0 | 1013,9 | 13,9 | 1,387 | 5,8 |

APPENDIX 5

## Mg KA1-HS-Tr/Wastewaters_151221
## Wastewaters_151221.evm

Abridged calibration data for line Mg KA1-HS-Tr/Wastewaters_151221
S/N 215396, Mask: 34 mm, Mode: Helium, 30 kV , 33 mA, Filter: None, Be: 75µm
Crystal (nominal): 2d = 55,1 Ao, Collimator aperture (nominal) = 0,46 degrees
Detector: flow counter LLD = 50, ULD = 150 % of nominal peak.
Adjusted peak at 20,752 degrees 2-theta, Wavelength = 9,893 Ao
Background 1 at 22,639 degrees 2-theta, weight 1
Calibration data for compound Mg in original sample
Absorption correction: None
Intensity model: net intensity
Minimization target: absolute error, 10 standards from 0 PPM to 1000 PPM
Standard deviation: 3 PPM
Squared correlation coefficient: 0,999897
Slope: 0,08314 %/kcps / Sensitivity: 12,03 kcps/% (Adjustable by regression)
Corrected intensity offset: -0,05184 kcps (Adjustable by regression) or 43,1 PPM

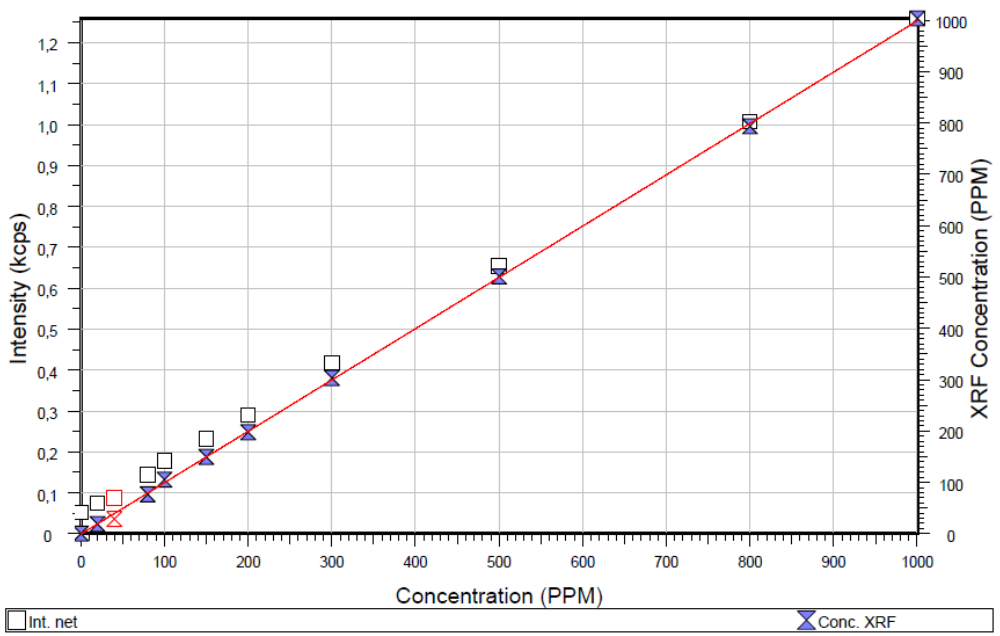


## Mg KA1-HS-Tr/Wastewaters_151221
## Wastewaters_151221.evm

| # | Name | Net. Int. | Chem.Conc. | XRF.Conc. | Abs.Dev. | Rel.Dev. | LLD(PPM) |
|---|---|---|---|---|---|---|---|
| 11 | Wastewater_Blank | 0,0518 | Trace | -0,1 | -0,1 | | 2,6 |
| 1 | Wastewater_STD1 | 0,0745 | 20,0 | 18,8 | -1,2 | -5,916 | 2,5 |
| ~~2~~ | ~~Wastewater_STD2~~ | ~~0,0863~~ | ~~40,0~~ | ~~28,7~~ | ~~-11,3~~ | ~~-28,334~~ | ~~2,5~~ |
| 3 | Wastewater_STD3 | 0,1440 | 80,0 | 76,6 | -3,4 | -4,196 | 2,6 |
| 4 | Wastewater_STD4 | 0,1783 | 100,0 | 105,2 | 5,2 | 5,156 | 2,6 |
| 5 | Wastewater_STD5 | 0,2319 | 150,0 | 149,7 | -0,3 | -0,216 | 2,6 |
| 6 | Wastewater_STD6 | 0,2898 | 200,0 | 197,9 | -2,1 | -1,059 | 2,6 |
| 7 | Wastewater_STD7 | 0,4167 | 300,0 | 303,4 | 3,4 | 1,119 | 2,6 |
| 8 | Wastewater_STD8 | 0,6548 | 500,0 | 501,3 | 1,3 | 0,264 | 2,7 |
| 9 | Wastewater_STD9 | 1,0065 | 800,0 | 793,7 | -6,3 | -0,791 | 2,7 |
| 10 | Wastewater_STD10 | 1,2589 | 1000,0 | 1003,5 | 3,5 | 0,353 | 2,7 |

APPENDIX 6

## Si KA1-HS-Tr/Wastewaters_151221
## Wastewaters_151221.evm

Abridged calibration data for line Si KA1-HS-Tr/Wastewaters_151221
S/N 215396, Mask: 34 mm, Mode: Helium, 30 kV , 33 mA, Filter: None, Be: 75µm
Crystal (nominal): 2d = 8,752 Ao, Collimator aperture (nominal) = 0,46 degrees
Detector: flow counter LLD = 60, ULD = 140 % of nominal peak.
Adjusted peak at 109,033 degrees 2-theta, Wavelength = 7,1254 Ao
Background 1 at 105,327 degrees 2-theta, weight 0,4443
Background 2 at 111,995 degrees 2-theta, weight 0,5557
Calibration data for compound Si in original sample
Absorption correction: None
Intensity model: net intensity
Minimization target: absolute error, 8 standards from 0 PPM to 200 PPM
Standard deviation: 4 PPM
Squared correlation coefficient: 0,998806
Slope: 0,06965 %/kcps / Sensitivity: 14,36 kcps/% (Adjustable by regression)

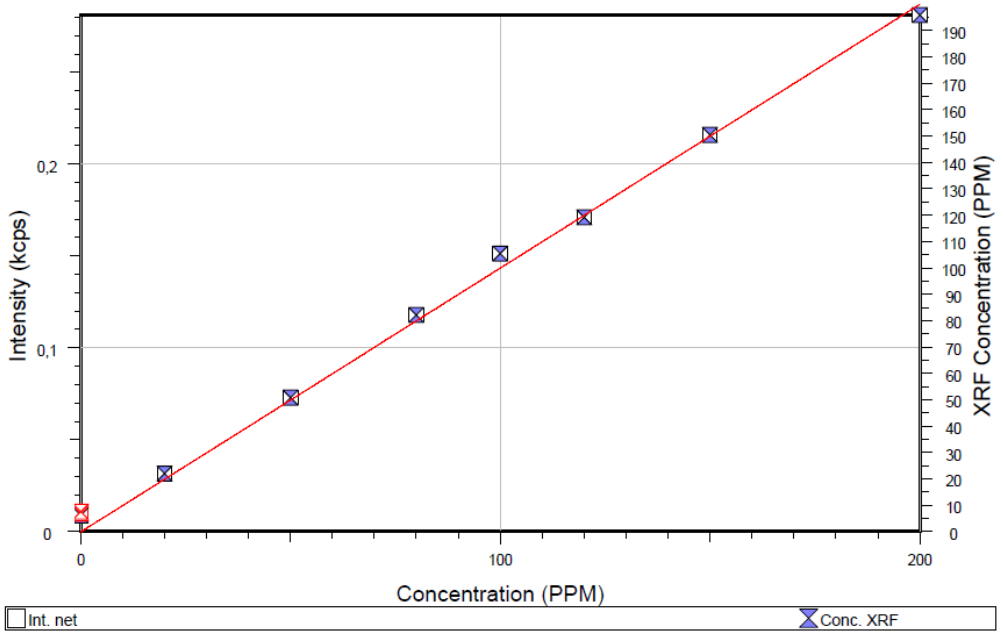


## Si KA1-HS-Tr/Wastewaters_151221
## Wastewaters_151221.evm

| # | Name | Net. Int. | Chem.Conc. | XRF.Conc. | Abs.Dev. | Rel.Dev. | LLD(PPM) |
|---|---|---|---|---|---|---|---|
| ~~8~~ | ~~Wastewater_STD8~~ | ~~0,0109~~ | ~~Trace~~ | ~~7,6~~ | ~~7,6~~ | | ~~1,3~~ |
| ~~9~~ | ~~Wastewater_STD9~~ | ~~0,0100~~ | ~~Trace~~ | ~~6,9~~ | ~~6,9~~ | | ~~1,3~~ |
| ~~10~~ | ~~Wastewater_STD10~~ | ~~0,0103~~ | ~~Trace~~ | ~~7,1~~ | ~~7,1~~ | | ~~1,3~~ |
| 11 | Wastewater_Blank | 0,0089 | Trace | 6,2 | 6,2 | | 1,3 |
| 1 | Wastewater_STD1 | 0,0317 | 20,0 | 22,1 | 2,1 | 10,273 | 1,3 |
| 2 | Wastewater_STD2 | 0,0729 | 50,0 | 50,8 | 0,8 | 1,520 | 1,3 |
| 3 | Wastewater_STD3 | 0,1180 | 80,0 | 82,2 | 2,2 | 2,708 | 1,3 |
| 4 | Wastewater_STD4 | 0,1513 | 100,0 | 105,4 | 5,4 | 5,405 | 1,3 |
| 5 | Wastewater_STD5 | 0,1710 | 120,0 | 119,1 | -0,9 | -0,736 | 1,3 |
| 6 | Wastewater_STD6 | 0,2159 | 150,0 | 150,4 | 0,4 | 0,262 | 1,3 |
| 7 | Wastewater_STD7 | 0,2811 | 200,0 | 195,8 | -4,2 | -2,104 | 1,3 |

APPENDIX 7

## P KA1-HS-Tr/Wastewaters_151221
## Wastewaters_151221.evm

Abridged calibration data for line P KA1-HS-Tr/Wastewaters_151221
S/N 215396, Mask: 34 mm, Mode: Helium, 30 kV , 33 mA, Filter: None, Be: 75µm
Crystal (nominal): 2d = 8,752 Ao, Collimator aperture (nominal) = 0,46 degrees
Detector: flow counter LLD = 60, ULD = 140 % of nominal peak.
Adjusted peak at 89,395 degrees 2-theta, Wavelength = 6,157 Ao
Background 1 at 92,022 degrees 2-theta, weight 1
Calibration data for compound P in original sample
Absorption correction: None
Intensity model: net intensity
Minimization target: absolute error, 10 standards from 0 PPM to 500 PPM
Standard deviation: 5 PPM
Squared correlation coefficient: 0,999190
Slope: 0,0503 %/kcps / Sensitivity: 19,88 kcps/% (Adjustable by regression)

## P KA1-HS-Tr/Wastewaters_151221
## Wastewaters_151221.evm

| # | Name | Net. Int. | Chem.Conc. | XRF.Conc. | Abs.Dev. | Rel.Dev. | LLD(PPM) |
|---|---|---|---|---|---|---|---|
| 1 | Wastewater_STD1 | 0,0440 | 20,0 | 22,1 | 2,1 | 10,608 | 1,6 |
| 2 | Wastewater_STD2 | 0,0927 | 50,0 | 46,6 | -3,4 | -6,760 | 1,7 |
| 3 | Wastewater_STD3 | 0,1517 | 80,0 | 76,3 | -3,7 | -4,615 | 1,6 |
| 4 | Wastewater_STD4 | 0,1981 | 100,0 | 99,7 | -0,3 | -0,323 | 1,7 |
| 5 | Wastewater_STD5 | 0,2282 | 120,0 | 114,8 | -5,2 | -4,320 | 1,6 |
| 6 | Wastewater_STD6 | 0,2789 | 150,0 | 140,3 | -9,7 | -6,479 | 1,6 |
| 7 | Wastewater_STD7 | 0,3968 | 200,0 | 199,6 | -0,4 | -0,191 | 1,7 |
| ~~8~~ | ~~Wastewater_STD8~~ | ~~0,0060~~ | ~~Trace~~ | ~~2,5~~ | ~~2,5~~ | | ~~1,7~~ |
| ~~9~~ | ~~Wastewater_STD9~~ | ~~0,0045~~ | ~~Trace~~ | ~~2,3~~ | ~~2,3~~ | | ~~1,7~~ |
| ~~10~~ | ~~Wastewater_STD10~~ | ~~0,0035~~ | ~~Trace~~ | ~~1,7~~ | ~~1,7~~ | | ~~1,7~~ |
| 11 | Wastewater_Blank | 0,0082 | Trace | 4,1 | 4,1 | | 1,7 |
| 12 | Vastewater_STD1 | 0,6033 | 300,0 | 303,5 | 3,5 | 1,165 | 1,7 |
| 13 | Vastewater_STD1 | 0,9994 | 500,0 | 502,7 | 2,7 | 0,549 | 1,7 |
| ~~14~~ | ~~Wastewater_STD13~~ | ~~0,0048~~ | ~~Trace~~ | ~~2,4~~ | ~~2,4~~ | | ~~1,8~~ |
| ~~15~~ | ~~Wastewater_STD14~~ | ~~0,0090~~ | ~~Trace~~ | ~~4,5~~ | ~~4,5~~ | | ~~1,8~~ |
| ~~16~~ | ~~Wastewater_STD15~~ | ~~0,0014~~ | ~~Trace~~ | ~~0,7~~ | ~~0,7~~ | | ~~1,8~~ |

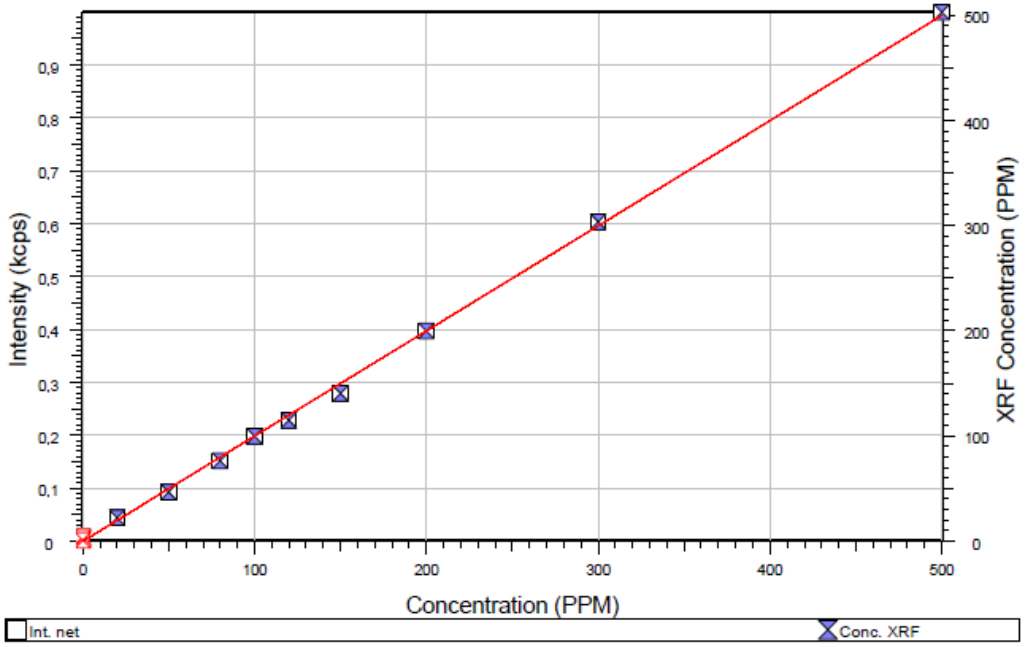

APPENDIX 8

## S KA1-HS-Min/Wastewaters_151221
## Wastewaters_151221.evm

Abridged calibration data for line S KA1-HS-Min/Wastewaters_151221
S/N 215396, Mask: 34 mm, Mode: Helium, 30 kV , 33 mA, Filter: None, Be: 75µm
Crystal (nominal): 2d = 8,752 Ao, Collimator aperture (nominal) = 0,46 degrees
Detector: flow counter LLD = 50, ULD = 150 % of nominal peak.
Adjusted peak at 75,747 degrees 2-theta, Wavelength = 5,3722 Ao
Background 1 at 79,275 degrees 2-theta, weight 1
Calibration data for compound S in original sample
Absorption correction: None
Intensity model: net intensity
Minimization target: absolute error, 9 standards from 0 PPM to 2000 PPM
Standard deviation: 15 PPM
Squared correlation coefficient: 0,999616
Slope: 0,02543 %/kcps / Sensitivity: 39,32 kcps/% (Adjustable by regression)

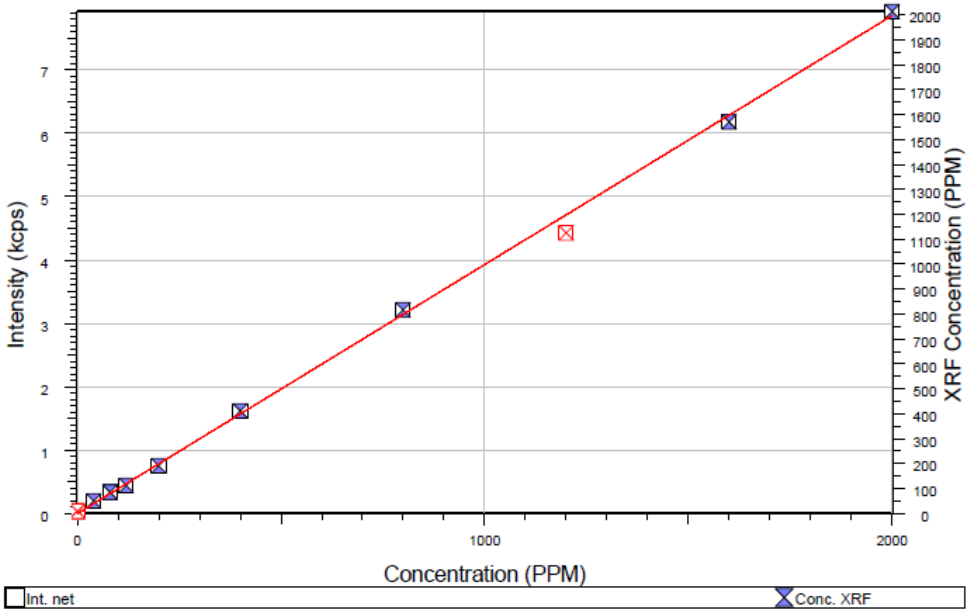


## S KA1-HS-Min/Wastewaters_151221
## Wastewaters_151221.evm

| # | Name | Net. Int. | Chem.Conc. | XRF.Conc. | Abs.Dev. | Rel.Dev. | LLD(PPM) |
|---|---|---|---|---|---|---|---|
| 1 | Wastewater_STD1 | 0,1956 | 40,0 | 49,7 | 9,7 | 24,369 | 1,2 |
| 2 | Wastewater_STD2 | 0,3355 | 80,0 | 85,3 | 5,3 | 6,664 | 1,2 |
| 3 | Wastewater_STD3 | 0,4397 | 120,0 | 111,8 | -8,2 | -6,818 | 1,1 |
| 4 | Wastewater_STD4 | 0,7501 | 200,0 | 190,8 | -9,2 | -4,610 | 1,1 |
| ~~5~~ | ~~Wastewater_STD5~~ | ~~0,0330~~ | ~~Trace~~ | ~~8,4~~ | ~~8,4~~ | | ~~1,1~~ |
| ~~6~~ | ~~Wastewater_STD6~~ | ~~0,0270~~ | ~~Trace~~ | ~~7,1~~ | ~~7,1~~ | | ~~1,2~~ |
| ~~7~~ | ~~Wastewater_STD7~~ | ~~0,0333~~ | ~~Trace~~ | ~~8,5~~ | ~~8,5~~ | | ~~1,1~~ |
| ~~8~~ | ~~Wastewater_STD8~~ | ~~0,0315~~ | ~~Trace~~ | ~~8,0~~ | ~~8,0~~ | | ~~1,2~~ |
| ~~9~~ | ~~Wastewater_STD9~~ | ~~0,0328~~ | ~~Trace~~ | ~~8,3~~ | ~~8,3~~ | | ~~1,2~~ |
| ~~10~~ | ~~Wastewater_STD10~~ | ~~0,0360~~ | ~~Trace~~ | ~~9,4~~ | ~~9,4~~ | | ~~1,2~~ |
| 11 | Wastewater_Blank | 0,0395 | Trace | 10,0 | 10,0 | | 1,2 |
| 12 | Wastewater_STD11 | 1,6154 | 400,0 | 410,8 | 10,8 | 2,707 | 1,2 |
| 13 | Wastewater_STD12 | 3,2100 | 800,0 | 816,4 | 16,4 | 2,047 | 1,2 |
| ~~14~~ | ~~Wastewater_STD13~~ | ~~4,4279~~ | ~~1200,0~~ | ~~1126,1~~ | ~~-73,9~~ | ~~-6,156~~ | ~~1,2~~ |
| 15 | Wastewater_STD14 | 6,1799 | 1600,0 | 1571,7 | -28,3 | -1,769 | 1,2 |
| 16 | Wastewater_STD15 | 7,9193 | 2000,0 | 2014,1 | 14,1 | 0,703 | 1,3 |

APPENDIX 9

## Cl KA1-HS-Tr/Wastewaters_151221
## Wastewaters_151221.evm

Abridged calibration data for line Cl KA1-HS-Tr/Wastewaters_151221
S/N 215396, Mask: 34 mm, Mode: Helium, 30 kV , 33 mA, Filter: None, Be: 75µm
Crystal (nominal): 2d = 8,752 Ao, Collimator aperture (nominal) = 0,46 degrees
Detector: flow counter LLD = 60, ULD = 140 % of nominal peak.
Adjusted peak at 65,411 degrees 2-theta, Wavelength = 4,7278 Ao
Background 1 at 66,638 degrees 2-theta, weight 1
Calibration data for compound Cl in original sample
Absorption correction: None
Intensity model: net intensity
Minimization target: absolute error, 10 standards from 0 PPM to 1234 PPM
Standard deviation: 4 PPM
Squared correlation coefficient: 0,999897
Slope: 0,04144 %/kcps / Sensitivity: 24,13 kcps/% (Adjustable by regression)
Corrected intensity offset: -0,2233 kcps (Adjustable by regression) or 92,5 PPM

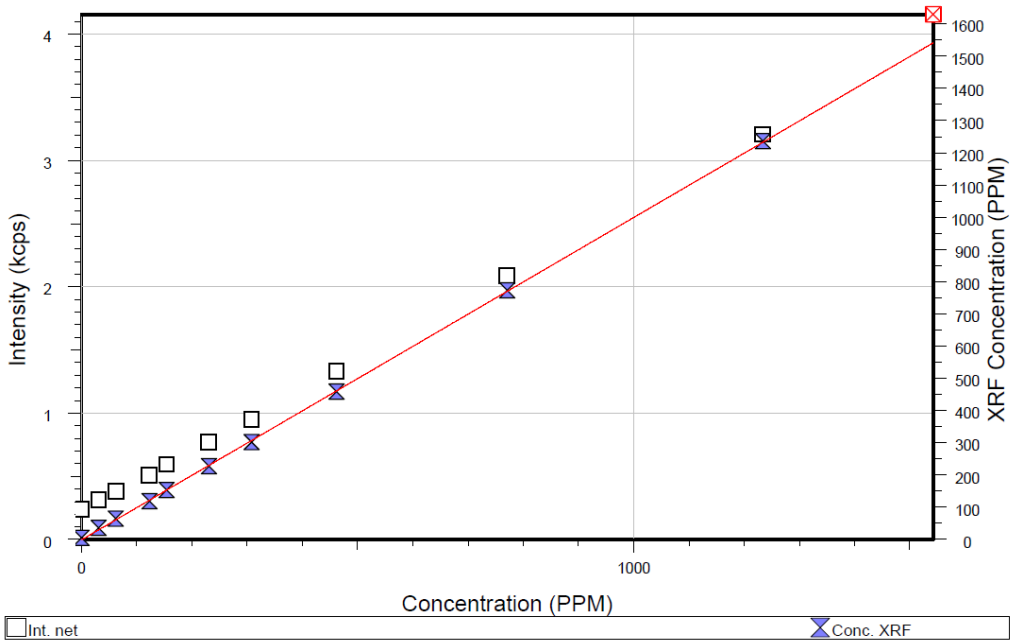


## Cl KA1-HS-Tr/Wastewaters_151221
## Wastewaters_151221.evm

| # | Name | Net. Int. | Chem.Conc. | XRF.Conc. | Abs.Dev. | Rel.Dev. | LLD(PPM) |
|---|---|---|---|---|---|---|---|
| 11 | Wastewater_Blank | 0,2355 | Trace | 5,1 | 5,1 | | 4,5 |
| 1 | Wastewater_STD1 | 0,3104 | 31,0 | 36,1 | 5,1 | 16,532 | 4,4 |
| 2 | Wastewater_STD2 | 0,3795 | 62,0 | 64,7 | 2,7 | 4,411 | 4,4 |
| 3 | Wastewater_STD3 | 0,5092 | 123,0 | 118,5 | -4,5 | -3,671 | 4,2 |
| 4 | Wastewater_STD4 | 0,5943 | 154,0 | 153,7 | -0,3 | -0,164 | 4,3 |
| 5 | Wastewater_STD5 | 0,7728 | 231,0 | 227,7 | -3,3 | -1,425 | 4,3 |
| 6 | Wastewater_STD6 | 0,9527 | 308,0 | 302,3 | -5,7 | -1,859 | 4,3 |
| 7 | Wastewater_STD7 | 1,3302 | 462,0 | 458,7 | -3,3 | -0,713 | 4,3 |
| 8 | Wastewater_STD8 | 2,0889 | 771,0 | 773,1 | 2,1 | 0,271 | 4,3 |
| 9 | Wastewater_STD9 | 3,2062 | 1234,0 | 1236,1 | 2,1 | 0,168 | 4,4 |
| ~~10~~ | ~~Wastewater_STD10~~ | ~~4,1550~~ | ~~1542,0~~ | ~~1629,3~~ | ~~87,3~~ | ~~5,659~~ | ~~4,5~~ |

## K KA1-HS-Tr/Wastewaters_151221 Wastewaters_151221.evm

Abridged calibration data for line K KA1-HS-Tr/Wastewaters_151221
S/N 215396, Mask: 34 mm, Mode: Helium, 50 kV , 20 mA, Filter: None, Be: 75µm
Crystal (nominal): 2d = 4,026 Ao, Collimator aperture (nominal) = 0,46 degrees
Detector: flow counter LLD = 60, ULD = 140 % of nominal peak.
Adjusted peak at 136,664 degrees 2-theta, Wavelength = 3,7414 Ao
Background 1 at 139,538 degrees 2-theta, weight 1
Calibration data for compound K in original sample
Absorption correction: None
Intensity model: net intensity
Minimization target: absolute error, 11 standards from 0 PPM to 1000 PPM
Standard deviation: 7 PPM
Squared correlation coefficient: 0,999622
Slope: 0,02003 %/kcps / Sensitivity: 49,94 kcps/% (Adjustable by regression)

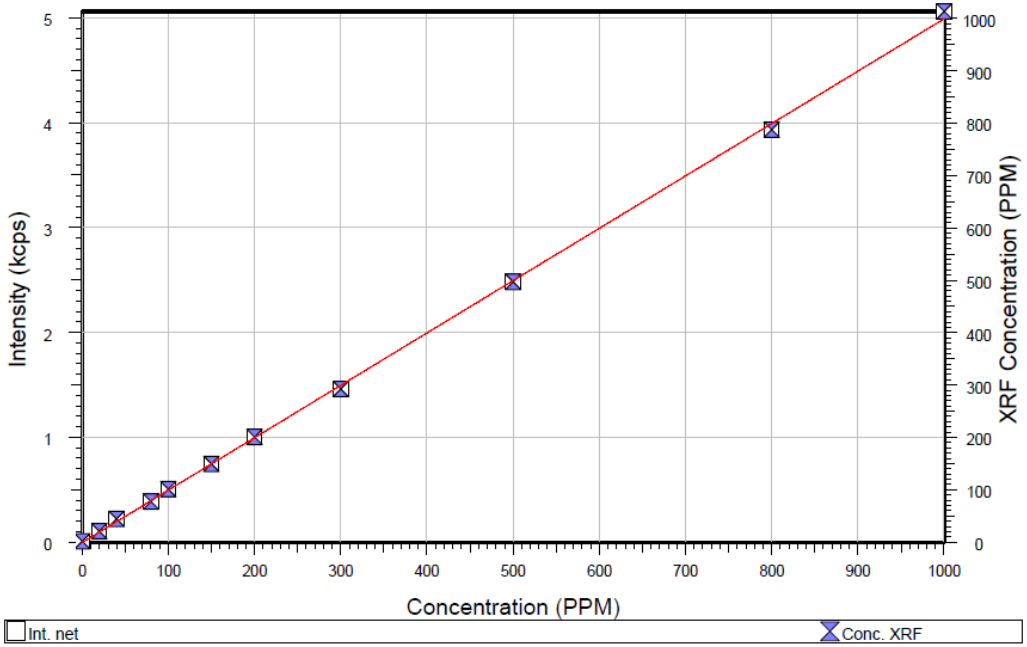


## K KA1-HS-Tr/Wastewaters_151221 Wastewaters_151221.evm

| # | Name | Net. Int. | Chem.Conc. | XRF.Conc. | Abs.Dev. | Rel.Dev. | LLD(PPM) |
|---|---|---|---|---|---|---|---|
| 11 | Wastewater_Blank | 0,0103 | Trace | 2,1 | 2,1 | | 1,4 |
| 1 | Wastewater_STD1 | 0,1053 | 20,0 | 21,1 | 1,1 | 5,442 | 1,4 |
| 2 | Wastewater_STD2 | 0,2228 | 40,0 | 44,6 | 4,6 | 11,552 | 1,3 |
| 3 | Wastewater_STD3 | 0,3876 | 80,0 | 77,6 | -2,4 | -2,970 | 1,3 |
| 4 | Wastewater_STD4 | 0,5065 | 100,0 | 101,4 | 1,4 | 1,425 | 1,3 |
| 5 | Wastewater_STD5 | 0,7457 | 150,0 | 149,3 | -0,7 | -0,444 | 1,3 |
| 6 | Wastewater_STD6 | 1,0040 | 200,0 | 201,1 | 1,1 | 0,530 | 1,3 |
| 7 | Wastewater_STD7 | 1,4607 | 300,0 | 292,5 | -7,5 | -2,494 | 1,3 |
| 8 | Wastewater_STD8 | 2,4824 | 500,0 | 497,1 | -2,9 | -0,577 | 1,3 |
| 9 | Wastewater_STD9 | 3,9318 | 800,0 | 787,4 | -12,6 | -1,578 | 1,4 |
| 10 | Vastewater_STD1 | 5,0589 | 1000,0 | 1013,1 | 13,1 | 1,309 | 1,4 |

APPENDIX 11

## Ca KA1-HS-Tr/Wastewaters_151221
## Wastewaters_151221.evm

Abridged calibration data for line Ca KA1-HS-Tr/Wastewaters_151221
S/N 215396, Mask: 34 mm, Mode: Helium, 50 kV , 20 mA, Filter: None, Be: 75µm
Crystal (nominal): 2d = 4,026 Ao, Collimator aperture (nominal) = 0,46 degrees
Detector: flow counter LLD = 60, ULD = 140 % of nominal peak.
Adjusted peak at 113,084 degrees 2-theta, Wavelength = 3,3584 Ao
Background 1 at 110,491 degrees 2-theta, weight 0,5322
Background 2 at 116,032 degrees 2-theta, weight 0,4678
Calibration data for compound Ca in original sample
Absorption correction: None
Intensity model: net intensity
Minimization target: absolute error, 9 standards from 0 PPM to 200 PPM
Standard deviation: 2 PPM
Squared correlation coefficient: 0,999314
Slope: 0,01748 %/kcps / Sensitivity: 57,21 kcps/% (Adjustable by regression)

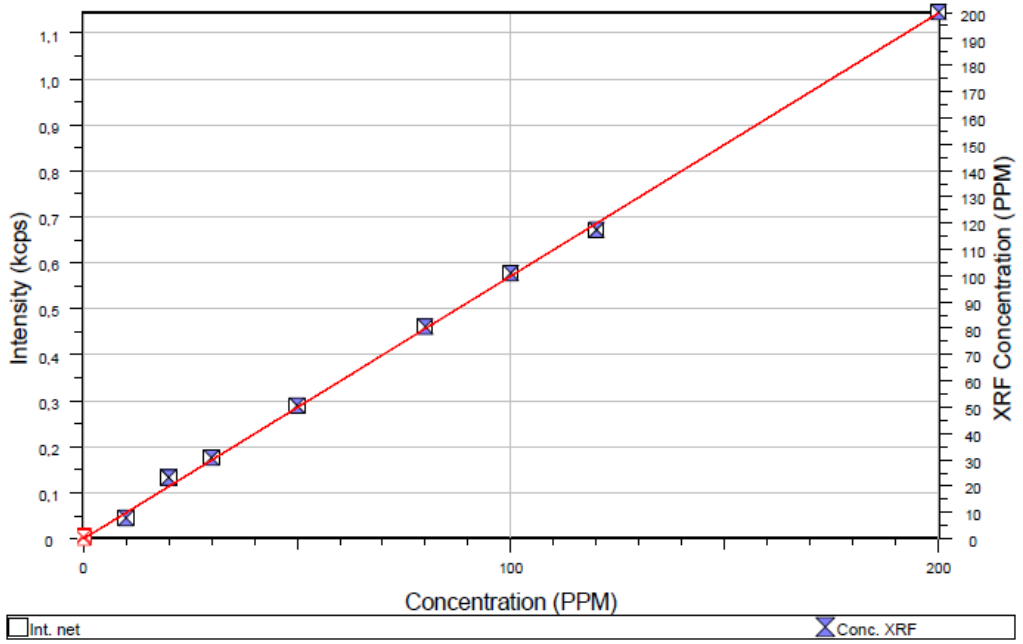


## Ca KA1-HS-Tr/Wastewaters_151221
## Wastewaters_151221.evm

| # | Name | Net. Int. | Chem.Conc. | XRF.Conc. | Abs.Dev. | Rel.Dev. | LLD(PPM) |
|---|---|---|---|---|---|---|---|
| ~~9~~ | ~~Wastewater_STD9~~ | ~~0,0028~~ | ~~Trace~~ | ~~0,5~~ | ~~0,5~~ | | ~~1,3~~ |
| ~~10~~ | ~~Wastewater_STD10~~ | ~~0,0066~~ | ~~Trace~~ | ~~1,2~~ | ~~1,2~~ | | ~~1,3~~ |
| 11 | Wastewater_Blank | 0,0050 | Trace | 0,9 | 0,9 | | 1,3 |
| 1 | Wastewater_STD1 | 0,0454 | 10,0 | 7,9 | -2,1 | | 1,4 |
| 2 | Wastewater_STD2 | 0,1331 | 20,0 | 23,3 | 3,3 | 16,332 | 1,3 |
| 3 | Wastewater_STD3 | 0,1761 | 30,0 | 30,8 | 0,8 | 2,581 | 1,3 |
| 4 | Wastewater_STD4 | 0,2896 | 50,0 | 50,6 | 0,6 | 1,246 | 1,3 |
| 5 | Wastewater_STD5 | 0,4612 | 80,0 | 80,6 | 0,6 | 0,750 | 1,3 |
| 6 | Wastewater_STD6 | 0,5777 | 100,0 | 101,0 | 1,0 | 0,972 | 1,3 |
| 7 | Wastewater_STD7 | 0,6718 | 120,0 | 117,4 | -2,6 | -2,146 | 1,2 |
| 8 | Wastewater_STD8 | 1,1454 | 200,0 | 200,2 | 0,2 | 0,100 | 1,3 |

## Mn KA1-HR-Tr/Wastewaters_151221 Wastewaters_151221.evm

Abridged calibration data for line Mn KA1-HR-Tr/Wastewaters_151221
S/N 215396, Mask: 34 mm, Mode: Helium, 50 kV , 20 mA, Filter: None, Be: 75µm
Crystal (nominal): 2d = 4,026 Ao, Collimator aperture (nominal) = 0,23 degrees
Detector: scintillation counter LLD = 60, ULD = 140 % of nominal peak.
Adjusted peak at 62,968 degrees 2-theta, Wavelength = 2,1018 Ao
Background 1 at 61,834 degrees 2-theta, weight 0,4988
Background 2 at 64,096 degrees 2-theta, weight 0,5012
Calibration data for compound Mn in original sample
Absorption correction: None
Intensity model: net intensity
Minimization target: absolute error, 11 standards from 0 PPM to 200 PPM
Standard deviation: 2 PPM
Squared correlation coefficient: 0,999463
Slope: 0,004725 %/kcps / Sensitivity: 211,6 kcps/% (Adjustable by regression)

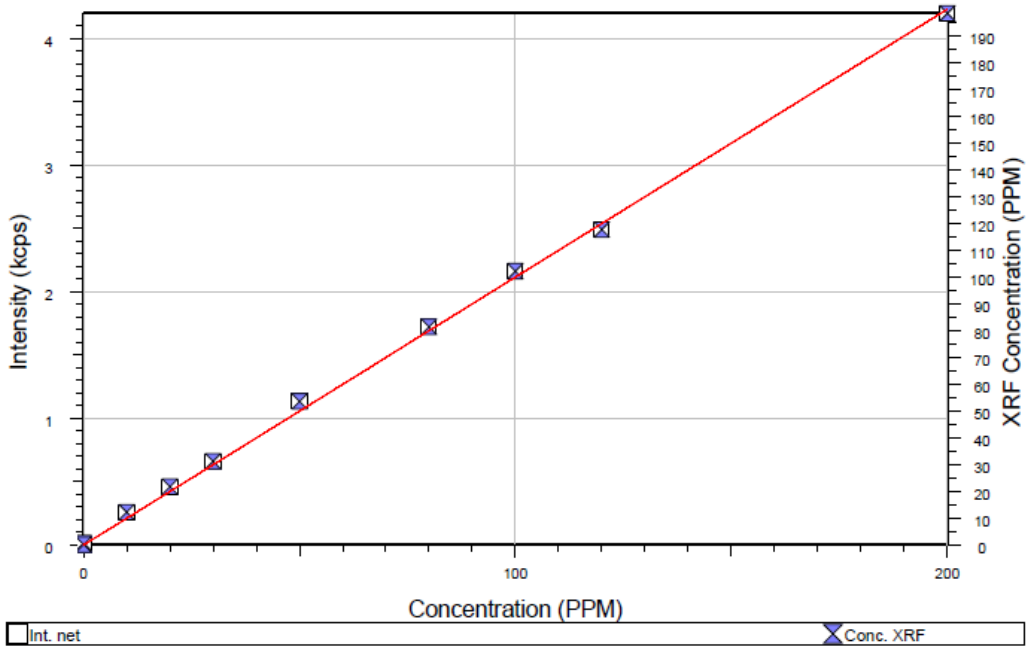


## Mn KA1-HR-Tr/Wastewaters_151221 Wastewaters_151221.evm

| # | Name | Net. Int. | Chem.Conc. | XRF.Conc. | Abs.Dev. | Rel.Dev. | LLD(PPM) |
|---|---|---|---|---|---|---|---|
| 9 | Wastewater_STD9 | 0,0014 | Trace | 0,1 | 0,1 | | 0,6 |
| 10 | Wastewater_STD10 | 0,0116 | Trace | 0,5 | 0,5 | | 0,6 |
| 11 | Wastewater_Blank | 0,0107 | Trace | 0,5 | 0,5 | | 0,7 |
| 1 | Wastewater_STD1 | 0,2568 | 10,0 | 12,1 | 2,1 | | 0,7 |
| 2 | Wastewater_STD2 | 0,4590 | 20,0 | 21,7 | 1,7 | 8,4371 | 0,7 |
| 3 | Wastewater_STD3 | 0,6597 | 30,0 | 31,2 | 1,2 | 3,8993 | 0,7 |
| 4 | Wastewater_STD4 | 1,1317 | 50,0 | 53,5 | 3,5 | 6,9458 | 0,7 |
| 5 | Wastewater_STD5 | 1,7212 | 80,0 | 81,3 | 1,3 | 1,6570 | 0,7 |
| 6 | Wastewater_STD6 | 2,1608 | 100,0 | 102,1 | 2,1 | 2,0954 | 0,7 |
| 7 | Wastewater_STD7 | 2,4907 | 120,0 | 117,7 | -2,3 | -1,9327 | 0,6 |
| 8 | Wastewater_STD8 | 4,1973 | 200,0 | 198,3 | -1,7 | -0,8421 | 0,7 |

## Fe KA1-HR-Tr/Wastewaters_151221 Wastewaters_151221.evm

Abridged calibration data for line Fe KA1-HR-Tr/Wastewaters_151221
S/N 215396, Mask: 34 mm, Mode: Helium, 50 kV , 20 mA, Filter: None, Be: 75µm
Crystal (nominal): 2d = 4,026 Ao, Collimator aperture (nominal) = 0,23 degrees
Detector: scintillation counter LLD = 60, ULD = 140 % of nominal peak.
Adjusted peak at 57,533 degrees 2-theta, Wavelength = 1,936 Ao
Background 1 at 58,758 degrees 2-theta, weight 1
Calibration data for compound Fe in original sample
Absorption correction: None
Intensity model: net intensity
Minimization target: absolute error, 7 standards from 0 PPM to 100 PPM
Standard deviation: 2 PPM
Squared correlation coefficient: 0,998311
Slope: 0,002999 %/kcps / Sensitivity: 333,5 kcps/% (Adjustable by regression)
Corrected intensity offset: -0,7373 kcps (Adjustable by regression) or 22,1 PPM

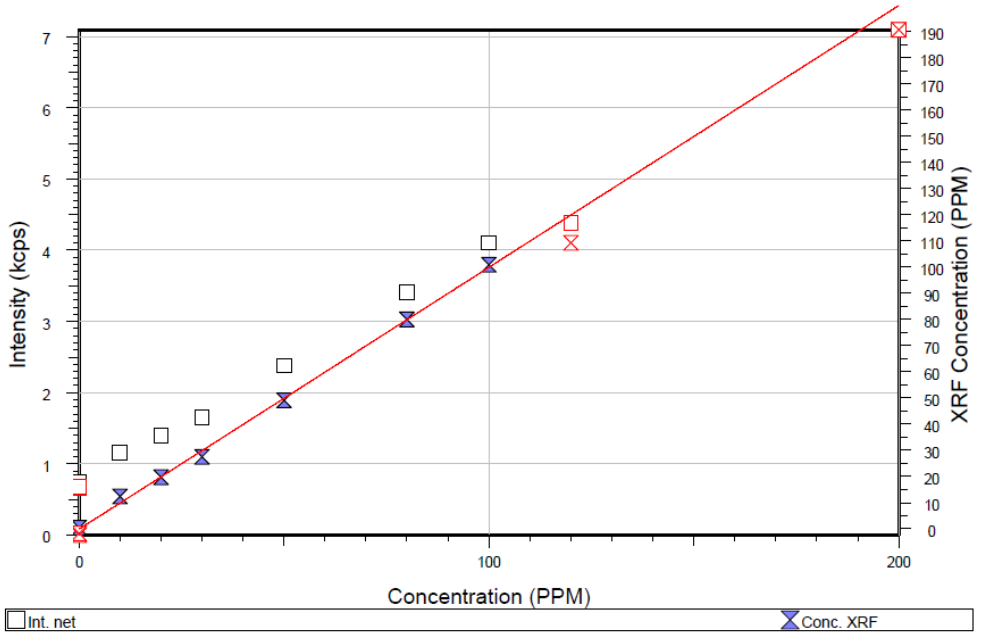


## Fe KA1-HR-Tr/Wastewaters_151221 Wastewaters_151221.evm

| # | Name | Net. Int. | Chem.Conc. | XRF.Conc. | Abs.Dev. | Rel.Dev. | LLD(PPM) |
|---|---|---|---|---|---|---|---|
| ~~9~~ | ~~Wastewater_STD9~~ | ~~0,6789~~ | ~~Trace~~ | ~~-1,8~~ | ~~-1,8~~ | | ~~0,7~~ |
| ~~10~~ | ~~Wastewater_STD10~~ | ~~0,6569~~ | ~~Trace~~ | ~~-2,4~~ | ~~-2,4~~ | | ~~0,7~~ |
| 11 | Wastewater_Blank | 0,7519 | Trace | 0,4 | 0,4 | | 0,7 |
| 1 | Wastewater_STD1 | 1,1509 | 10,0 | 12,4 | 2,4 | | 0,7 |
| 2 | Wastewater_STD2 | 1,3939 | 20,0 | 19,7 | -0,3 | -1,5528 | 0,7 |
| 3 | Wastewater_STD3 | 1,6534 | 30,0 | 27,5 | -2,5 | -8,4335 | 0,7 |
| 4 | Wastewater_STD4 | 2,3750 | 50,0 | 49,1 | -0,9 | -1,7829 | 0,7 |
| 5 | Wastewater_STD5 | 3,4064 | 80,0 | 80,0 | 0,0 | 0,0410 | 0,7 |
| 6 | Wastewater_STD6 | 4,1009 | 100,0 | 100,9 | 0,9 | 0,8604 | 0,7 |
| ~~7~~ | ~~Wastewater_STD7~~ | ~~4,3813~~ | ~~120,0~~ | ~~109,3~~ | ~~-10,7~~ | ~~-8,9445~~ | ~~0,7~~ |
| ~~8~~ | ~~Wastewater_STD8~~ | ~~7,0940~~ | ~~200,0~~ | ~~190,6~~ | ~~-9,4~~ | ~~-4,6950~~ | ~~0,7~~ |

APPENDIX 14

| XRF results for test solutions 5 and 6 (ppm) | | | | | | | | | | | | | |
|---|---|---|---|---|---|---|---|---|---|---|---|---|---|
| Sample Name | Measurement Finished | Na | Mg | Si | P | S | Cl | K | Ca | Mn | Fe | H2O (%) | Compton (%) |
| Testiliuos5_6 | 14.1.2022 10.38 | 27.8 | 27.5 | 27.4 | 12 | 14.7 | 2.3 | 11.8 | 7 | 4.2 | 6.9 | 99.9859 | 97.627 |
| Testiliuos5_5 | 14.1.2022 10.17 | 11 | 31.4 | 30.3 | 12.1 | 17.1 | 2.3 | 12.9 | 6.6 | 5.6 | 6.6 | 99.9864 | 98.629 |
| Testiliuos5_4 | 14.1.2022 9.57 | 12.6 | 32.8 | 28.3 | 12.1 | 18.5 | 16.6 | 12.4 | 7.4 | 5.7 | 6 | 99.9847 | 97.478 |
| Testiliuos5_3 | 14.1.2022 9.13 | 10.9 | 24.8 | 28.1 | 15 | 20.7 | 14.7 | 12.4 | 4.9 | 6.1 | 6.8 | 99.9856 | 96.831 |
| Testiliuos5_2 | 14.1.2022 8.53 | 34.8 | 27.8 | 23.9 | 12 | 19 | 12.4 | 12.6 | 7.6 | 6 | 5.7 | 99.9838 | 97.628 |
| Testiliuos5_1 | 14.1.2022 8.32 | 25.5 | 26.7 | 26.7 | 12.5 | 19.3 | 14.8 | 14 | 7.2 | 6.2 | 6.4 | 99.984 | 97.137 |
| Sample Name | Measurement Finished | | | | | | | | | | | | |
| Testiliuos6_6 | 17.1.2022 13.02 | 60.5 | 43.6 | 50.6 | 24.8 | 897.1 | 21.6 | 27.9 | 17.7 | 16.2 | 14.6 | 99.8825 | 98.122 |
| Testiliuos6_5 | 17.1.2022 12.41 | 48.1 | 57.1 | 63.4 | 31.4 | 1019.5 | 33.3 | 29.1 | 17.4 | 16 | 14.5 | 99.867 | 99.418 |
| Testiliuos6_4 | 17.1.2022 11.36 | 56.1 | 50.6 | 56.8 | 24.6 | 887.1 | 18.5 | 27.8 | 17.5 | 16.2 | 15.7 | 99.8829 | 98.056 |
| Testiliuos6_3 | 17.1.2022 11.13 | 54 | 53.4 | 57.2 | 25.8 | 889.6 | 19.8 | 25.5 | 16.6 | 14 | 14.8 | 99.8829 | 98.178 |
| Testiliuos6_2 | 17.1.2022 10.53 | 56.2 | 55.6 | 61.7 | 27.8 | 1047.2 | 35.7 | 30 | 17.5 | 16 | 15.7 | 99.8636 | 98.81 |
| Testiliuos6_1 | 17.1.2022 10.32 | 59.4 | 55.9 | 59.5 | 26.4 | 981.3 | 25.9 | 26.8 | 16.6 | 16.6 | 13 | 99.8719 | 99.186 |

APPENDIX 15

| XRF results for sample 22-00430 (ppm) | | | | | | | | | | | | |
|---|---|---|---|---|---|---|---|---|---|---|---|---|
| Sample Name | Na | Mg | Si | P | S | Cl | K | Ca | Mn | Fe | H2O (%) | Compton (%) |
| 22-00430-001_3 | 36 | 10.8 | 17 | 56.1 | 843.8 | 5.3 | 13 | 3.1 | 1.3 | 2.4 | 99.9011 | 96.761 |
| 22-00430-001_2 | 33.3 | 6.8 | 8.3 | 55.2 | 861.5 | 3.2 | 12.3 | 3.1 | 0.5 | 1.8 | 99.9014 | 96.935 |
| 22-00430-001_1 | 59.7 | 4.8 | 11.9 | 52.8 | 832.8 | 2.7 | 12.2 | 3.5 | 0.7 | 2 | 99.9017 | 96.66 |
| ICP-OES / IC results for sample 22-00430 (ppm) | | | | | | | | | | | | |
| 22-00430-001-1 | 53.284 | 1.229 | 2.821 | 45.014 | 188.493 | N/A | 8.962 | 2.411 | N/A | 0.105 | 10x dilution | |
| 22-00430-001-2 | 54.705 | 1.253 | 2.949 | 46.129 | 186.731 | N/A | 9.328 | 2.470 | N/A | 0.110 | 10x dilution | |
| 22-00430-001-3 | 54.041 | 1.227 | 2.911 | 45.686 | 184.946 | N/A | 9.136 | 2.441 | N/A | 0.109 | 10x dilution | |
| 22-00430-001-1 | 50.680 | 1.116 | 2.773 | 43.550 | 177.906 | 0.802 | 8.812 | 2.302 | 0.257 | 0.108 | 1.1x dilution | |
| 22-00430-001-2 | 50.684 | 1.108 | 2.812 | 43.362 | 178.710 | 0.794 | 8.793 | 2.290 | 0.256 | 0.108 | 1.1x dilution | |
| 22-00430-001-3 | 50.225 | 1.116 | 2.768 | 43.522 | 180.211 | 0.792 | 8.769 | 2.292 | 0.257 | 0.112 | 1.1x dilution | |
| XRF results for sample 22-00434 (ppm) | | | | | | | | | | | | |
| Sample Name | Na | Mg | Si | P | S | Cl | K | Ca | Mn | Fe | H2O (%) | Compton (%) |
| 22-00434-001_3 | 11.7 | 6.1 | 11.4 | 62.6 | 2374.4 | 4.9 | 9.4 | 0 | 0.9 | 1.9 | 99.7517 | 96.9 |
| 22-00434-001_2 | 6.7 | 6.3 | 10.7 | 66.2 | 2342.3 | 3.6 | 9.9 | 1 | 0.6 | 2.1 | 99.7551 | 96.253 |
| 22-00434-001_1 | 6.6 | 7.6 | 10.1 | 63.6 | 2368.5 | 6.2 | 8.8 | 1.1 | 0 | 2.7 | 99.7525 | 96.396 |
| ICP-OES / IC results for sample 22-00434 (ppm) | | | | | | | | | | | | |
| 22-00434-001-1 | 19.724 | 0.532 | 4.425 | 52.096 | 1393.469 | N/A | 6.876 | 0.101 | N/A | 0.434 | 10x dilution | |
| 22-00434-001-2 | 19.842 | 0.537 | 4.466 | 52.305 | 1397.779 | N/A | 6.727 | 0.147 | N/A | 0.435 | 10x dilution | |
| 22-00434-001-3 | 19.840 | 0.536 | 4.478 | 52.084 | 1397.095 | N/A | 6.964 | 0.104 | N/A | 0.435 | 10x dilution | |
| 22-00434-001-1 | 18.633 | 0.492 | 4.233 | 50.850 | N/A | 0.562 | 6.725 | 0.209 | 0.100 | 0.414 | 1.1x dilution | |
| 22-00434-001-2 | 18.709 | 0.486 | 4.262 | 50.923 | N/A | 0.599 | 6.727 | 0.178 | 0.100 | 0.411 | 1.1x dilution | |
| 22-00434-001-3 | 18.683 | 0.489 | 4.291 | 50.948 | N/A | 0.600 | 6.722 | 0.178 | 0.100 | 0.415 | 1.1x dilution | |

APPENDIX 16

| XRF results for sample 22-00435, addition-1 (ppm) | | | | | | | | | | | | |
|---|---|---|---|---|---|---|---|---|---|---|---|---|
| Sample Name | Na | Mg | Si | P | S | Cl | K | Ca | Mn | Fe | H2O (%) | Compton (%) |
| 00435_stdlis_1_3 | 34.4 | 14.2 | 14.8 | 86.9 | 2112.3 | 17.1 | 25.7 | 1.8 | 0.3 | 2.5 | 99.769 | 96.258 |
| 00435_stdlis_1_2 | 39.4 | 14.2 | 13.1 | 85.3 | 2110.8 | 21.4 | 25.5 | 0.6 | 0.9 | 2.4 | 99.7687 | 96.25 |
| 00435_stdlis_1_1 | 45.2 | 18 | 12.1 | 85.9 | 2100.4 | 14.6 | 26.1 | 0 | 0.3 | 2.6 | 99.7695 | 96.165 |
| ICP-OES / IC results for sample 22-00435, addition-1 (ppm) | | | | | | | | | | | | |
| 22-00435-002-1 | 58.633 | 12.023 | 6.017 | 72.099 | 1365.925 | N/A | 21.240 | 0.264 | 0.146 | 0.708 | 10x dilution | |
| 22-00435-002-2 | 58.517 | 12.019 | 6.220 | 72.031 | 1355.712 | N/A | 21.063 | 0.196 | 0.145 | 0.699 | 10x dilution | |
| 22-00435-002-3 | 58.759 | 12.052 | 6.233 | 71.888 | 1356.114 | N/A | 21.110 | 0.228 | 0.144 | 0.699 | 10x dilution | |
| 22-00435-002-1 | 55.761 | 10.259 | 5.852 | 73.181 | 1111.512 | 9.863 | 19.884 | 0.290 | 0.132 | 0.641 | 1.1x dilution | |
| 22-00435-002-2 | 55.268 | 10.255 | 5.418 | 72.893 | 1102.423 | 10.353 | 19.632 | 0.223 | 0.130 | 0.640 | 1.1x dilution | |
| 22-00435-002-3 | 55.128 | 10.272 | 5.508 | 72.806 | 1100.810 | 10.360 | 19.595 | 0.223 | 0.129 | 0.641 | 1.1x dilution | |
| XRF results for sample 22-00435, addition-5 (ppm) | | | | | | | | | | | | |
| Sample Name | Na | Mg | Si | P | S | Cl | K | Ca | Mn | Fe | H2O (%) | Compton (%) |
| 00435 stdlis5_3 | 9 | 3 | 35.8 | 145 | 2143.6 | 3.7 | 12.5 | 12.8 | 12.8 | 15.4 | 99.7606 | 96.369 |
| 00435 stdlis5_2 | 14.7 | 6 | 36.7 | 144 | 2156.4 | 0 | 12.2 | 12.4 | 12.3 | 15 | 99.7591 | 96.658 |
| 00435 stdlis5_1 | 9.1 | 9.1 | 35.5 | 142 | 2133.7 | 4 | 14.6 | 13.2 | 12.8 | 15 | 99.7611 | 96.335 |
| ICP-OES / IC results for sample 22-00435, addition-5 (ppm) | | | | | | | | | | | | |
| 22-00435-003-1 | 29.717 | 0.865 | 33.423 | 123.653 | 1349.514 | N/A | 10.331 | 10.896 | 10.608 | 11.918 | 10x dilution | |
| 22-00435-003-2 | 29.722 | 0.859 | 33.657 | 123.358 | 1345.997 | N/A | 10.292 | 10.866 | 10.536 | 11.914 | 10x dilution | |
| 22-00435-003-3 | 29.611 | 0.855 | 33.383 | 122.790 | 1346.803 | N/A | 10.271 | 10.897 | 10.506 | 11.915 | 10x dilution | |
| 22-00435-003-1 | 28.029 | 0.746 | 66.257 | 131.346 | 1100.940 | 0.561 | 9.588 | 10.136 | 10.143 | 11.084 | 1.1x dilution | |
| 22-00435-003-2 | 28.192 | 0.740 | 66.344 | 132.258 | 1110.253 | 0.574 | 9.648 | 10.149 | 10.096 | 11.093 | 1.1x dilution | |
| 22-00435-003-3 | 27.746 | 0.743 | 66.904 | 132.566 | 1102.758 | 0.583 | 9.524 | 10.135 | 10.115 | 11.093 | 1.1x dilution | |

APPENDIX 17

| XRF results for standard addition series of sample 22-00435 | | Na | Mg | Si | P | S | Cl | K | Ca | Mn | Fe | H2O (%) | Compton (%) |
|---|---|---|---|---|---|---|---|---|---|---|---|---|---|
| Reference | | | | | | | | | | | | | |
| 22-00435-001_3 | | 19.9 | 4.8 | 15.4 | 101.2 | 2696 | 2.4 | 16.1 | 0 | 0.4 | 2.5 | 99.7141 | 96.501 |
| 22-00435-001_2 | | 24.6 | 5.4 | 16.9 | 102.4 | 2677.6 | 4.8 | 16.1 | 0 | 0.5 | 1.9 | 99.715 | 96.356 |
| 22-00435-001_1 | | 35.8 | 6.4 | 13.5 | 100.3 | 2678 | 5.9 | 13.7 | 1.4 | 0.3 | 2.4 | 99.7142 | 96.466 |
| ADDITION-1 | Added concentrations | 26.5 | 10 | 0 | 0 | 0 | 10 | 10 | 0 | 0 | 0 | | |
| 00435_stdlis_1_3 | | 34.4 | 14.2 | 14.8 | 86.9 | 2112.3 | 17.1 | 25.7 | 1.8 | 0.3 | 2.5 | 99.769 | 96.258 |
| 00435_stdlis_1_2 | | 39.4 | 14.2 | 13.1 | 85.3 | 2110.8 | 21.4 | 25.5 | 0.6 | 0.9 | 2.4 | 99.7687 | 96.25 |
| 00435_stdlis_1_1 | | 45.2 | 18 | 12.1 | 85.9 | 2100.4 | 14.6 | 26.1 | 0 | 0.3 | 2.6 | 99.7695 | 96.165 |
| ADDITION-2 | Added concentrations | 53 | 20 | 0 | 0 | 0 | 20 | 20 | 0 | 0 | 0 | | |
| 00435 stdlis2_3 | | 78.4 | 27.1 | 11.7 | 85.3 | 2055.3 | 33 | 36.6 | 1.7 | 1 | 3 | 99.7667 | 96.663 |
| 00435 stdlis2_2 | | 62.2 | 26.8 | 11.6 | 83.6 | 2055.7 | 33.1 | 37.8 | 0.7 | 0.8 | 1.9 | 99.7686 | 96.784 |
| 00435_stdlis2_1 | | 63.5 | 29 | 13.9 | 85.4 | 2053.6 | 31.3 | 38.8 | 1.4 | 0.9 | 2.9 | 99.7679 | 96.562 |
| ADDITION-3 | Added concentrations | 83 | 50 | 0 | 0 | 0 | 50 | 50 | 0 | 0 | 0 | | |
| 00435 stdlis3_3 | | 103.2 | 54.4 | 12.9 | 83.6 | 1947.4 | 67.6 | 75.1 | 2 | 0.6 | 3.4 | 99.765 | 96.478 |
| 00435 stdlis3_2 | | 95.1 | 57.4 | 14.7 | 85.9 | 1951.4 | 67 | 73.4 | 0.8 | 0.8 | 3.2 | 99.765 | 96.728 |
| 00435 stdlis3_1 | | 96.3 | 61 | 13.5 | 85.1 | 1943.7 | 65.6 | 73.5 | 2.2 | 0.9 | 3 | 99.7655 | 96.569 |
| ADDITION-4 | Added concentrations | 0 | 0 | 10 | 20 | 0 | 0 | 0 | 20 | 20 | 20 | | |
| 00435 stdlis4_3 | | 0 | 2.2 | 22.9 | 110.3 | 2165.4 | 5.9 | 12.6 | 24.6 | 24.6 | 28.2 | 99.7603 | 96.276 |
| 00435 stdlis4_2 | | 7.8 | 2.1 | 24.1 | 114.4 | 2150.5 | 0.5 | 12.9 | 26.2 | 24.4 | 26.4 | 99.7611 | 96.404 |
| 00435 stdlis4_1 | | 11.2 | 8 | 22.8 | 109.6 | 2168.5 | 4.6 | 12.6 | 25.2 | 24.5 | 27.2 | 99.7586 | 96.492 |
| ADDITION-5 | Added concentrations | 0 | 0 | 20 | 50 | 0 | 0 | 0 | 10 | 10 | 10 | | |
| 00435 stdlis5_3 | | 9 | 3 | 35.8 | 145 | 2143.6 | 3.7 | 12.5 | 12.8 | 12.8 | 15.4 | 99.7606 | 96.369 |
| 00435 stdlis5_2 | | 14.7 | 6 | 36.7 | 144 | 2156.4 | 0 | 12.2 | 12.4 | 12.3 | 15 | 99.7591 | 96.658 |
| 00435 stdlis5_1 | | 9.1 | 9.1 | 35.5 | 142 | 2133.7 | 4 | 14.6 | 13.2 | 12.8 | 15 | 99.7611 | 96.335 |
| ADDITION-6 | Added concentrations | 0 | 0 | 50 | 100 | 0 | 0 | 0 | 50 | 0 | 0 | | |
| 00435 stdlis6_3 | | 9.4 | 2.7 | 69.1 | 209.2 | 1984.9 | 3.9 | 13.3 | 62.3 | 0.7 | 2.9 | 99.7642 | 96.686 |
| 00435 stdlis6_2 | | 11.7 | 3.4 | 67.8 | 210.3 | 2004.5 | 3 | 12.1 | 60.8 | 0 | 3.2 | 99.7623 | 96.178 |
| 00435 stdlis6_1 | | 19 | 4.1 | 70.8 | 208.8 | 2014.5 | 4.7 | 12.5 | 61.4 | 0 | 2.9 | 99.7601 | 96.348 |

APPENDIX 18

| XRF results for samples 22-00430 and 22-00434 (ppm), spiked with 10ppm Na, Mg and K, 15.4 ppm Cl, 5 ppm Mn and Fe | | | | | | | | | | | | | |
|---|---|---|---|---|---|---|---|---|---|---|---|---|---|
| | | | | | | | | | | | | | |
| Sample Name | Measurement Finished | Na | Mg | Si | P | S | Cl | K | Ca | Mn | Fe | H2O (%) | Compton (%) |
| 22-00430-002 | 10.2.2022 8.56 | 56.0 | 18.0 | 11.1 | 53.2 | 722.9 | 29.3 | 23.8 | 4.9 | 6.3 | 9.5 | 99.9065 | 96.762 |
| 22-00430-002_2 | 10.2.2022 10.32 | 43.6 | 16.3 | 10.1 | 52.6 | 739.6 | 26.9 | 25.3 | 4.4 | 6.8 | 9.0 | 99.9065 | 96.092 |
| 22-00430-002_3 | 10.2.2022 10.58 | 48.5 | 14.1 | 9.1 | 53.8 | 716.7 | 24.0 | 24.9 | 4.0 | 6.9 | 8.3 | 99.909 | 95.959 |
| 22-00430-002_4 | 11.2.2022 7.40 | 56.2 | 16.4 | 10.3 | 51.7 | 744.8 | 23.4 | 23.8 | 4.4 | 7.5 | 9.1 | 99.9052 | 96.636 |
| 22-00430-002_5 | 11.2.2022 8.05 | 38 | 15.9 | 10.6 | 54.3 | 730.8 | 27.4 | 24.7 | 3.1 | 7 | 8.7 | 99.9079 | 96.281 |
| 22-00430-002_6 | 11.2.2022 8.31 | 53.9 | 16.6 | 14.2 | 54.4 | 719.9 | 24.2 | 24 | 4.1 | 7.3 | 8.6 | 99.9073 | 96.457 |
| Sample Name | Measurement Finished | | | | | | | | | | | | |
| 22-00434-002 | 10.2.2022 12.52 | 6.9 | 14.8 | 12 | 62 | 2234.8 | 22.4 | 20.9 | 1.4 | 6.5 | 8.1 | 99.761 | 95.914 |
| 22-00434-002_2 | 10.2.2022 13.12 | 12.4 | 17.6 | 11 | 63.3 | 2228.6 | 30.5 | 21.6 | 0 | 6.4 | 7.4 | 99.7601 | 95.764 |
| 22-00434-002_3 | 10.2.2022 13.39 | 9.4 | 15.5 | 10.6 | 59.6 | 2250.5 | 25.2 | 21.6 | 0 | 6.8 | 8 | 99.7593 | 96.265 |
| 22-00434-002_4 | 11.2.2022 9.52 | 23.7 | 16.5 | 10.4 | 62.8 | 2240.4 | 26.3 | 22 | 0.9 | 6.6 | 8.4 | 99.7582 | 96.4 |
| 22-00434-002_5 | 11.2.2022 10.14 | 22.3 | 15.7 | 10.2 | 63.3 | 2220.6 | 26.1 | 21 | 0.8 | 6.9 | 8.5 | 99.7605 | 96.429 |
| 22-00434-002_6 | 11.2.2022 10.34 | 22.4 | 13.8 | 11.1 | 60.8 | 2250.5 | 25.4 | 20.3 | 1.1 | 6.6 | 7.6 | 99.7581 | 96.6 |

APPENDIX 19

| XRF results for sample 22-02255, pretreatment tests (ppm) | | | | | | | | | | | | | |
|---|---|---|---|---|---|---|---|---|---|---|---|---|---|
| Sample Name | Measurement Finished | Na | Mg | Si | P | S | Cl | K | Ca | Mn | Fe | H2O (%) | Compton (%) |
| Reference | | | | | | | | | | | | | |
| 22-02255-001_rep2 | 16.2.2022 14.56 | 68.8 | 3.6 | 23.7 | 36.5 | 350 | 3 | 15 | 0 | 0.7 | 6.7 | 99.9492 | 95.197 |
| 22-02255-001 | 16.2.2022 11.18 | 55.7 | 6.3 | 25.2 | 40.2 | 386.3 | 6.8 | 14.8 | 1.8 | 0.3 | 8.2 | 99.9454 | 94.874 |
| Separation, room temp. | | | | | | | | | | | | | |
| 22-02255-002 | 17.2.2022 8.48 | 68.5 | 4.6 | 24.6 | 37.8 | 326.1 | 3.9 | 13.8 | 0 | 0.4 | 6.8 | 99.9514 | 95.398 |
| 22-02255-002_2 | 17.2.2022 9.52 | 65.7 | 6.4 | 23.8 | 40.6 | 320.9 | 8.8 | 13.5 | 1.6 | 0 | 6.7 | 99.9512 | 95.188 |
| Separation, fridge | | | | | | | | | | | | | |
| 22-02255-003 | 17.2.2022 10.12 | 61.7 | 5.4 | 24.4 | 37.4 | 338.9 | 5.5 | 15.1 | 0.5 | 0.4 | 7.7 | 99.9503 | 94.855 |
| 22-02255-003_2 | 17.2.2022 10.35 | 69.4 | 0.9 | 22.9 | 38.7 | 328.8 | 6.6 | 14.6 | 0.5 | 0 | 7.5 | 99.951 | 94.898 |
| Centrifuged | | | | | | | | | | | | | |
| 22-02255-004_2 | 16.2.2022 14.34 | 71 | 2.4 | 22.8 | 35.8 | 320.9 | 7.3 | 15 | 1.4 | 0 | 6.1 | 99.9517 | 95.974 |
| 22-02255-004_1 | 16.2.2022 14.13 | 54.9 | 1 | 23.6 | 38.5 | 321.9 | 7.5 | 14.2 | 0.5 | 0.6 | 6.4 | 99.9531 | 95.614 |
| Filtrated | | | | | | | | | | | | | |
| 22-02255-005 | 17.2.2022 14.00 | 66.4 | 6.2 | 25.3 | 39.2 | 303.8 | 9.6 | 15.4 | 1.9 | 0.6 | 6.5 | 99.9525 | 93.657 |
| 22-02255-005_2 | 18.2.2022 10.58 | 65.9 | 3.9 | 22.3 | 37.1 | 313.2 | 9.1 | 14.5 | 2.7 | 0.3 | 8.1 | 99.9523 | 94.988 |

APPENDIX 20

| XRF results for sample 22-03412, pretreatment tests (ppm) | | | | | | | | | | | | | |
|---|---|---|---|---|---|---|---|---|---|---|---|---|---|
| Sample Name | Measurement Finished | Na | Mg | Si | P | S | Cl | K | Ca | Mn | Fe | H2O (%) | Compton (%) |
| Reference | | | | | | | | | | | | | |
| 22-03412-001_2 | 10.3.2022 11.49 | 66 | 1 | 28.2 | 35.6 | 3941.8 | 6.5 | 15.8 | 0 | 0.5 | 15.8 | 99.5889 | 95.686 |
| 22-03412-001_1 | 10.3.2022 11.29 | 58.8 | 3.3 | 27.6 | 35.6 | 3955.3 | 4.3 | 15.8 | 0 | 0.7 | 15.8 | 99.5883 | 95.804 |
| Separated, room temp. | | | | | | | | | | | | | |
| 22-03412-002_2 | 11.3.2022 9.12 | 69.2 | 2.2 | 29.7 | 39 | 2757.9 | 4.2 | 16.4 | 1.4 | 0 | 16 | 99.7064 | 96.707 |
| 22-03412-002_1 | 11.3.2022 8.50 | 62.9 | 5.3 | 29.7 | 37.4 | 2799.6 | 8.7 | 16.9 | 0 | 0 | 16.2 | 99.7023 | 96.684 |
| Separated, fridge | | | | | | | | | | | | | |
| 22-03412-003_2 | 11.3.2022 9.57 | 63 | 7.1 | 28.8 | 38.9 | 2632.1 | 4.1 | 18.8 | 0.9 | 0.4 | 15.7 | 99.719 | 96.808 |
| 22-03412-003_1 | 11.3.2022 9.33 | 74.5 | 4.1 | 27.8 | 37.5 | 2638.3 | 4.4 | 17.8 | 0.7 | 0.8 | 16.1 | 99.7178 | 97.115 |
| Centrifuged | | | | | | | | | | | | | |
| 22-03412-004_2 | 10.3.2022 12.58 | 68.3 | 7.6 | 28.4 | 36.1 | 2634.9 | 4.6 | 17.1 | 0.5 | 0.3 | 15.6 | 99.7187 | 96.942 |
| 22-03412-004_1 | 10.3.2022 12.09 | 59.9 | 4.5 | 29.2 | 37.1 | 2648.1 | 6.4 | 18.6 | 0 | 1 | 16 | 99.7179 | 96.925 |
| Filtrated | | | | | | | | | | | | | |
| 22-03412-005_2 | 10.3.2022 13.40 | 71.2 | 4.4 | 26.6 | 39.9 | 2678.5 | 1.2 | 17 | 0 | 0.9 | 15.5 | 99.7145 | 96.805 |
| 22-03412-005_1 | 10.3.2022 13.18 | 57.9 | 5.4 | 29.5 | 37.8 | 2670.2 | 7 | 17.3 | 0 | 0 | 17 | 99.7158 | 96.556 |
| Afternoon measurement | | | | | | | | | | | | | |
| 22-03412-001_iltapvä | 10.3.2022 14.00 | 56.3 | 8.2 | 27.7 | 36.8 | 3110.9 | 3.7 | 17 | 1.2 | 0.3 | 15.2 | 99.6723 | 96.586 |